Péptidos derivados del GB virus C como potenciales inhibidores del virus de la inmunodeficiencia humana tipo 1

Ramona Galatola

UNIVERSIDAD DE BARCELONA
FACULTAD DE FARMACIA
DEPARTAMENTO DE FISICOQUÍMICA

Péptidos derivados del GB virus C como potenciales inhibidores del virus de la inmunodeficiencia humana tipo 1

Ramona Galatola.

Barcelona, 2014

CONCLUSIONES

1. Tras la realización de ensayos biofísicos, se demuestra la capacidad de las secuencias peptídicas de la glicoproteína E2 del GBV-C, E2(175-192), E2(289-306) y E2(313-330), de interaccionar con el PF-HIV-1. Preferentemente el dominio E2(175-192), esto es el péptido E2P59, es el que presenta una mayor inhibición, sugiriendo que éste podría intervenir a nivel de la entrada del virus HIV-1 en las células.
2. Se han obtenido de forma satisfactoria, siguiendo procedimientos de síntesis semiautomática de péptidos en fase solida, 23 análogos peptídicos de la región E1(22-39) del GBV-C. Asimismo, se ha derivatizado esta secuencia con ácido palmítico y ácido mirístico para obtener lipopéptidos. La formación en solución de un puente disulfuro, entre las Cisteínas en posiciones 25 y 29, permitió la obtención de un derivado cíclico de esta secuencia.
3. Tras la realización del estudio de interacción de los análogos de la región E1(22-39) con el PF-HIV-1 por el ensayo de liberación de contenidos vesiculares, se han seleccionado seis regiones peptídicas que presentan una mayor capacidad de inhibir la actividad del PF-HIV-1 según este ensayo.
4. Todos los análogos de E1(22-39) seleccionados inhiben la actividad hemolítica del PF-HIV-1 de forma dosis dependiente.
5. Los estudios realizados con monocapas lipídicas de POPG y DPPG indican que los análogos de E1(22-39) seleccionados modifican la interacción del PF-HIV-1 con lípidos aniónicos.
6. Los estudios realizados por dicroísmo circular con los análogos de E1(22-39) seleccionados sugieren que, aunque los péptidos no presentan una estructura secundaria definida en solución acuosa, interaccionan con el PF-HIV-1 impidiendo la agregación de éste, lo cual podría afectar a su inserción en la membrana celular.
7. Los ensayos de susceptibilidad del HIV-1 a los péptidos potencialmente inhibidores del PF-HIV-1 análogos de E1(22-39), permiten concluir que la secuencia nativa es la que presenta mayor actividad inhibitoria, indicando que tanto la estructura primaria como la

carga son fundamentales para la actividad anti-HIV-1 del péptido. Los resultados alcanzados con los lipopéptidos y con el péptido cíclico, derivado de esta región, indican que la ciclación de la secuencia E1(22-39) es la modificación más idónea para el diseño de nuevos péptidos derivados del GBV-C con actividad anti-HIV-1.

8. Los estudios biofísicos realizados por fluorescencia, dicroísmo circular y balanza de Langmuir, demuestran la interacción del péptido cíclico derivados de E1(22-39) con el PF-HIV-1 y evidencian el papel de este péptido como potencial inhibidor de la entrada del virus HIV-1 a la célula huésped.

ANEXOS

Anexo 1: Espectros de fluorescencia de: A) PF-HIV-1/P59 y B) PF-HIV-1/P105 (1/1) en presencia de concentraciones crecientes de LUV de POPG (de 0 a 400 µM).

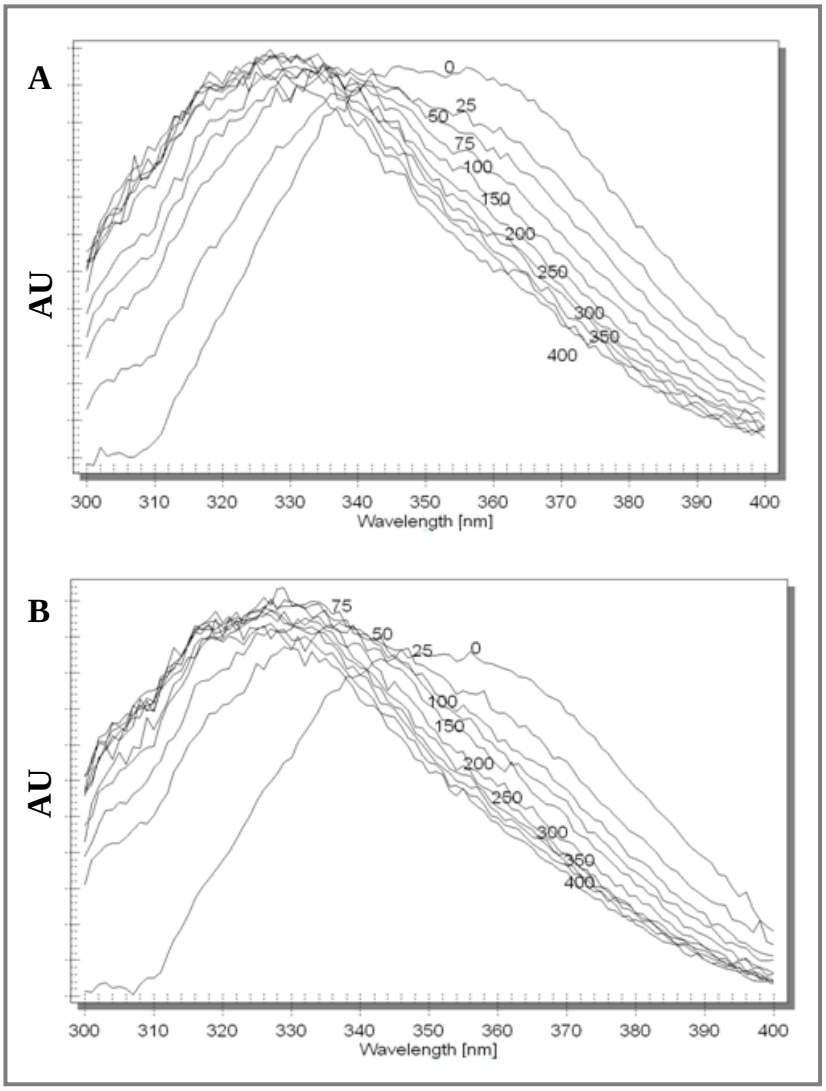

Anexo 2: Energía de Gibbs de exceso (G^E) para las mezclas de PF HIV-1 con POPG, a las presiones superficiales de 5 mN m^{-1}, 10 mN m^{-1}, 20 mN m^{-1} y 25 mN m^{-1}**.**

	G^E (J mol^{-1})			
$X_{PF\text{-}HIV\text{-}1}$	5 mN m^{-1}	10 mN m^{-1}	20 mN m^{-1}	25 mN m^{-1}
0,1	72,88	126,60	65	220,14
0,2	-16,86	114,78	-15,66	130,10
0,4	*-274,65*	*-463,28*	*203,58*	*-196,95*
0,6	-321,63	-499,18	91,55	-673,37

Anexo 3: Energía de Gibbs de exceso (G^E) para las mezclas de POPG con E1P8/PF-HIV-1, E1P8-12/PF-HIV-1, E1P8-13/PF-HIV-1 y E1P8-21/PF-HIV-1, a las presiones superficiales 5 mN m^{-1} y 25 mN m^{-1}**.**

$X_{Peptidos}$	$G^E(J\ mol^{-1})$			
	Π (mN m^{-1})	**E1P8 cyc**	**PF-HIV-1**	**E1P8 cyc/PF-HIV-1**
0,1	5	198,28	72,88	367,01
	10	129,86	126,60	374,95
	20	226,22	65,05	430,98
	25	366,26	220,14	561,97
0,2	5	214,66	16,86	117,46
	10	226,59	114,79	115,46
	20	528,94	15,66	155,71
	25	747,57	130,10	255,63
0,4	5	535,32	274,65	103,03
	10	588,69	463,29	114,41
	20	872,97	203,58	122,59
	25	1063,30	196,95	197,77
0,6	5	1162,56	321,63	217,30
	10	1511,53	499,19	305,42
	20	2475,81	91,55	364,76
	25	3002,83	-673,37	580,41

Anexo 4: Espectros de CD obtenidos a 50 µM de los péptidos solos y la mezcla de los péptidos a diferentes fracciones molares de los E1. A) PF –HIV-1 y E1P8-7, B) PF –HIV-1 y E1P8-12, C) PF –HIV-1 y E1P8-13 y D) PF–HIV-1 y E1P8-21. Los Espectros teóricos del CD se calcularon a partir de la suma de los espectros de cada uno por separado.

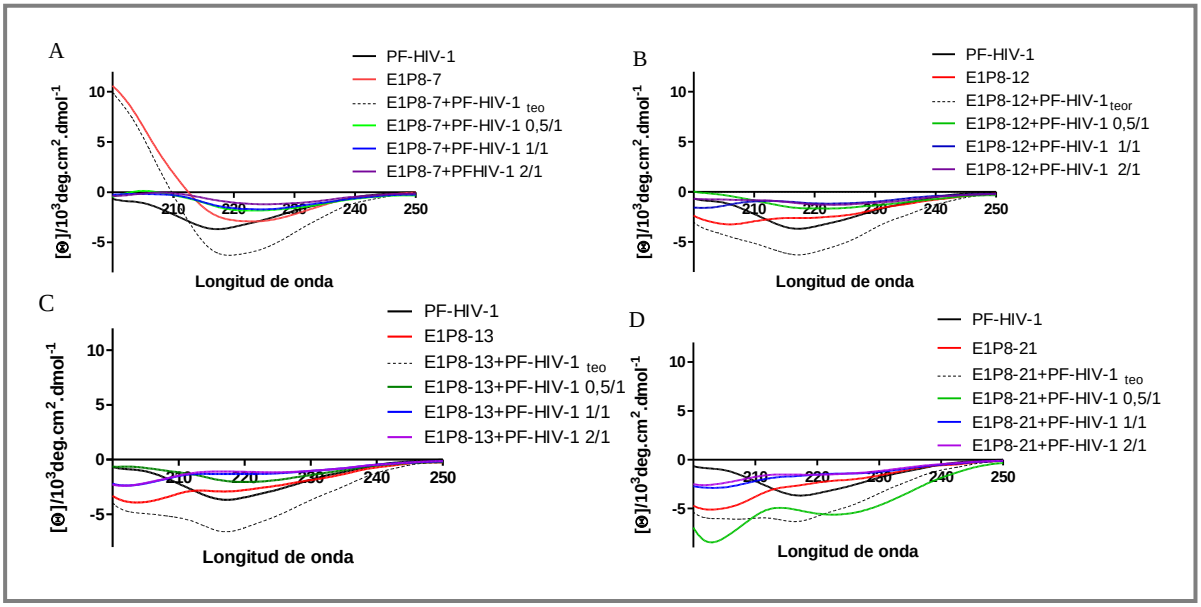

Anexo 5: Espectros UPLC: (A) Mir-E1P8 y (C) Pal-E1P8. Condiciones: 10 mM de acetato de amonio en H_2O; (B) 10 mM de acetato de amonio en Metanol. Gradiente lineal de 50%B a 100%B en 16 minutos a un flujo de 0,2 ml/min. Masa experimental de los péptidos obtenida por Electrospray (ES-MS) (B) Mir-E1P8 y (D) Pal-E1P8.

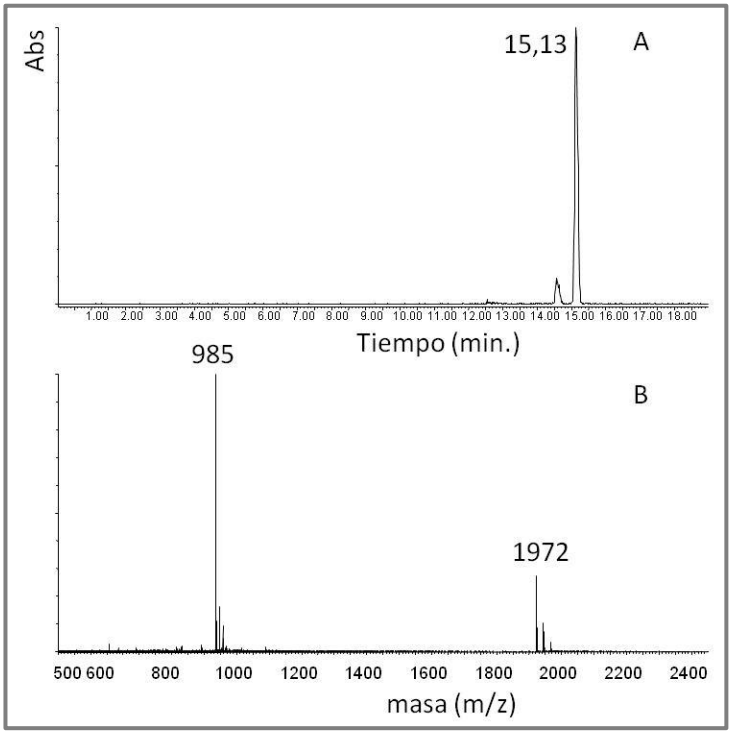

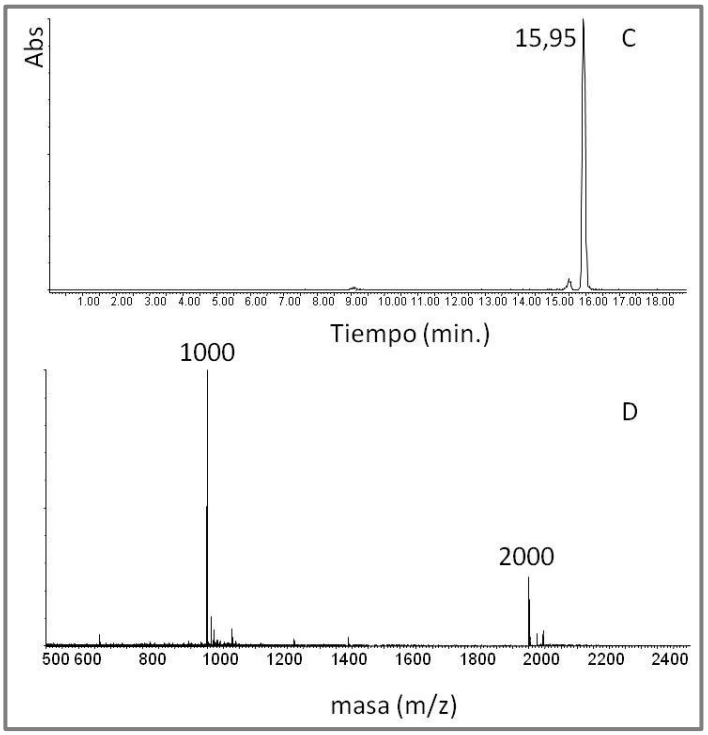
Abs
15,95
C
1.00 2.00 3.00 4.00 5.00 6.00 7.00 8.00 9.00 10.00 11.00 12.00 13.00 14.00 15.00 16.00 17.00 18.00
Tiempo (min.)
1000
D
2000
500 600 800 1000 1200 1400 1600 1800 2000 2200 2400
masa (m/z)

BIBLIOGRAFÍA

[1] T.P. Leary, A.S. Muerhoff, J.N. Simons, T.J. Pilot-Matias, J.C. Erker, M.L. Chalmers, G.G. Schlauder, G.J. Dawson, S.M. Desai, I.K. Mushahwar, Sequence and genomic organization of GBV-C: A novel member of the flaviviridae associated with human Non-A-E hepatitis, Journal of Medical Virology, 48 (1996) 60-67.
[2] J. Linnen, J. Wages Jr, Z.Y. Zhang-Keck, K.E. Fry, K.Z. Krawczynski, H. Alter, E. Koonin, M. Gallagher, M. Alter, S. Hadziyannis, P. Karayiannis, K. Fung, Y. Nakatsuji, J.W.K. Shin, L. Young, M. Piatak Jr, C. Hoover, J. Fernandez, S. Chen, J.C. Zou, T. Morris, K.C. Hyams, S. Ismay, J.D. Lifson, G. Hess, S.K.H. Foung, H. Thomas, D. Bradley, H. Margolis, J.P. Kim, Molecular cloning and disease association of hepatitis G virus: A transfusion-transmissible agent, Science, 271 (1996) 505-508.
[3] E.L. Mohr, J.T. Stapleton, GB virus type C interactions with HIV: The role of envelope glycoproteins, Journal of Viral Hepatitis, 16 (2009) 757-768.
[4] C.F. Williams, D. Klinzman, T.E. Yamashita, J. Xiang, P.M. Polgreen, C. Rinaldo, C. Liu, J. Phair, J.B. Margolick, D. Zdunek, G. Hess, J.T. Stapleton, Persistent GB Virus C Infection and Survival in HIV-Infected Men, New England Journal of Medicine, 350 (2004) 981-990.
[5] H.L. Tillmann, M.P. Manns, C. Claes, H. Heiken, R.E. Schmidt, M. Stoll, GB virus C infection and quality of life in HIV-positive patients, AIDS Care - Psychological and Socio-Medical Aspects of AIDS/HIV, 16 (2004) 736-743.
[6] J. Xiang, S. Wunschmann, D.J. Diekema, D. Klinzman, K.D. Patrick, S.L. George, J.T. Stapleton, Effect of coinfection with GB virus C on survival among patients with HIV infection, New England Journal of Medicine, 345 (2001) 707-714.
[7] J.T. Stapleton, K. Chaloner, J.A. Martenson, J. Zhang, D. Klinzman, J. Xiang, W. Sauter, S.N. Desai, A. Landay, GB Virus C Infection Is Associated with Altered Lymphocyte Subset Distribution and Reduced T Cell Activation and Proliferation in HIV-Infected Individuals, PLoS ONE, 7 (2012).
[8] N. Bhattarai, J.T. Stapleton, GB virus C: The good boy virus?, Trends in Microbiology, 20 (2012) 124-130.
[9] J.N. Simons, T.P. Leary, G.J. Dawson, T. Pilot-Matias, A.S. Muerhoff, G.G. Schlauder, S.M. Desai, I.K. Kushahwar, Isolation of novel virus-like sequences associated with human hepatitis, Nature Medicine, 1 (1995) 564-569.
[10] S. Saito, K. Tanaka, M. Kondo, K. Morita, T. Kitamura, T. Kiba, K. Numata, H. Sekihara, Plus- and minus-stranded hepatitis G virus RNA in liver tissue and in peripheral blood mononuclear cells, Biochemical and Biophysical Research Communications, 237 (1997) 288-291.
[11] J.T. Stapleton, GB virus type C/hepatitis G virus, Seminars in Liver Disease, 23 (2003) 137-148.

[12] J.T. Stapleton, S. Foung, A.S. Muerhoff, J. Bukh, P. Simmonds, The GB viruses: A review and proposed classification of GBV-A, GBV-C (HGV), and GBV-D in genus Pegivirus within the family Flaviviridae, Journal of General Virology, 92 (2011) 233-246.
[13] J. Xiang, D. Klinzman, J. McLinden, W.N. Schmidt, D.R. LaBrecque, R. Gish, J.T. Stapleton, Characterization of hepatitis G virus (GB-C virus) particles: Evidence for a nucleocapsid and expression of sequences upstream of the E1 protein, Journal of Virology, 72 (1998) 2738-2744.
[14] S.L. George, D. Varmaz, J.T. Stapleton, GB virus C replicates in primary T and B lymphocytes, Journal of Infectious Diseases, 193 (2006) 451-454.
[15] M. Tacke, K. Kiyosawa, K. Stark, V. Schlueter, B. Ofenloch-Haehnle, G. Hess, A.M. Engel, Detection of antibodies to a putative hepatitis G virus envelope protein, Lancet, 349 (1997) 318-320.
[16] M. Tacke, S. Schmolke, V. Schlueter, S. Sauleda, J.I. Esteban, E. Tanaka, K. Kiyosawa, H.J. Alter, U. Schmitt, G. Hess, B. Ofenloch-Haehnle, A.M. Engel, Humoral immune response to the E2 protein of hepatitis G virus is associated with long-term recovery from infection and reveals a high frequency of hepatitis G virus exposure among healthy blood donors, Hepatology, 26 (1997) 1626-1633.
[17] D.L. Thomas, D. Vlahov, H.J. Alter, J.C. Hunt, R. Marshall, J. Astemborski, K.E. Nelson, Association of antibody to GB virus C (hepatitis G virus) with viral clearance and protection from reinfection, Journal of Infectious Diseases, 177 (1998) 539-542.
[18] J.T. Stapleton, K. Chaloner, GB virus C infection and non-Hodgkin lymphoma: Important to know but the jury is out, International Journal of Cancer, 126 (2010) 2759-2761.
[19] J.J. Lefrère, F. Roudot-Thoraval, L. Morand-Joubert, Y. Brossard, F. Parnet-Mathieu, M. Mariotti, F. Agis, G. Rouet, J. Lerable, G. Lefèvre, R. Girot, P. Loiseau, Prevalence of GB virus type C/hepatitis G virus RNA and of anti-E2 in individuals at high or low risk for blood-borne or sexually transmitted viruses: Evidence of sexual and parenteral transmission, Transfusion, 39 (1999) 83-94.
[20] A.J. Nahmias, J. Weiss, X. Yao, F. Lee, R. Kodsi, M. Schanfield, T. Matthews, D. Bolognesi, D. Durack, A. Motulsky, Evidence for human infection with an HTLV III/LAV-like virus in central Africa, 1959, Lancet, 1 (1986) 1279-1280.
[21] F. Clavel, K. Mansinho, S. Chamaret, D. Guetard, V. Favier, J. Nina, M.O. Santos-Ferreira, J.L. Champalimaud, L. Montagnier, Human immunodeficiency virus type 2 infection associated with AIDS in West Africa, New England Journal of Medicine, 316 (1987) 1180-1185.

[22] C. Beyrer, S.D. Baral, F. Van Griensven, S.M. Goodreau, S. Chariyalertsak, A.L. Wirtz, R. Brookmeyer, Global epidemiology of HIV infection in men who have sex with men, The Lancet, 380 (2012) 367-377.
[23] G. Chêne, Epidemiology of HIV/AIDS, Epidemiologie de l'infection par le VIH, 49 (1999) 1732-1737.
[24] F. Barre Sinoussi, J.C. Chermann, F. Rey, Isolation of a T-lymphotropic retrovirus from a patient at risk for acquired immune deficiency syndrome (AIDS), Science, 220 (1983) 868-871.
[25] R.C. Gallo, A. Sliski, F. Wong-Staal, Origin of human T-cell leukaemia-lymphoma virus, Lancet, 2 (1983) 962-963.
[26] M. Emerman, M.H. Malim, HIV-1 regulatory/accessory genes: Keys to unraveling viral and host cell biology, Science, 280 (1998) 1880-1884.
[27] H. Varmus, N. Nathanson, Science and the control of AIDS, Science, 280 (1998) 1815.
[28] A. Seelamgari, A. Maddukuri, R. Berro, C. de la Fuente, K. Kehn, L. Deng, S. Dadgar, M.E. Bottazzi, E. Ghedin, A. Pumfery, F. Kashanchi, Role of viral regulatory and accessory proteins in HIV-1 replication, Frontiers in bioscience : a journal and virtual library., 9 (2004) 2388-2413.
[29] P. Monini, C. Sgadari, E. Toschi, G. Barillari, B. Ensoli, Antitumour effects of antiretroviral therapy, Nature Reviews Cancer, 4 (2004) 861-875.
[30] C. Boggiano, S. Jiang, H. Lu, Q. Zhao, S. Liu, J. Binley, S.E. Blondelle, Identification of a d-amino acid decapeptide HIV-1 entry inhibitor, Biochemical and Biophysical Research Communications, 347 (2006) 909-915.
[31] C.K. Leonard, M.W. Spellman, L. Riddle, R.J. Harris, J.N. Thomas, T.J. Gregory, Assignment of intrachain disulfide bonds and characterization of potential glycosylation sites of the type 1 recombinant human immunodeficiency virus envelope glycoprotein (gp120) expressed in Chinese hamster ovary cells, Journal of Biological Chemistry, 265 (1990) 10373-10382.
[32] D.C. Chan, P.S. Kim, HIV entry and its inhibition, Cell, 93 (1998) 681-684.
[33] E. De Clercq, Antiviral drugs in current clinical use, Journal of Clinical Virology, 30 (2004) 115-133.
[34] D.C. Chan, D. Fass, J.M. Berger, P.S. Kim, Core Structure of gp41 from the HIV Envelope Glycoprotein, Cell, 89 (1997) 263-273.
[35] F. Yu, L. Lu, L. Du, X. Zhu, A. Debnath, S. Jiang, Approaches for Identification of HIV-1 Entry Inhibitors Targeting gp41 Pocket, Viruses, 5 (2013) 127-149.
[36] Y. He, J. Cheng, J. Li, Z. Qi, H. Lu, M. Dong, S. Jiang, Q. Dai, Identification of a Critical Motif for the Human Immunodeficiency Virus Type 1 (HIV-1) gp41 Core

Structure: Implications for Designing Novel Anti-HIV Fusion Inhibitors, Journal of Virology, 82 (2008) 6349-6358.
[37] H. Chong, X. Yao, Z. Qiu, B. Qin, R. Han, S. Waltersperger, M. Wang, S. Cui, Y. He, Discovery of Critical Residues for Viral Entry and Inhibition through Structural Insight of HIV-1 Fusion Inhibitor CP621–652, Journal of Biological Chemistry, 287 (2012) 20281-20289.
[38] H. Chong, X. Yao, J. Sun, Z. Qiu, M. Zhang, S. Waltersperger, M. Wang, S. Cui, Y. He, The M-T Hook Structure Is Critical for Design of HIV-1 Fusion Inhibitors, Journal of Biological Chemistry, 287 (2012) 34558-34568.
[39] S. Heringlake, J. Ockenga, H.L. Tillmann, C. Trautwein, D. Meissner, M. Stoll, J. Hunt, C. Jou, N. Solomon, R.E. Schmidt, M.P. Manns, GB virus C/hepatitis G virus infection: A favorable prognostic factor in human immunodeficiency virus-infected patients?, Journal of Infectious Diseases, 177 (1998) 1723-1726.
[40] A.E.T. Yeo, A. Matsumoto, M. Hisada, J.W. Shih, H.J. Alter, J.J. Goedert, Effect of hepatitis g virus infection on progression of HIV infection in patients with hemophilia, Annals of Internal Medicine, 132 (2000) 959-963.
[41] H.L. Tillmann, H. Heiken, A. Knapik-Botor, S. Heringlake, J. Ockenga, J.C. Wilber, B. Goergen, J. Detmer, M. McMorrow, M. Stoll, R.E. Schmidt, M.P. Manns, Infection with GB virus C and reduced mortality among HIV-infected patients, New England Journal of Medicine, 345 (2001) 715-724.
[42] A.K. Van Der Bij, N. Kloosterboer, M. Prins, B. Boeser-Nunnink, R.B. Geskus, J.M.A. Lange, R.A. Coutinho, H. Schuitemaker, GB virus C coinfection and HIV-1 disease progression: The Amsterdam cohort study, Journal of Infectious Diseases, 191 (2005) 678-685.
[43] W. Zhang, K. Chaloner, H.L. Tillmann, C.F. Williams, J.T. Stapleton, Effect of early and late GB virus C viraemia on survival of HIV-infected individuals: A meta-analysis, HIV Medicine, 7 (2006) 173-180.
[44] W.B. Supapol, R.S. Remis, J. Raboud, M. Millson, J. Tappero, R. Kaul, P. Kulkarni, M.S. McConnell, P.A. Mock, M. Culnane, J. McNicholl, A. Roongpisuthipong, T. Chotpitayasunondh, N. Shaffer, S. Butera, Reduced mother-to-child transmission of HIV associated with infant but not maternal GB virus C infection, Journal of Infectious Diseases, 197 (2008) 1369-1377.
[45] H. Toyoda, Y. Fukuda, T. Hayakawa, J. Takamatsu, H. Saito, Effect of GB virus C/hepatitis G virus coinfection on the course of HIV infection in hemophilia patients in Japan, Journal of Acquired Immune Deficiency Syndromes and Human Retrovirology, 17 (1998) 209-213.
[46] J.J. Lefrère, F. Roudot-Thoraval, L. Morand-Joubert, J.C. Petit, J. Lerable, M. Thauvin, M. Mariotti, Carriage of GB virus C/hepatitis G virus RNA is associated

with a slower immunologic, virologic, and clinical progression of human immunodeficiency virus disease in coinfected persons, Journal of Infectious Diseases, 179 (1999) 783-789.
[47] J.P. Moore, S.G. Kitchen, P. Pugach, J.A. Zack, The CCR5 and CXCR4 Coreceptors - Central to Understanding the Transmission and Pathogenesis of Human Immunodeficiency Virus Type 1 Infection, AIDS Research and Human Retroviruses, 20 (2004) 111-126.
[48] M.M. Lederman, A. Penn-Nicholson, M. Cho, D. Mosier, Biology of CCR5 and its role in HIV infection and treatment, Journal of the American Medical Association, 296 (2006) 815-826.
[49] C. Schwarze-Zander, M. Neibecker, S. Othman, C. Tural, B. Clotet, J.T. Blackard, B. Kupfer, G. Luechters, R.T. Chung, J.K. Rockstroh, U. Spengler, GB virus C coinfection in advanced HIV type-1 disease is associated with low CCR5 and CXCR4 surface expression on CD4+ T-cells, Antiviral Therapy, 15 (2010) 745-752.
[50] J. Xiang, S.L. George, S. Wünschmann, Q. Chang, D. Klinzman, J.T. Stapleton, Inhibition of HIV-1 replication by GB virus C infection through increases in RANTES, MIP-1α, MIP-1β, and SDF-1, Lancet, 363 (2004) 2040-2046.
[51] J.A. Levy, The importance of the innate immune system in controlling HIV infection and disease, Trends in Immunology, 22 (2001) 312-316.
[52] V. Soumelis, L. Scott, F. Gheyas, D. Bouhour, G. Cozon, L. Cotte, L. Huang, J.A. Levy, Y.J. Liu, Depletion of circulating natural type 1 interferon-producing cells in HIV-infected AIDS patients, Blood, 98 (2001) 906-912.
[53] I. Kamga, S. Kahi, L. Develioglu, M. Lichtner, C. Marañón, C. Deveau, L. Meyer, C. Goujard, P. Lebon, M. Sinet, A. Hosmalin, Type I interferon production is profoundly and transiently impaired in primary HIV-1 infection, Journal of Infectious Diseases, 192 (2005) 303-310.
[54] S. Feldman, D. Stein, S. Amrute, T. Denny, Z. Garcia, P. Kloser, Y. Sun, N. Megjugorac, P. Fitzgerald-Bocarsly, Decreased interferon-α production in HIV-infected patients correlates with numerical and functional deficiencies in circulating type 2 dendritic cell precursors, Clinical Immunology, 101 (2001) 201-210.
[55] E. Lalle, A. Sacchi, I. Abbate, A. Vitale, F. Martini, G. D'Offizi, G. Antonucci, C. Castilletti, F. Poccia, M.R. Capobianchi, Activation of interferon response genes and of plasmacytoid dendritic cells in HIV-1 positive subjects with GB virus C co-infection, International Journal of Immunopathology and Pharmacology, 21 (2008) 161-171.
[56] M.R. Capobianchi, E. Lalle, F. Martini, F. Poccia, G. D'Offizi, G. Antonucci, I. Abbate, F. Dianzani, Influence of GBV-C infection on the endogenous activation of

the IFN system in HIV-1 co-infected patients, Cellular and Molecular Biology, 52 (2006) 3-8.
[57] N. Bhattarai, J.H. McLinden, J. Xiang, T.M. Kaufman, J.T. Stapleton, GB virus C envelope protein E2 inhibits TCR-induced IL-2 production and alters IL-2-signaling pathways, Journal of Immunology, 189 (2012) 2211-2216.
[58] M.D. Berzsenyi, D.S. Bowden, S.K. Roberts, GB virus C: Insights into co-infection, Journal of Clinical Virology, 33 (2005) 257-266.
[59] W. Barcellini, G.P. Rizzardi, M.O. Borghi, C. Fain, A. Lazzarin, P.L. Meroni, TH1 and TH2 cytokine production by peripheral blood mononuclear cells from HIV-infected patients, AIDS, 8 (1994) 757-762.
[60] R.T. Rydze, J. Xiang, J.H. McLinden, J.T. Stapleton, GB virus type C infection polarizes T-cell cytokine gene expression toward a Th1 cytokine profile via NS5A protein expression, Journal of Infectious Diseases, 206 (2012) 69-72.
[61] G. Nunnari, L. Nigro, F. Palermo, M. Attanasio, A. Berger, H.W. Doerr, R.J. Pomerantz, B. Cacopardo, Slower Progression of HIV-1 Infection in Persons with GB Virus C Co-Infection Correlates with an Intact T-Helper 1 Cytokine Profile, Annals of Internal Medicine, 139 (2003) 26-30+I65.
[62] M. Moenkemeyer, R.E. Schmidt, H. Wedemeyer, H.L. Tillmann, H. Heiken, GBV-C coinfection is negatively correlated to Fas expression and Fas-mediated apoptosis in HIV-1 infected patients, Journal of Medical Virology, 80 (2008) 1933-1940.
[63] U. Dianzani, T. Bensi, A. Savarino, S. Sametti, M. Indelicato, R. Mesturini, A. Chiocchetti, Role of FAS in HIV infection, Curr HIV Res, 1 (2003) 405-417.
[64] Y. Koedel, K. Eissmann, H. Wend, B. Fleckenstein, H. Reil, Peptides derived from a distinct region of GB virus c glycoprotein E2 mediate strain-specific HIV-1 entry inhibition, Journal of Virology, 85 (2011) 7037-7047.
[65] S. Jung, M. Eichenmüller, N. Donhauser, F. Neipel, A.M. Engel, G. Hess, B. Fleckenstein, H. Reil, HIV entry inhibition by the envelope 2 glycoprotein of GB virus C, AIDS, 21 (2007) 645-647.
[66] Q. Chang, J.H. McLinden, J.T. Stapleton, M.A. Sathar, J. Xiang, Expression of GB virus C NS5A protein from genotypes 1, 2, 3 and 5 and a 30 aa NS5A fragment inhibit human immunodeficiency virus type 1 replication in a CD4+ T-lymphocyte cell line, Journal of General Virology, 88 (2007) 3341-3346.
[67] J. Xiang, J.H. McLinden, Q. Chang, T.M. Kaufman, J.T. Stapleton, An 85-aa segment of the GB virus type C NS5A phosphoprotein inhibits HIV-1 replication in CD4+ Jurkat T cells, Proceedings of the National Academy of Sciences of the United States of America, 103 (2006) 15570-15575.

[68] J. Xiang, J.H. McLinden, T.M. Kaufman, E.L. Mohr, N. Bhattarai, Q. Chang, J.T. Stapleton, Characterization of a peptide domain within the GB virus C envelope glycoprotein (E2) that inhibits HIV replication, Virology, 430 (2012) 53-62.
[69] E. Herrera, S. Tenckhoff, M.J. Gómara, R. Galatola, M.J. Bleda, C. Gil, G. Ercilla, J.M. Gatell, H.L. Tillmann, I. Haro, Effect of synthetic peptides belonging to E2 envelope protein of GB virus C on human immunodeficiency virus type 1 infection, Journal of Medicinal Chemistry, 53 (2010) 6054-6063.
[70] M.J. Sánchez-Martín, A. Cruz, M.A. Busquets, I. Haro, M.A. Alsina, M. Pujol, Physicochemical characterization of GBV-C E1 peptides as potential inhibitors of HIV-1 fusion peptide: Interaction with model membranes, International Journal of Pharmaceutics, 436 (2012) 593-601.
[71] J. Xiang, J.H. McLinden, R.A. Rydze, Q. Chang, T.M. Kaufman, D. Klinzman, J.T. Stapleton, Viruses within the Flaviviridae decrease CD4 expression and inhibit HIV replication in human CD4+ cells, Journal of Immunology, 183 (2009) 7860-7869.
[72] E.L. Mohr, J. Xiang, J.H. McLinden, T.M. Kaufman, Q. Chang, D.C. Montefiori, D. Klinzman, J.T. Stapleton, GB virus type C envelope protein E2 elicits antibodies that react with a cellular antigen on HIV-1 particles and neutralize diverse HIV-1 isolates, Journal of Immunology, 185 (2010) 4496-4505.
[73] C.T. Wild, D.C. Shugars, T.K. Greenwell, C.B. McDanal, T.J. Matthews, Peptides corresponding to a predictive α-helical domain of human immunodeficiency virus type 1 gp41 are potent inhibitors of virus infection, Proceedings of the National Academy of Sciences of the United States of America, 91 (1994) 9770-9774.
[74] A. Burton, Enfuvirtide approved for defusing HIV, The Lancet Infectious Diseases, 3 (2003) 260.
[75] J.M. Kilby, S. Hopkins, T.M. Venetta, B. Dimassimo, G.A. Cloud, J.Y. Lee, L. Alldredge, E. Hunter, D. Lambert, D. Bolognesi, T. Matthews, M.R. Johnson, M.A. Nowak, G.M. Shaw, M.S. Saag, Potent suppression of HIV-1 replication in humans by T-20, a peptide inhibitor of gp41-mediated virus entry, Nature Medicine, 4 (1998) 1302-1307.
[76] E. Poveda, V. Briz, V. Soriano, Enfuvirtide, the first fusion inhibitor to treat HIV infection, AIDS Reviews, 7 (2005) 139-147.
[77] M.L. Heil, J.M. Decker, J.N. Sfakianos, G.M. Shaw, E. Hunter, C.A. Derdeyn, Determinants of human immunodeficiency virus type 1 baseline susceptibility to the fusion inhibitors enfuvirtide and T-649 reside outside the peptide interaction site, Journal of Virology, 78 (2004) 7582-7589.

[78] C.A. Derdeyn, J.M. Decker, J.N. Sfakianos, Z. Zhang, W.A. O'Brien, L. Ratner, G.M. Shaw, E. Hunter, Sensitivity of human immunodeficiency virus type 1 to fusion inhibitors targeted to the gp41 first heptad repeat involves distinct regions of gp41 and is consistently modulated by gp120 interactions with the coreceptor, Journal of Virology, 75 (2001) 8605-8614.
[79] A. Otaka, M. Nakamura, D. Nameki, E. Kodama, S. Uchiyama, S. Nakamura, H. Nakano, H. Tamamura, Y. Kobayashi, M. Matsuoka, N. Fujii, Remodeling of gp41-C34 Peptide Leads to Highly Effective Inhibitors of the Fusion of HIV-1 with Target Cells, Angewandte Chemie International Edition, 41 (2002) 2937-2940.
[80] J.J. Eron, R.M. Gulick, J.A. Bartlett, T. Merigan, R. Arduino, J.M. Kilby, B. Yangco, A. Diers, C. Drobnes, R. DeMasi, M. Greenberg, T. Melby, C. Raskino, P. Rusnak, Y. Zhang, R. Spence, G.D. Miralles, Short-Term Safety and Antiretroviral Activity of T-1249, a Second-Generation Fusion Inhibitor of HIV, Journal of Infectious Diseases, 189 (2004) 1075-1083.
[81] J.P. Lalezari, N.C. Bellos, K. Sathasivam, G.J. Richmond, C.J. Cohen, R.A. Myers, D.H. Henry, C. Raskino, T. Melby, H. Murchison, Y. Zhang, R. Spence, M.L. Greenberg, R.A. DeMasi, G.D. Miralles, T-1249 Retains Potent Antiretroviral Activity in Patients Who Had Experienced Virological Failure while on an Enfuvirtide-Containing Treatment Regimen, Journal of Infectious Diseases, 191 (2005) 1155-1163.
[82] L. Martin-Carbonero, Discontinuation of the clinical development of fusion inhibitor T-1249, AIDS Reviews, 61 (2004) 61.
[83] D. Eggink, C.E. Baldwin, Y. Deng, J.P.M. Langedijk, M. Lu, R.W. Sanders, B. Berkhout, Selection of T1249-Resistant Human Immunodeficiency Virus Type 1 Variants, Journal of Virology, 82 (2008) 6678-6688.
[84] Y. He, Synthesized Peptide Inhibitors of HIV-1 gp41-dependent Membrane Fusion, Current Pharmaceutical Design, 19 (2013) 1800-1809.
[85] Y. He, Y. Xiao, H. Song, Q. Liang, D. Ju, X. Chen, H. Lu, W. Jing, S. Jiang, L. Zhang, Design and Evaluation of Sifuvirtide, a Novel HIV-1 Fusion Inhibitor, Journal of Biological Chemistry, 283 (2008) 11126-11134.
[86] X. Yao, H. Chong, C. Zhang, S. Waltersperger, M. Wang, S. Cui, Y. He, Broad Antiviral Activity and Crystal Structure of HIV-1 Fusion Inhibitor Sifuvirtide, Journal of Biological Chemistry, 287 (2012) 6788-6796.
[87] L. Li, Y. Ben, S. Yuan, S. Jiang, J. Xu, X. Zhang, Efficacy, stability, and biosafety of sifuvirtide gel as a microbicide candidate against HIV-1, PLoS ONE, 7 (2012) e37381.

[88] H. Chong, X. Yao, Z. Qiu, B. Qin, R. Han, S. Waltersperger, M. Wang, S. Cui, Y. He, Structural insight of HIV-1 fusion inhibitor CP621-652 discovers the critical residues for viral entry and inhibition, Journal of Biological Chemistry, (2012).
[89] Y. He, J. Cheng, H. Lu, J. Li, J. Hu, Z. Qi, Z. Liu, S. Jiang, Q. Dai, Potent HIV fusion inhibitors against Enfuvirtide-resistant HIV-1 strains, Proceedings of the National Academy of Sciences, 105 (2008) 16332-16337.
[90] T. Naito, K. Izumi, E. Kodama, Y. Sakagami, K. Kajiwara, H. Nishikawa, K. Watanabe, S.G. Sarafianos, S. Oishi, N. Fujii, M. Matsuoka, SC29EK, a Peptide Fusion Inhibitor with Enhanced α-Helicity, Inhibits Replication of Human Immunodeficiency Virus Type 1 Mutants Resistant to Enfuvirtide, Antimicrobial Agents and Chemotherapy, 53 (2009) 1013-1018.
[91] H. Nishikawa, S. Oishi, M. Fujita, K. Watanabe, R. Tokiwa, H. Ohno, E. Kodama, K. Izumi, K. Kajiwara, T. Naitoh, M. Matsuoka, A. Otaka, N. Fujii, Identification of minimal sequence for HIV-1 fusion inhibitors, Bioorganic & Medicinal Chemistry, 16 (2008) 9184-9187.
[92] D.M. Eckert, V.N. Malashkevich, L.H. Hong, P.A. Carr, P.S. Kim, Inhibiting HIV-1 Entry: Discovery of D-Peptide Inhibitors that Target the gp41 Coiled-Coil Pocket, Cell, 99 (1999) 103-115.
[93] B.D. Welch, A.P. VanDemark, A. Heroux, C.P. Hill, M.S. Kay, Potent D-peptide inhibitors of HIV-1 entry, Proceedings of the National Academy of Sciences, 104 (2007) 16828-16833.
[94] B.D. Welch, J.N. Francis, J.S. Redman, S. Paul, M.T. Weinstock, J.D. Reeves, Y.S. Lie, F.G. Whitby, D.M. Eckert, C.P. Hill, M.J. Root, M.S. Kay, Design of a potent D-peptide HIV-1 entry inhibitor with a strong barrier to resistance, Journal of Virology, 84 (2010) 11235-11244.
[95] J. Munch, L. Standker, K. Adermann, A. Schulz, M. Schindler, R. Chinnadurai, S. Pohlmann, C. Chaipan, T. Biet, T. Peters, B. Meyer, D. Wilhelm, H. Lu, W. Jing, S. Jiang, W.G. Forssmann, F. Kirchhoff, Discovery and Optimization of a Natural HIV-1 Entry Inhibitor Targeting the gp41 Fusion Peptide, Cell, 129 (2007) 263-275.
[96] W.-G. Forssmann, Y.-H. The, M. Stoll, K. Adermann, U. Albrecht, H.-C. Tillmann, K. Barlos, A. Busmann, A. Canales-Mayordomo, G. Giménez-Gallego, J. Hirsch, J. Jiménez-Barbero, D. Meyer-Olson, J. Münch, J. Pérez-Castells, L. Ständker, F. Kirchhoff, R.E. Schmidt, Short-Term Monotherapy in HIV-Infected Patients with a Virus Entry Inhibitor Against the gp41 Fusion Peptide, Science Translational Medicine, 2 (2010) 63re63-63re63.
[97] E. Gonzalez, E. Ballana, B. Clotet, J.A. Esté, Development of resistance to VIR-353 with cross-resistance to the natural HIV-1 entry virus inhibitory peptide (VIRIP), AIDS, 25 (2011) 1575-1583.

[98] E. González-Ortega, E. Ballana, R. Badia, B. Clotet, J.A. Esté, Compensatory mutations rescue the virus replicative capacity of VIRIP-resistant HIV-1, Antiviral Research, 92 (2011) 479-483.
[99] M.E. Quiñones-Mateu, D. Schols, Virus-inhibitory peptide: A natural HIV entry inhibitor in search for a formal target in the viral genome, AIDS, 25 (2011) 1663-1664.
[100] J. Xiang, J.H. McLinden, Q. Chang, E.L. Jordan, J.T. Stapleton, Characterization of a Peptide Domain within the GB Virus C NS5A Phosphoprotein that Inhibits HIV Replication, PLoS ONE, 3 (2008).
[101] E. Herrera, M.J. Gomara, S. Mazzini, E. Ragg, I. Haro, Synthetic peptides of hepatitis G virus (GBV-C/HGV) in the selection of putative peptide inhibitors of the HIV-1 fusion peptide, Journal of Physical Chemistry B, 113 (2009) 7383-7391.
[102] K. Eissmann, S. Mueller, H. Sticht, S. Jung, P. Zou, S. Jiang, A. Gross, J. Eichler, B. Fleckenstein, H. Reil, HIV-1 Fusion Is Blocked through Binding of GB Virus C E2D Peptides to the HIV-1 gp41 Disulfide Loop, PLoS ONE, 8 (2013).
[103] J.H. McLinden, J.T. Stapleton, D. Klinzman, K.K. Murthy, Q. Chang, T.M. Kaufman, N. Bhattarai, J. Xiang, Chimpanzee GB virus C and GB virus A E2 envelope glycoproteins contain a peptide motif that inhibits human immunodeficiency virus type 1 replication in human CD4+ T-cells, Journal of General Virology, 94 (2013) 774-782.
[104] S. Mazzini, M. Fernandez-Vidal, V. Galbusera, F. Castro-Roman, M.C. Bellucci, E. Ragg, I. Haro, 3D-Structure of the interior fusion peptide of HGV/GBV-C by 1H NMR, CD and molecular dynamics studies, Archives of Biochemistry and Biophysics, 465 (2007) 187-196.
[105] C. Larios, J. Casas, M.A. Alsina, C. Mestres, M.J. Gómara, I. Haro, Characterization of a putative fusogenic sequence in the E2 hepatitis G virus protein, Archives of Biochemistry and Biophysics, 442 (2005) 149-159.
[106] C. Larios, B. Christiaens, M.J. Gómara, M.A. Alsina, I. Haro, Interaction of synthetic peptides corresponding to hepatitis G virus (HGV/GBV-C) E2 structural protein with phospholipid vesicles, FEBS Journal, 272 (2005) 2456-2466.
[107] M.J. Sánchez-Martín, M.A. Busquets, V. Girona, I. Haro, M.A. Alsina, M. Pujol, Effect of E1(64-81) hepatitis G peptide on the in vitro interaction of HIV-1 fusion peptide with membrane models, Biochimica et Biophysica Acta - Biomembranes, 1808 (2011) 2178-2188.
[108] M.J. Sánchez-Martín, K. Hristova, M. Pujol, M.J. Gómara, I. Haro, M. Asunción Alsina, M. Antònia Busquets, Analysis of HIV-1 fusion peptide inhibition by synthetic peptides from E1 protein of GB virus C, Journal of Colloid and Interface Science, 360 (2011) 124-131.

[109] M.J. Sánchez-Martín, P. Urbán, M. Pujol, I. Haro, M.A. Alsina, M.A. Busquets, Biophysical investigations of GBV-C E1 peptides as potential inhibitors of HIV-1 fusion peptide, ChemPhysChem, 12 (2011) 2816-2822.
[110] R. Jahn, T.C. Südhof, MEMBRANE FUSION AND EXOCYTOSIS, Annual Review of Biochemistry, 68 (1999) 863-911.
[111] J.M. White, Viral and Cellular Membrane Fusion Proteins, Annual Review of Physiology, 52 (1990) 675-697.
[112] T.S. Jardetzky, R.A. Lamb, Virology: A class act, Nature, 427 (2004) 307-308.
[113] Y.G. Yu, D.S. King, Y.K. Shin, Insertion of coiled-coil peptide from influenza virus hemagglutinin into membranes, Science (New York, N. Y.), 266 (1994) 274-276.
[114] J.K. Ghosh, Y. Shai, Direct Evidence that the N-Terminal Heptad Repeat of Sendai Virus Fusion Protein Participates in Membrane Fusion, Journal of molecular biology, 292 (1999) 531-546.
[115] N.C. Santos, M. Prieto, M.A.R.B. Castanho, Interaction of the Major Epitope Region of HIV Protein gp41 with Membrane Model Systems. A Fluorescence Spectroscopy Study†, Biochemistry, 37 (1998) 8674-8682.
[116] V.D.D. Angel, F. Dupuis, J.-P. Mornon, I. Callebaut, Viral fusion peptides and identification of membrane-interacting segments, Biochemical and Biophysical Research Communications, 293 (2002) 1153-1160.
[117] J.M. White, Membrane fusion, Science, 258 (1992) 917-924.
[118] T. Suárez, W.R. Gallaher, A. Agirre, F.M. Goñi, J.L. Nieva, Membrane Interface-Interacting Sequences within the Ectodomain of the Human Immunodeficiency Virus Type 1 Envelope Glycoprotein: Putative Role during Viral Fusion, Journal of Virology, 74 (2000) 8038-8047.
[119] J.J. Skehel, D.C. Wiley, RECEPTOR BINDING AND MEMBRANE FUSION IN VIRUS ENTRY: The Influenza Hemagglutinin, Annual Review of Biochemistry, 69 (2000) 531-569.
[120] W. Weissenhorn, A. Dessen, L.J. Calder, S.C. Harrison, J.J. Skehel, D.C. Wiley, Structural basis for membrane fusion by enveloped viruses, Molecular Membrane Biology, 16 (1999) 3-9.
[121] K.A. Baker, R.E. Dutch, R.A. Lamb, T.S. Jardetzky, Structural Basis for Paramyxovirus-Mediated Membrane Fusion, Molecular Cell, 3 (1999) 309-319.
[122] F.X. Heinz, S.L. Allison, Flavivirus structure and membrane fusion, Advances in Virus Research, 59 (2003) 63-67.

[123] S.E. Delos, J.M. Gilbert, J.M. White, The Central Proline of an Internal Viral Fusion Peptide Serves Two Important Roles, Journal of Virology, 74 (2000) 1686-1693.
[124] Y. Gaudin, C. Tuffereau, P. Durrer, J. Brunner, A. Flamand, R. Ruigrok, Rabies virus-induced membrane fusion., Molecular Membrane Biology, 16 (1999) 21-31.
[125] S.L. Allison, J. Schalich, K. Stiasny, C.W. Mandl, F.X. Heinz, Mutational Evidence for an Internal Fusion Peptide in Flavivirus Envelope Protein E, Journal of Virology, 75 (2001) 4268-4275.
[126] J. Lescar, A. Roussel, M.W. Wien, J. Navaza, S.D. Fuller, G. Wengler, G. Wengler, F.A. Rey, The Fusion Glycoprotein Shell of Semliki Forest Virus: An Icosahedral Assembly Primed for Fusogenic Activation at Endosomal pH, Cell, 105 (2001) 137-148.
[127] N.M. Qureshi, D.H. Coy, R.F. Garry, L.A. Henderson, Characterization of a putative cellular receptor for HIV-1 transmembrane glycoprotein using synthetic peptides., AIDS, 4 (1990) 553-558.
[128] J.L. Nieva, A. Agirre, Are fusion peptides a good model to study viral cell fusion?, Biochimica et Biophysica Acta - Biomembranes, 1614 (2003) 104-115.
[129] A.D. Bangham, R.W. Horne, NEGATIVE STAINING OF PHOSPHOLIPIDS AND THEIR STRUCTURAL MODIFICATION BY SURFACE-ACTIVE AGENTS AS OBSERVED IN THE ELECTRON MICROSCOPE., Journal of molecular biology, 8 (1964) 660-668.
[130] G. Cevc, M. Derek, In Phospholipid Bilayers: Physical Principles and Models. Ed: New York, (1987) 2-28.
[131] R. Verger, F. Pattus, Lipid-protein interactions in monolayers, Chemistry and Physics of Lipids, 30 (1982) 189-227.
[132] R. Maget-Dana, The monolayer technique: A potent tool for studying the interfacial properties of antimicrobial and membrane-lytic peptides and their interactions with lipid membranes, Biochimica et Biophysica Acta - Biomembranes, 1462 (1999) 109-140.
[133] D. Lukovic, A. Cruz, A. Gonzalez-Horta, A. Almlen, T. Curstedt, I. Mingarro, J. Pérez-Gil, Interfacial behavior of recombinant forms of human pulmonary surfactant protein SP-C, Langmuir, 28 (2012) 7811-7825.
[134] N.A. Williams, N.D. Weiner, Interactions of small polypeptides with dimyristoylphosphatidylcholine monolayers: Effect of size and hydrophobicity, International Journal of Pharmaceutics, 50 (1989) 261-266.
[135] I. Langmuir, The constitution and fundamental properties of solids and liquids. II. Liquids, Journal of the American Chemical Society, 39 (1917) 1848-1906.

[136] G.L. Gaines, Insoluble Monolayers at Liquid-Gas Interface Wiley-Interscience, New York, (1966) 286.
[137] M.M. Lipp, K.Y.C. Lee, J.A. Zasadzinski, A.J. Waring, Phase and morphology changes in lipid monolayers induced by SP-B protein and its amino-terminal peptide, Science, 273 (1996) 1196-1199.
[138] C. McFate, D. Ward, J. Olmsted Iii, Organized collapse of fatty acid monolayers, Langmuir, 9 (1993) 1036-1039.
[139] P. Cea, C. Lafuente, J.S. Urieta, M.C. López, F.M. Royo, Langmuir and Langmuir-Blodgett films of a phosphorus derivative, Langmuir, 12 (1996) 5881-5887.
[140] L. Dei, A. Casnati, P. Lo Nostro, P. Baglioni, Selective complexation by p-tert-butylcalix[6]arene in monolayers at the water-air interface, Langmuir, 11 (1995) 1268-1272.
[141] J.M. Smit, B.L. Waarts, R. Bittman, J. Wilschut, Liposomes as Target Membranes in the Study of Virus Receptor Interaction and Membrane Fusion, in, vol. 372, 2003, pp. 374-392.
[142] Y. Cajal, J.M. Boggs, M.K. Jain, Salt-triggered intermembrane exchange of phospholipids and hemifusion by myelin basic protein, Biochemistry, 36 (1997) 2566-2576.
[143] O. Korazim, K. Sackett, Y. Shai, Functional and Structural Characterization of HIV-1 gp41 Ectodomain Regions in Phospholipid Membranes Suggests that the Fusion-active Conformation Is Extended, Journal of molecular biology, 364 (2006) 1103-1117.
[144] R.B. Merrifield, Solid phase peptide synthesis. I. The synthesis of a tetrapeptide, Journal of the American Chemical Society, 85 (1963) 2149-2154.
[145] E. Bayer, Towards the Chemical Synthesis of Proteins, Angewandte Chemie International Edition in English, 30 (1991) 113-129.
[146] W. Rapp, PEG Grafted Polystyrene Tentacle Polymers: Physico-Chemical Properties and Application in Chemical Synthesis, in: Combinatorial Peptide and Nonpeptide Libraries, Wiley-VCH Verlag GmbH, 2007, pp. 425-464.
[147] F. Garcia-Martín, M. Quintanar-Audelo, Y. Garcia-Ramos, L.J. Cruz, C. Gravel, R. Furic, S. Cote, J. Tulla-Puche, F. Albericio, ChemMatrix, a poly(ethylene glycol)-based support for the solid-phase synthesis of complex peptides, Journal of Combinatorial Chemistry, 8 (2006) 213-220.
[148] J.C. Sheehan, G.P. Hess, A new method of forming peptide bonds [6], Journal of the American Chemical Society, 77 (1955) 1067-1068.
[149] R.B. Merrifield, Solid-phase peptide synthesis. III. An improved synthesis of bradykinin, Biochemistry, 3 (1964) 1385-1390.

[150] D. Sarantakis, J. Teichman, E.L. Lien, R.L. Fenichel, A novel cyclic undecapeptide, WY-40,770, with prolonged growth hormone release inhibiting activity, Biochemical and Biophysical Research Communications, 73 (1976) 336-342.
[151] W. Konig, R. Geiger, A new method for the synthesis of peptides: activation of the carboxy group with dicyclohexylcarbodiimide and 3-hydroxy-4-oxo-3,4-dihydro-1,2,3-benzotriazine, Eine neue Methode zur Synthese von Peptiden: Aktivierung der Carboxylgruppe mit Dicyclohexylcarbodiimid und 3-Hydroxy-4-oxo-3.4-dihydro-1.2.3-benzotriazin., 103 (1970) 2034-2040.
[152] B. Castro, J.R. Dormoy, G. Evin, C. Selve, Reactifs de couplage peptidique I (1) - l'hexafluorophosphate de benzotriazolyl N-oxytrisdimethylamino phosphonium (B.O.P.), Tetrahedron Letters, 16 (1975) 1219-1222.
[153] J. Martinez, J.P. Bali, M. Rodriguez, B. Castro, R. Magous, J. Laur, M.F. Lignon, Synthesis and biological activities of some pseudo-peptide analogues of tetragastrin: The importance of the peptide backbone, Journal of Medicinal Chemistry, 28 (1985) 1874-1879.
[154] J. Coste, D. Le-Nguyen, B. Castro, PyBOP®: a new peptide coupling reagent devoid of toxic by-product, Tetrahedron Letters, 31 (1990) 205-208.
[155] L.P. Miranda, P.F. Alewood, Accelerated chemical synthesis of peptides and small proteins, Proceedings of the National Academy of Sciences of the United States of America, 96 (1999) 1181-1186.
[156] F. Albericio, M. Cases, J. Alsina, S.A. Triolo, L.A. Carpino, S.A. Kates, On the use of PyAOP, a phosphonium salt derived from HOAt, in solid-phase peptide synthesis, Tetrahedron Letters, 38 (1997) 4853-4856.
[157] F. Albericio, J.M. Bofill, A. El-Faham, S.A. Kates, Use of onium salt-based coupling reagents in peptide synthesis, Journal of Organic Chemistry, 63 (1998) 9678-9683.
[158] E. Kaiser, R.L. Colescott, C.D. Bossinger, P.I. Cook, Color test for detection of free terminal amino groups in the solid-phase synthesis of peptides, Analytical Biochemistry, 34 (1970) 595-598.
[159] T. Christensen, Qualitative Test for Monitoring Coupling Completeness in Solid-Phase Peptide-Synthesis Using Chloranil, Acta Chemica Scandinavica Series B-Organic Chemistry and Biochemistry, 33 (1979) 763-766.
[160] W.S. Hancock, J.E. Battersby, A new micro test for the detection of incomplete coupling reactions in solid phase peptide synthesis using 2,4,6 trinitrobenzene sulphonic acid, Analytical Biochemistry, 71 (1976) 260-264.
[161] G.L. Ellman, Tissue sulfhydryl groups, Archives of Biochemistry and Biophysics, 82 (1959) 70-77.

[162] C.W.F. McClare, An accurate and convenient organic phosphorus assay, Analytical Biochemistry, 39 (1971) 527-530.
[163] E.M. Reuven, Y. Dadon, M. Viard, N. Manukovsky, R. Blumenthal, Y. Shai, HIV-1 gp41 transmembrane domain interacts with the fusion peptide: Implication in lipid mixing and inhibition of virus-cell fusion, Biochemistry, 51 (2012) 2867-2878.
[164] S.H. White, W.C. Wimley, A.S. Ladokhin, K. Hristova, Protein Folding in Membranes: Determining Energetics of Peptide–Bilayer Interactions, *Methods in Enzymology*, (1998) 62-87.
[165] C. Larios, J. Miñones Jr, I. Haro, M.A. Alsina, M.A. Busquets, J. Miñones Trillo, Study of adsorption and penetration of E2(279-298) peptide into langmuir phospholipid monolayers, Journal of Physical Chemistry B, 110 (2006) 23292-23299.
[166] A. Chávez, M. Pujol, I. Haro, M.A. Alsina, Y. Cajal, Miscibility of the Hepatocyte Membrane Lipids at the Air/Water Interface and Interaction with the Sequence (110-121) of the Capsid Protein VP3 of Hepatitis A Virus, Langmuir, 15 (1999) 1101-1107.
[167] M. Rafalski, J.D. Lear, W.F. DeGrado, Phospholipid interactions of synthetic peptides representing the N-terminus of HIV gp41, Biochemistry, 29 (1990) 7917-7922.
[168] A. Cruz, L.A. Worthman, A.G. Serrano, C. Casals, K.M.W. Keough, J. Pérez-Gil, Microstructure and dynamic surface properties of surfactant protein SP-B/dipalmitoylphosphatidylcholine interfacial films spread from lipid-protein bilayers, European Biophysics Journal, 29 (2000) 204-213.
[169] L. Wang, A. Cruz, C.R. Flach, J. Pérez-Gil, R. Mendelsohn, Langmuir-blodgett films formed by continuously varying surface pressure. Characterization by IR spectroscopy and epifluorescence microscopy, Langmuir, 23 (2007) 4950-4958.
[170] N.J. Greenfield, Methods to estimate the conformation of proteins and polypeptides from circular dichroism data, Analytical Biochemistry, 235 (1996) 1-10.
[171] Y.H. Chen, J.T. Yang, K.H. Chau, Determination of the helix and β form of proteins in aqueous solution by circular dichroism, Biochemistry, 13 (1974) 3350-3359.
[172] N.J. Greenfield, Using circular dichroism collected as a function of temperature to determine the thermodynamics of protein unfolding and binding interactions, Nature Protocols, 1 (2006) 2527-2535.
[173] Z. Oren, Y. Shai, Selective lysis of bacteria but not mammalian cells by diastereomers of melittin: Structure-function study, Biochemistry, 36 (1997) 1826-1835.

[174] M. Tejuca, G. Anderluh, P. Maček, R. Marcet, D. Torres, J. Sarracent, C. Alvarez, M.E. Lanio, M. Dalla Serra, G. Menestrina, Antiparasite activity of sea-anemone cytolysins on Giardia duodenalis and specific targeting with anti-Giardia antibodies, International Journal for Parasitology, 29 (1999) 489-498.
[175] P.W. Mobley, C.C. Curtain, a. Kirkpatrick, M. Rostamkhani, A.J. Waring, L.M. Gordon, The amino-terminal peptide of HIV-1 glycoprotein 41 lyses human erythrocytes and CD4+ lymphocytes, BBA - Molecular Basis of Disease, 1139 (1992) 251-256.
[176] M.J. Gómara, M. Lorizate, N. Huarte, I. Mingarro, E. Perez-Payá, J.L. Nieva, Hexapeptides that interfere with HIV-1 fusion peptide activity in liposomes block GP41-mediated membrane fusion, FEBS Letters, 580 (2006) 2561-2566.
[177] S.A. Gallo, W. Wang, S.S. Rawat, G. Jung, A.J. Waring, A.M. Cole, H. Lu, X. Yan, N.L. Daly, D.J. Craik, S. Jiang, R.I. Lehrer, R. Blumenthal, θ-defensins prevent HIV-1 Env-mediated fusion by binding gp41 and blocking 6-helix bundle formation, Journal of Biological Chemistry, 281 (2006) 18787-18792.
[178] E. Gustchina, J.M. Louis, C.A. Bewley, G.M. Clore, Synergistic Inhibition of HIV-1 Envelope-Mediated Membrane Fusion by Inhibitors Targeting the N and C-Terminal Heptad Repeats of gp41, Journal of molecular biology, 364 (2006) 283-289.
[179] S. Jiang, H. Lu, S. Liu, Q. Zhao, Y. He, A.K. Debnath, N-substituted pyrrole derivatives as novel human immunodeficiency virus type 1 entry inhibitors that interfere with the gp41 six-helix bundle formation and block virus fusion, Antimicrobial Agents and Chemotherapy, 48 (2004) 4349-4359.
[180] F. Denizot, R. Lang, Rapid colorimetric assay for cell growth and survival - Modifications to the tetrazolium dye procedure giving improved sensitivity and reliability, Journal of Immunological Methods, 89 (1986) 271-277.
[181] D.D. Richman, R.S. Kornbluth, D.A. Carson, Failure of dideoxynucleosides to inhibit human immunodeficiency virus replication in cultured human macrophages, Journal of Experimental Medicine, 166 (1987) 1144-1149.
[182] A.J. Japour, D.L. Mayers, V.A. Johnson, D.R. Kuritzkes, L.A. Beckett, J.M. Arduino, J. Lane, R.J. Black, P.S. Reichelderfer, R.T. D'Aquila, C.S. Crumpacker, L. Abrams, F. McCutchan, D. Burke, L. Gardner, C. Roberts, R. Chung, C. Hicks, E. Shellie, Standardized peripheral blood mononuclear cell culture assay for determination of drug susceptibilities of clinical human immunodeficiency virus type 1 isolates, Antimicrobial Agents and Chemotherapy, 37 (1993) 1095-1101.
[183] V.D.D. Angel, F. Dupuis, J.P. Mornon, I. Callebaut, Viral fusion peptides and identification of membrane-interacting segments, Biochemical and Biophysical Research Communications, 293 (2002) 1153-1160.

[184] L. Cai, M. Gochin, K. Liu, Biochemistry and Biophysics of HIV-1 gp41 – Membrane Interactions and Implications for HIV-1 Envelope Protein Mediated Viral-Cell Fusion and Fusion Inhibitor Design, Current Topics in Medicinal Chemistry, 11 (2011) 2959-2984.
[185] T. Cserhati, M. Szogyi, Interaction of phospholipids with proteins and peptides. New advances III, International Journal of Biochemistry, 25 (1993) 123-146.
[186] J.H. Hwang, Q. Jin, E.-R. Woo, D.G. Lee, Antifungal property of hibicuslide C and its membrane-active mechanism in Candida albicans, Biochimie, 95 (2013) 1917-1922.
[187] J.J. Cheetham, S. Hilfiker, F. Benfenati, T. Weber, P. Greengard, A.J. Czernik, Identification of synapsin I peptides that insert into lipid membranes, Biochemical Journal, 354 (2001) 57-66.
[188] W.C. Wimley, S.H. White, Designing transmembrane α-helices that insert spontaneously, Biochemistry, 39 (2000) 4432-4442.
[189] B. Christiaens, S. Symoens, S. Vanderheyden, Y. Engelborghs, A. Joliot, A. Prochiantz, J. Vandekerckhove, M. Rosseneu, B. Vanloo, Tryptophan fluorescence study of the interaction of penetratin peptides with model membranes, European Journal of Biochemistry, 269 (2002) 2918-2926.
[190] M.K. Callahan, P.M. Popernack, S. Tsutsui, L. Truong, R.A. Schlegel, A.J. Henderson, Phosphatidylserine on HIV Envelope Is a Cofactor for Infection of Monocytic Cells, The Journal of Immunology, 170 (2003) 4840-4845.
[191] I. Haro, M.J. Gómara, R. Galatola, O. Domenech, J. Prat, V. Girona, M.A. Busquets, Study of the inhibition capacity of an 18-mer peptide domain of GBV-C virus on gp41-FP HIV-1 activity, Biochimica et Biophysica Acta - Biomembranes, 1808 (2011) 1567-1573.
[192] M.J. Sánchez-Martín, J.M. Amigo, M. Pujol, I. Haro, M.A. Alsina, M.A. Busquets, Fluorescence study of the dynamic interaction between E1(145-162) sequence of hepatitis GB virus C and liposomes, Analytical and Bioanalytical Chemistry, 394 (2009) 1003-1010.
[193] M.J. Sánchez-Martin, I. Haro, M.A. Alsina, M.A. Busquets, M. Pujol, A langmuir monolayer study of the interaction of E1(145-162) hepatitis G virus peptide with phospholipid membranes, Journal of Physical Chemistry B, 114 (2010) 448-456.
[194] F.B. Pereira, F.M. Goñi, A. Muga, J.L. Nieva, Permeabilization and fusion of uncharged lipid vesicles induced by the HIV-1 fusion peptide adopting an extended conformation: Dose and sequence effects, Biophysical Journal, 73 (1997) 1977-1986.

[195] M. Fivash, E.M. Towler, R.J. Fisher, BIAcore for macromolecular interaction, Current Opinion in Biotechnology, 9 (1998) 97-101.
[196] P. Pattnaik, Surface plasmon resonance: Applications in understanding receptor-ligand interaction, Applied Biochemistry and Biotechnology, 126 (2005) 79-92.
[197] A. Szabo, L. Stolz, R. Granzow, Surface plasmon resonance and its use in biomolecular interaction analysis (BIA), Current Opinion in Structural Biology, 5 (1995) 699-705.
[198] D.J. O'Shannessy, M. Brigham-Burke, K. Peck, Immobilization chemistries suitable for use in the BIAcore surface plasmon resonance detector, Analytical Biochemistry, 205 (1992) 132-136.
[199] J. Homola, Present and future of surface plasmon resonance biosensors, Analytical and Bioanalytical Chemistry, 377 (2003) 528-539.
[200] R.L. Rich, D.G. Myszka, Survey of the year 2004 commercial optical biosensor literature, Journal of Molecular Recognition, 18 (2005) 431-478.
[201] R.L. Rich, D.G. Myszka, Survey of the year 2003 commercial optical biosensor literature, Journal of Molecular Recognition, 18 (2005) 1-39.
[202] W. Huber, F. Mueller, Biomolecular interaction analysis in drug discovery using surface plasmon resonance technology, Current Pharmaceutical Design, 12 (2006) 3999-4021.
[203] H. Sota, Y. Hasegawa, M. Iwakura, Detection of Conformational Changes in an Immobilized Protein Using Surface Plasmon Resonance, Analytical Chemistry, 70 (1998) 2019-2024.
[204] L.M. May, D.A. Russell, The characterization of biomolecular secondary structures by surface plasmon resonance, Analyst, 127 (2002) 1589-1595.
[205] T.H. Lee, H. Mozsolits, M.I. Aguilar, Measurement of the affinity of melittin for zwitterionic and anionic membranes using immobilized lipid biosensors, Journal of Peptide Research, 58 (2001) 464-476.
[206] H. Mozsolits, M.I. Aguilar, Surface plasmon resonance spectroscopy: An emerging tool for the study of peptide-membrane interactions, Biopolymers - Peptide Science Section, 66 (2002) 3-18.
[207] R. Koenker, In: *Quantile Regression*. New York: Cambridge University Press, (2005).
[208] XV International Symposium on Luminescence Spectrometry – Biophysical and Analytical Aspects, Extended Abstracts, 19-22 June 2012, Barcelona,Spain - (ISLS 2012), Luminescence, 27 (2012) 534-572.
[209] P. Bougis, H. Rochat, G. Piéroni, R. Verger, Penetration of phospholipid monolayers by cardiotoxins, Biochemistry, 20 (1981) 4915-4920.

[210] D. Marsh, Lateral pressure in membranes, Biochimica et Biophysica Acta - Reviews on Biomembranes, 1286 (1996) 183-223.
[211] M.A. Alsina, A. Ortiz, D. Polo, F. Comelles, F. Reig, Synthesis and study of molecular interactions between phosphatidyl choline and two laminin derived peptides hydrophobically modified, Journal of Colloid and Interface Science, 294 (2006) 385-390.
[212] R. Maget-Dana, D. Lelivre, Comparative interaction of α-helical and β-sheet amphiphilic isopeptides with phospholipid monolayers, Biopolymers, 59 (2001) 1-10.
[213] J.T. Davies, G.R.A. Mayers, The effect of interfacial films on mass transfer rates in liquid-liquid extraction, Chemical Engineering Science, 16 (1961) 55-68.
[214] F. Takeda, M. Matsumoto, T. Takenaka, Y. Fujiyoshi, N. Uyeda, Surface pressure dependence of monolayer structure of poly-ε{lunate}-benzyloxycarbonyl-l-lysine, Journal of Colloid and Interface Science, 91 (1983) 267-271.
[215] M. Kaku, H. Hsiung, D.Y. Sogah, M. Levy, J.M. Rodríguez-Parada, Monolayers and Langmuir-Blodgett films of poly(N-acylethylenimines), Langmuir, 8 (1992) 1239-1242.
[216] K. Hac-Wydro, J. Kapusta, A. Jagoda, P. Wydro, P. Dynarowicz-Łatka, The influence of phospholipid structure on the interactions with nystatin, a polyene antifungal antibiotic. A Langmuir monolayer study, Chemistry and Physics of Lipids, 150 (2007) 125-135.
[217] D.K. Chattoraj, K.S. Birdi, Adsortion and the Gibbs Surface Excess, Plenum Press, New York, (1984) 219-222.
[218] R.E. Pagano, N.L. Gershfeld, A millidyne film balance for measuring intermolecular energies in lipid films, Journal of Colloid and Interface Science, 41 (1972) 311-317.
[219] L. Picas, C. Suárez-Germà, M.T. Montero, O. Domènech, J. Hernández-Borrell, Miscibility behavior and nanostructure of monolayers of the main phospholipids of escherichia coli inner membrane, Langmuir, 28 (2012) 701-706.
[220] A. Cruz, J. Pérez-Gil, Langmuir films to determine lateral surface pressure on lipid segregation, in, vol. 400, 2007, pp. 439-457.
[221] K. Nag, J. Perez-Gil, A. Cruz, K.M.W. Keough, Fluorescently labeled pulmonary surfactant protein C in spread phospholipid monolayers, Biophysical Journal, 71 (1996) 246-256.
[222] K. Nag, S.G. Taneva, J. Perez-Gil, A. Cruz, K.M.W. Keough, Combinations of fluorescently labeled pulmonary surfactant proteins SP- B and SP-C in phospholipid films, Biophysical Journal, 72 (1997) 2638-2650.

[223] W.C. Wimley, K. Hristova, A.S. Ladokhin, L. Silvestro, P.H. Axelsen, S.H. White, Folding of β-sheet membrane proteins: A hydrophobic hexapeptide model, Journal of molecular biology, 277 (1998) 1091-1110.
[224] S. Liu, H. Lu, J. Niu, Y. Xu, S. Wu, S. Jiang, Different from the HIV fusion inhibitor C34, the anti-HIV drug fuzeon (T-20) inhibits HIV-1 entry by targeting multiple sites in gp41 and gp120, Journal of Biological Chemistry, 280 (2005) 11259-11273.
[225] H. Zhang, S.E. Schneider, B.L. Bray, P.E. Friedrich, N.A. Tvermoes, C.J. Mader, S.R. Whight, T.E. Niemi, P. Silinski, T. Picking, M. Warren, S.A. Wring, Process development of TRI-999, a fatty-acid-modified HIV fusion inhibitory peptide, Organic Process Research and Development, 12 (2008) 101-110.
[226] Q. Jia, X. Jiang, F. Yu, J. Qiu, X. Kang, L. Cai, L. Li, W. Shi, S. Liu, S. Jiang, K. Liu, Short cyclic peptides derived from the C-terminal sequence of α1-antitrypsin exhibit significant anti-HIV-1 activity, Bioorganic & Medicinal Chemistry Letters, 22 (2012) 2393-2395.
[227] T. Okada, B.K. Patterson, S.-Q. Ye, M.E. Gurney, Aurothiolates Inhibit HIV-1 Infectivity by Gold(I) Ligand Exchange with a Component of the Virion Surface, Virology, 192 (1993) 631-642.
[228] F.M. Veronese, G. Pasut, PEGylation, successful approach to drug delivery, Drug Discovery Today, 10 (2005) 1451-1458.
[229] W. Huang, S. Groothuys, A. Heredia, B.H.M. Kuijpers, F.P.J.T. Rutjes, F.L. van Delft, L.-X. Wang, Enzymatic Glycosylation of Triazole-Linked GlcNAc/Glc–Peptides: Synthesis, Stability and Anti-HIV Activity of Triazole-Linked HIV-1 gp41 Glycopeptide C34 Analogues, ChemBioChem, 10 (2009) 1234-1242.
[230] C.A. Stoddart, G. Nault, S.A. Galkina, K. Thibaudeau, P. Bakis, N. Bousquet-Gagnon, M. Robitaille, M. Bellomo, V. Paradis, P. Liscourt, A. Lobach, M.-È. Rivard, R.G. Ptak, M.K. Mankowski, D. Bridon, O. Quraishi, Albumin-conjugated C34 Peptide HIV-1 Fusion Inhibitor: EQUIPOTENT TO C34 AND T-20 IN VITRO WITH SUSTAINED ACTIVITY IN SCID-HU THY/LIV MICE, Journal of Biological Chemistry, 283 (2008) 34045-34052.
[231] Y. Wexler-Cohen, A. Ashkenazi, M. Viard, R. Blumenthal, Y. Shai, Virus-cell and cell-cell fusion mediated by the HIV-1 envelope glycoprotein is inhibited by short gp41 N-terminal membrane-anchored peptides lacking the critical pocket domain, FASEB Journal, 24 (2010) 4196-4202.
[232] A. Gori, R. Longhi, C. Peri, G. Colombo, Peptides for immunological purposes: Design, strategies and applications, Amino Acids, 45 (2013) 257-268.

[233] Y. Wexler-Cohen, Y. Shai, Demonstrating the C-terminal boundary of the HIV 1 fusion conformation in a dynamic ongoing fusion process and implication for fusion inhibition, FASEB Journal, 21 (2007) 3677-3684.
[234] R. Consden, A.H. Gordon, Gramicidin S; the sequence of the amino-acid residues, The Biochemical journal, 41 (1947) 596-602.
[235] R.M. Kohli, C.T. Walsh, M.D. Burkart, Biomimetic synthesis and optimization of cyclic peptide antibiotics, Nature, 418 (2002) 658-661.
[236] J. Alsina, F. Rabanal, E. Giralt, F. Albericio, Solid-phase synthesis of 'head-to-tail' cyclic peptides via lysine side-chain anchoring, Tetrahedron Letters, 35 (1994) 9633-9636.
[237] F. Albericio, Developments in peptide and amide synthesis, Current Opinion in Chemical Biology, 8 (2004) 211-221.
[238] P. Li, P.P. Roller, J. Xu, Current synthetic approaches to peptide and peptidomimetic cyclization, Current Organic Chemistry, 6 (2002) 411-440.
[239] K. Hristova, C.E. Dempsey, S.H. White, Structure, location, and lipid perturbations of melittin at the membrane interface, Biophysical Journal, 80 (2001) 801-811.
[240] A.S. Ladokhin, S.H. White, 'Detergent-like' permeabilization of anionic lipid vesicles by melittin, Biochimica et Biophysica Acta - Biomembranes, 1514 (2001) 253-260.
[241] M. Wu, S.-Q. Nie, Y. Qiu, K.-C. Lin, S.-X. Wang, S.-F. Sui, Study of the relationship between structure and function of HIV-1 gp 41 N terminus fusion peptide, in: X.-Y. Hu, R. Wang, J. Tam (Eds.) Peptides Biology and Chemistry, Springer Netherlands, 2002, pp. 104-107.

TRABAJOS RELACIONADOS

6054 J. Med. Chem. 2010, 53, 6054–6063
DOI: 10.1021/jm100452c

Journal of Medicinal Chemistry Article

Effect of Synthetic Peptides Belonging to E2 Envelope Protein of GB Virus C on Human Immunodeficiency Virus Type 1 Infection

Elena Herrera,[†] Solveig Tenckhoff,[‡] María J. Gómara,[†] Ramona Galatola,[†] María J. Bleda,[†] Cristina Gil,[∥] Guadalupe Ercilla,[⊥] José M. Gatell,[∥,⊥] Hans L. Tillmann,[‡,§] and Isabel Haro*,[†]

[†]*Unit of Synthesis and Biomedical Applications of Peptides (IQAC-CSIC), Barcelona, Spain,* [‡]*Faculty of Medicine, University of Leipzig, Leipzig, Germany,* [§]*GI/Hepatology Research Program, Division of Gastroenterology, Duke Clinical Research Institute, Duke University, Durham, North Carolina,* [∥]*AIDS-Research Group, IDIBAPS, Barcelona, Spain, and* [⊥]*Services of Infectious Diseases and Immunology, Hospital Clinic Barcelona, University of Barcelona, Spain*

Received April 13, 2010

The use of synthetic peptides as HIV-1 inhibitors has been subject to research over recent years. Although the initial therapeutic attempts focused on HIV-coded enzymes, structural HIV proteins and, more specifically, the mechanisms that the virus uses to infect and replicate are now also considered therapeutic targets. The interest for viral fusion and entry inhibitors is growing significantly, given that they are applicable in combined therapies or when resistance to other antiretroviral drugs is seen and that they act before the virus enters the cell. The 124 synthetic sequences of the GBV-C E2 envelope protein have been obtained by SPPS. The interaction of certain GBV-C peptide sequences with the HIV-1 fusion peptide has been proven through the use of biophysical techniques. We also show how GBV-C E2 domains notably decrease cellular membrane fusion and interfere with the HIV-1 infectivity in a dose-dependent manner, highlighting their potential utility in future anti-HIV-1 therapies.

Introduction

When a supposedly new hepatitis virus, the GB virus C (GBV-C[a]), also known as the hepatitis G virus (HGV),[1,2] was discovered in the mid-1990s, many research groups sought to correlate it to hepatic inflammation or other associated diseases. However, no impact on health[3,4] could be identified until the research group of Prof. Tillmann demonstrated GBV-C viraemia to be associated with significant survival benefit in HIV-infected patients.[5] These results were subsequently confirmed by this and other research groups.[6,7] Although the results were sometimes not clearly significant,[8] a meta-analysis underlined GBV-C's association with a more beneficial course of disease.[9,10]

Several mechanisms seem to be involved in the beneficial effect: down-regulation of HIV co-receptors (C−C chemokine receptor type 5 (CCR5) and CXC chemokine receptor 4 (CXCR4)), the induction of natural ligands for these chemokine receptors (regulated on activation normal T expressed and secreted (RANTES), macrophage inflammatory protein 1 α and β (MIP-1α and MIP-1β), stromal derived factor 1 (SDF-1),[11,12] and decrease of Fas-induced lymphocyte apoptosis, the expression of which is higher in HIV-infected patients.[13]

Recently it has been shown that two GBV-C proteins inhibit HIV replication in vitro.[14,15] Thus, there is evidence for a casual relation of GBV-C and a more prolonged survival rate in patients co-infected with GBV-C and HIV.

It was further demonstrated that some effects can be achieved by two different GBV-C proteins: the envelope glycoprotein E2 inhibits R5 and X4-tropism HIV isolates by decreasing the surface expression of CCR5 co-receptors and inducing RANTES, one of the three known ligands for CCR5. The mechanism by which E2 inhibits the X4 virus has not been fully classified, although results point to the fact that the E2 protein of the GBV-C inhibits stages prior to replication, such as the binding or fusion of membranes. The second protein proposed by Prof. Stapleton's group is the nonstructural GBV-C NS5A. The NS5A protein decreases the surface expression of CXCR4 and increases the release of SDF-1, the CXCR4 ligand, in cell culture supernatants.[16] Furthermore, this group classified the peptide requirements of the GBV-C NS5A protein involved in HIV inhibition through mutagenesis and proved that synthetic peptides are capable of reproducing the effects of NS5A peptides expressed intracellularly, suggesting the use of these synthetic peptide sequences from a therapeutic stance.[17]

Though peptides have the disadvantage of requiring parenteral application, effective peptides are better than no further treatment option, as in the setting of resistance to several oral agents. HIV-1-inhibiting peptides have been identified and/or developed using different methods. Some therapeutic peptides such as enfuvirtide, already approved for clinical use,[18] are derived from the HIV-1, whereas others are natural peptides such as the chemokines, defensins, or the "virus inhibitory peptide" (VIRIP)[19] or have been designed and synthesized

*To whom correspondence should be addressed. Phone: +34934006109. Fax: +34932045904. E-mail: isabel.haro@iqac.csic.es.

[a] Abbreviations: FP, fusion peptide; GBV-C, GB virus C; HGV, hepatitis G virus; HIV-1, human immunodeficiency type 1; IC_{50}, half maximal inhibitory concentration; ITC, isothermal titration calorimetry; LUV, large unilamellar lipid vesicles; moi, multiplicity of infection; PBMC, peripheral blood mononuclear cell; SPPS, solid phase peptide synthesis; SPR, surface plasmon resonance; $TCID_{50}$, 50% tissue culture infective dose; VIRIP, virus inhibitory peptide.

 Published on Web 07/22/2010

E2 (U45966_USA)

APASVLGSRPFDYGLTWQSCSCRANGSRYTTGEKVWDRGNVTLLCDCPNGPWV
WLPAFCQAIGWGDPITHWSHGQNRWPLSCPQYVYGSVSVTCVWGSVSWFASTG
GRDSKIDVWSLVPVGSASCTIAALGSSDRDTVVELSEWGVPCATCILDRRPASCG
TCVRDCWPETGSVRFPFHRCGAGPKLTKDLEAVPFVNRTTPFTIRGPLGNQGRGN
PVRSPLGFGSYAMTKIRDSLHLVKCPTPAIEPPTGTFGFFPGVPPLNNCLLLGTEVS
EALGGAGLTGGFYEPLVRRRSELMGRRNPVCPGFAWLSSGRPDGFIHVQGHLQE
VDAGNFIPPPRWLLLDFVFVLLYLMKLAEARLVPLILLLLWWWVNQLAVLGLPA
VDAAVA

Figure 1. Primary sequence of E2 GBV-C protein.

from crystallographic data on HIV-1 proteins or from peptide libraries.[20] Furthermore, understanding the mechanism of how GBV-C E2 protein inhibits HIV might open other avenues of treatment for this devastating disease.

At present, the interest for viral fusion and entry inhibitors is growing significantly,[21] given that they are applicable in combined therapies or when resistance to other antiretroviral drugs is seen and that they act before the virus enters the cell, which could have the same potential as the inducing of immunity provided by a vaccine. In our group, synthetic sequences of the GBV-C E2 envelope protein have been obtained by solid-phase peptide synthesis (SPPS). The interaction of certain GBV-C peptide sequences with the HIV-1 fusion peptide has been proven through the use of biophysical techniques such as circular dichroism, Fourier transform infrared spectroscopy, isothermal titration calorimetry, and ^{1}H nuclear magnetic resonance.[22]

In the present article we show how certain E2 domains interfere with the HIV-1 fusion peptide−vesicle interaction and notably decrease cellular membrane fusion and interfere with the HIV-1 infectivity in a dose-dependent manner, highlighting a potential utility of some peptides in future anti-HIV-1 therapies.

Results

Biophysical Characterization of GBV-C Peptides/FP gp41 HIV-1 Interaction. In order to study the possible interaction of the envelope protein E2 with the fusion peptide (FP) of glycoprotein gp41 of the HIV-1 virus during the entry process of the virus into the cell, a scan of this glycoprotein was carried out by means of the synthesis of peptide sequences of 18 amino acids overlapped in 15 residues. The best preserved primary structure of the E2 protein taken from the Genbank database is shown in Figure 1, and multiple syntheses were carried out in parallel to obtain 124 peptides corresponding to this protein. All peptides were characterized using high performance liquid chromatography (HPLC) and HPLC−mass spectrometry (HPLC−MS) and showed purity greater than 90% (Table 1 in Supporting Information).

These peptides were evaluated in regard to their capacity to inhibit the destabilization process of lipid vesicles induced by the HIV-1 FP. As shown in Figure 2, the peptides P45−P46, P59, and P97 inhibit the leakage induced by the HIV-1 FP at a relationship of $^{1}/_{10}$ (FP/E2 peptide) in an extent higher than 50%, with P11, P40−41, P80−82, P88−P91, P96, P105−P109, and P124 peptide regions also being capable of inhibiting the activity of the HIV-1 FP

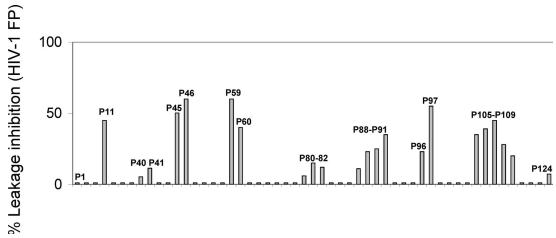

Figure 2. Inhibitory effect of the E2 GBV-C overlapped peptides on the HIV-1 FP induced leakage assay.

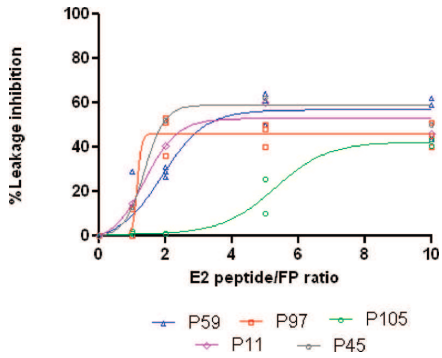

Figure 3. Inhibitory effect on HIV-1 FP induced leakage of P59, P97, P105, P11, and P45 E2 peptides. The extent of leakage inhibition was plotted as a function of the P*x*/HIV-1 FP molar ratio.

Table 1. Area under the Curve and Coordinates of the Peak for the Inhibitory Effect on HIV-1 FP Induced Leakage of P11, P45, P59, P97, and P105 E2 Peptides

	P11	P45	P59	P97	P105
area under the curve	449.8	491.7	438.0	394.7	180.6
	% Inhibition for E2 Peptide/FP Ratio of 5				
Y = % inhibition	52.9	59.0	56.3	46.0	17.9

although to a lower extent. The intrinsic lytic effect of the GBV-C peptides alone was null or negligible.

To confirm the anti-HIV-1 FP activity observed and thus to exclude the possibility that a contaminating agent might be responsible for the observed effects of E2 peptides, we next resynthesized manually and purified by preparative HPLC the selected peptides. Further experiments confirmed the inhibitory capacity of the selected E2 18-mer peptides.

Several ratios of the HIV-1 FP and the P11, P45, P59, P97, and P105 (1:1, 1:2, 1:5, and 1:10) were tested in leakage assays. As shown in Figure 3, these peptides inhibit the permeabilization vesicular process induced by the HIV-1 FP, the percentage of inhibition for a E2 peptide/HIV-1 FP ratio being higher for P45 (Table 1). The plateau observed during the leakage assay was in all cases lower than 65%. Despite an increase of the E2 peptides/HIV-1 FP ratio, the total inhibition of the permeabilization process induced by HIV-1 FP was not observed.

In order to test the specificity of the interaction between the E2 peptides and HIV-1 FP, we used melittin as a control peptide. Melittin induced 8-aminonaphthalene-1,3,6-trisulfonic acid, disodium salt (ANTS), and *p*-xylenebispiridinium bromide (DPX) leakage from palmitoyloleoylphosphatidylglycerol (POPG) large unilamellar lipid vesicles (LUVs) at

peptide-to-lipid mole ratios higher than $^1/_{50}$. The 50% of POPG vesicular content leakage induced by melittin was established at a peptide-to-lipid mole ratio of $^1/_{10}$. When the assay was performed in the same conditions as using the HIV-1 FP, a relationship of $^1/_{10}$ of melittin/E2 peptides was premixed in dimethyl sulfoxide (DMSO) and tested in the leakage assay (data not shown). The results showed that E2 peptides were unable to inhibit the membrane lytic activity of melittin, thus indicating the specificity of the interaction between GBV-C E2 peptides and the HIV-1 FP.

The interactions of E2 peptides with HIV-1 FP were examined by measuring their partitioning in POPG liposomes. As shown in Figure 4A, relative to fluorescence in buffer, the maximum wavelength of Trp emission (λ_{max}) of HIV-1 FP shifted dramatically toward the blue in the presence of 75 μM POPG LUV. Specifically λ_{max} decreased by more than 20 nm consistent with the movement of HIV-1 FP into a nonpolar environment of vesicles bilayers. The

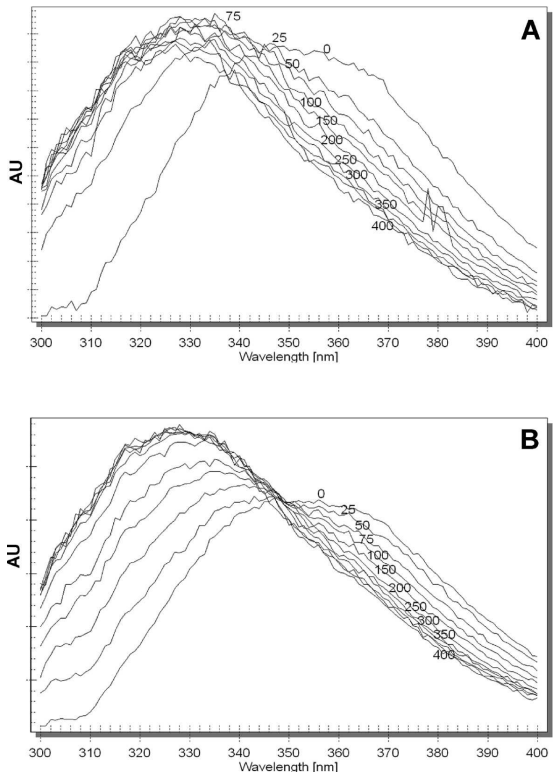

Figure 4. Fluorescence emission spectra of (A) FP and (B) equimolar mixture of FP and p97 upon titration with POPG LUVs. FP concentration is 2 μM.

incubation of E2 peptides with HIV-1 FP in an equimolar ratio prior to the POPG titration notoriously avoids the shift of the Trp emission fluorescence, thus indicating an interaction of E2 peptides with HIV-1 FP that prevents the movement of the Trp residue to an environment of lower polarity provided by the vesicles. As an example, in Figure 4B we show the fluorescence emission spectra of an equimolar mixture of HIV-1 FP and P97.

Fluorescence titration was used to measure HIV-1 partitioning quantitatively by measuring fluorescence intensity at the λ_{max} (327 nm). The partitioning isotherms (Figure 1 in Supporting Information) show that HIV-1 FP partitioned strongly into POPG vesicles ($K_x = (9.7 \pm 1.7) \times 10^5$). The mole fraction partition coefficients ranged from $(1.7 \pm 0.4) \times 10^5$ for HIV-1 FP/P59 to $(7.5 \pm 0.8) \times 10^5$ for HIV-1 FP/P105, with P59 and P97 thus being the GBV-C E2 peptides that more efficiently prevented the HIV-1 FP binding to the POPG vesicles and with P105 being the less active peptide in this assay.

To quantify the interaction of E2 peptides with the HIV-1 FP, we performed surface plasmon resonance (SPR) and isothermal titration calorimetry (ITC) studies. We used a Biacore T-100 SPR biosensor to screen the direct interactions of E2 peptides to HIV-1 FP. The kinetic binding parameters and equilibrium constants for the peptides are given in Table 2. Results obtained using immobilized HIV-1 FP and the selected E2 synthetic peptides as analytes showed a clear interaction between P11, P45, P97, and P105 and the HIV-1 FP, the K_D values being between 2.24×10^{-6} and 5.86×10^{-5} M. Of note is that the dissociation constant of P97 was 1 order of magnitude lower. Between 30- and 100-fold faster associations were observed for P97 compared to P11, P45, and P105. Figure 5 shows as an example the adjusted sensorgram for the P105 peptide.

The values for the binding affinities to HIV-1 FP were validated by ITC. Figure 6 shows ITC results where HIV-1 FP was titrated with P11. The ITC experiments yielded K_D values of 3.3×10^{-5}, 6.3×10^{-5}, 3.9×10^{-6}, and 2.0×10^{-5} M for P11, P45, P97, and P105, respectively, in excellent agreement with the values determined by SPR. The very low interaction observed for P59 could not be fitted into any of the defined binding models. Then, it was quantified neither by ITC nor by SPR.

Anti-HIV-1 Activities of E2 GBV-C Peptides. The antiviral activity of E2 GBV-C synthetic peptides was analyzed by means of three complementary assays. We first examined the effect of E2 peptides on cell−cell fusion assays, analyzing their capacity to block syncytium formation between HeLa cells expressing the envelope protein of HIV-1 and TZM-bl cells expressing the human CD4 receptor CXCR4 or CCR5 HIV-1 co-receptors in the presence of various amounts of each peptide.

The half maximal inhibitory concentration (IC_{50}) as a measure of the effectiveness of each E2 peptide in inhibiting

Table 2. Kinetics Parameters of the Interaction between the E2 GBV-C Peptides and HIV-1 FP Determined Using ITC and SPR

	ITC		SPR		
peptide	K_A (M^{-1})	K_D (M)	K_a (M^{-1} s^{-1})	K_d (s^{-1})	K_D (M)
P11	$(3.00 \pm 0.58) \times 10^4$	3.33×10^{-5}	$(0.23 \pm 0.005) \times 10^3$	$(5.8 \pm 0.13) \times 10^{-3}$	2.52×10^{-5}
P45	$(1.57 \pm 1.05) \times 10^4$	6.36×10^{-5}	$(0.13 \pm 0.005) \times 10^3$	$(7.74 \pm 0.34) \times 10^{-3}$	5.86×10^{-5}
P59	ND	ND	ND	ND	ND
P97	$(2.52 \pm 1.16) \times 10^5$	3.96×10^{-6}	$(1.28 \pm 0.004) \times 10^4$	$(2.86 \pm 0.23) \times 10^{-3}$	2.24×10^{-6}
P105	$(5.00 \pm 0.73) \times 10^4$	2.00×10^{-5}	$(0.41 \pm 0.008) \times 10^3$	$(7.17 \pm 0.14) \times 10^{-3}$	1.76×10^{-5}

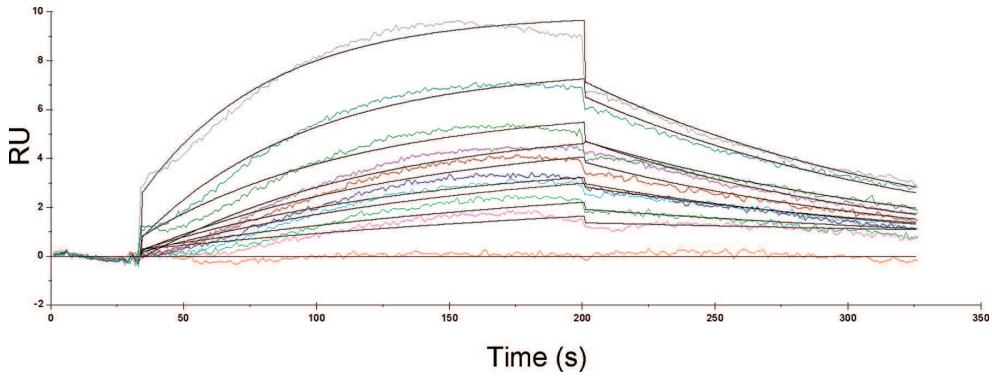

Figure 5. Sensorgrams for the direct binding of P105 to immobilized HIV-1 FP. P105 concentrations ranged from 0 to 100 μM. Black lines are fits to a 1:1 Langmuir binding model.

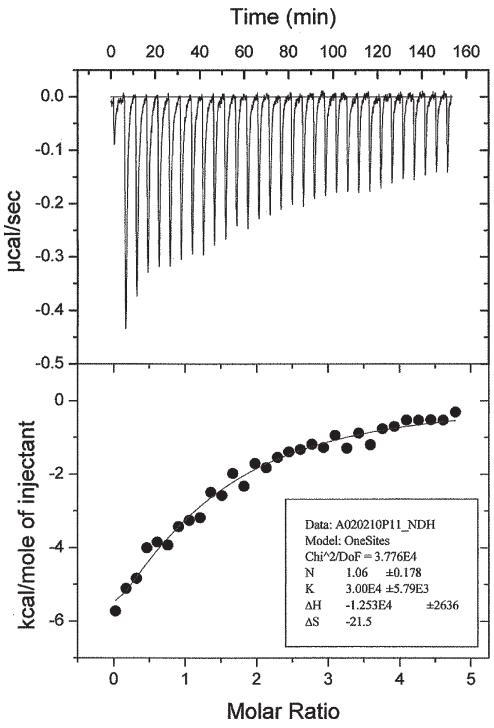

Figure 6. Calorimetric titration of HIV-1 FP with the P11 GBV-C peptide at 25 °C.

syncytium formation is shown in Table 3. The following 18-mer peptides P11, P19−21, P23, P25, P45−47, P59, P97, P109, and P124 inhibited the gp41-induced cell−cell fusion in a dose-dependent manner, showing IC_{50} values between 141.2 and 832.9 μM (Figure 2 in Supporting Information). The remaining peptides showed less than 50% of inhibition or had a non-sigmoidal (neither linear) shape of the dose-response curve, and they were discarded. C34 peptide was used as positive control (IC_{50} = 0.023 μM; 95% CI = 0.021−0.025). As an example, in Figures 7 and 8 we show how P45 inhibits syncytium formation in a dose-dependent manner.

The preliminary analysis performed to assess the capability of the 124 E2-peptides to inhibit the HIV-1 infection of CEM174 showed that all of them were able to inhibit the p24 antigen release at a high concentration of 500 μM, but only a subset of them produced more than 50% HIV-1 inhibition at 250 μM (P11, P19−P21, P23, P25, P34, P46, P47, P97, and P109) at day 7 postinfection (Figure 9).

These data were confirmed when the inhibitory effect of viral infection was analyzed using the TZM-bl cell line. Only the peptides P11, P19−P21, P34, P45−P47, P109, and P124 were able to inhibit the HIV-1 infection of HIV-1_{HXB2} (R4), the primary isolate HIV-$1_{69/7}$ (R5X4 dual or mixed tropism (DM)), and HIV-1_{BaL} (R5) in a dose-dependent manner (Figure 3 in Supporting Information). The inhibitory effect was differentially efficient between the X4 and the R5 strains. The IC_{50} obtained with peptides P11, P19, P20, and P21 for HIV-1_{HXB2} was as follows: < HIV-$1_{69/7}$ < HIV-1_{BaL}; nevertheless, the IC_{50} obtained with peptides P34, P45, P46, P47, and P109 for HIV-$1_{69/7}$ was < HIV-1_{HXB2} < HIV-1_{BaL}. In Figure 10 we show as an example the dose-response curves obtained for P47. In general, all peptides tested showed an IC_{50} that was 1 log higher for the virus R5 than for the virus X4 or R5X4 DM (Table 4). Of note was that the P124 was only effective for the HIV-1_{BaL} strain.

With the aim of locating where the most active peptide fragments lie on the E2 protein, a computerized prediction analysis of hydrophilicity, accessibility, and presence of β-turns of the E2 protein according to Hopp and Woods,[23] Janin,[24] and Chou and Fasman[25] was performed. In general, it was observed that the selected peptide regions showed high indexes of hydrophilicity and accessibility and a large number of residues with high turn probability that tend to distribute on the surface of the protein. In Supporting Information (Figure 4) we have incorporated the profiles of the E2 protein as well as noted the selected peptide regions.

New experiments performed in TZM-bl on which the peptides were incubated with the cell for 2 h before the virus adsorption did not prevent the viral infection.

The inhibitory effect of peptides P11, P19−P21, P34, P45−P47, P109, and P124 to inhibit infection of peripheral blood mononuclear cells (PBMCs) was also observed. In this case, the qualitative analysis of p24 antigen produced in these cell cultures showed (1) that the concentrations up to which viral production was almost undetectable were lower than the IC_{50} observed in TZM-bl cell cultures, (2) that these concentrations were lower in HIV-1_{HXB2} (R4) than HIV-1_{BaL} (R5) with the exceptions of P19, P46, and P124, and (3)

Table 3. Inhibitory Activity of E2 Peptides on Gp41-Mediated Cell−Cell Fusion Assay

peptide	residue no.[a]	sequence	IC_{50}[b] (μM)	95% CI[c]
P11	31−48	TGEKVWDRGNVTLLCDCP	439.7	361.4−535.0
P19	55−72	LPAFCQAIGWGDPITHWS	369.5	314.8−433.7
P20	58−75	FCQAIGWGDPITHWSHGQ	347.6	305.1−396.0
P21	61−78	AIGWGDPITHWSHGQNRW	832.9	754.5−919.4
P23	67−84	PITHWSHGQNRWPLSCPQ	508.8	496.9−520.9
P25	73−90	HGQNRWPLSCPQYVYGSV	304.4	260.9−355.3
P45	133−150	SDRDTVVELSEWGVPCAT	141.2	129.1−154.4
P46	136−153	DTVVELSEWGVPCATCIL	428.8	373.1−429.7
P47	139−156	VELSEWGVPCATCILDRR	330.8	277.4−394.5
P59	175−192	RFPFHRCGAGPKLTKDLE	529.6	514.0−545.8
P97	289−306	LVRRRSELMGRRNPVCPG	537.6	476.9−606.0
P109	325−342	LQEVDAGNFIPPPRWLLL	687.1	616.3−766.1
P124	370−387	WVNQLAVLGLPAVDAAVA	332.7	265.4−417.1

[a] The residue number of each region corresponds to its position in E2 (U45966_usa) of GBV-C. [b] IC_{50}: concentration of a peptide causing 50% inhibition of cell−cell fusion (μM). [c] 95% CI: 95% confidence interval of IC_{50}.

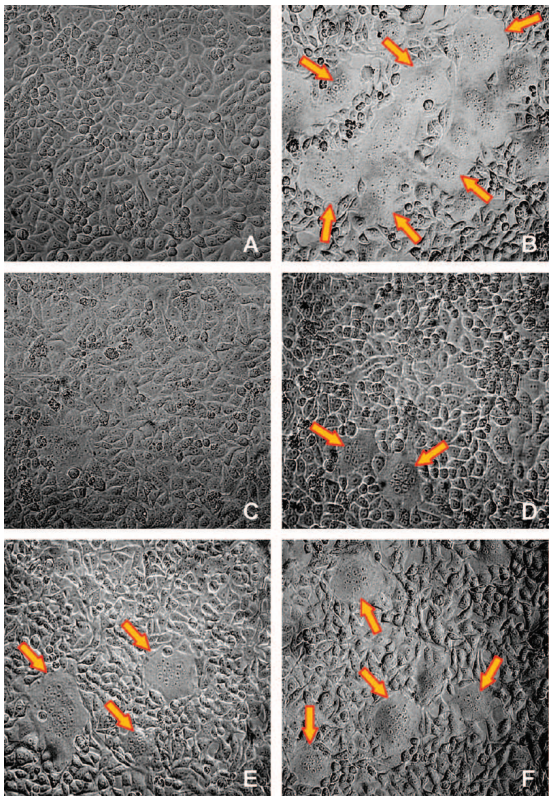

Figure 7. Inhibition of gp41-induced cell−cell fusion by incubation with P45 peptide. The arrow indicates syncytia (large cell-like structure filled with cytoplasm containing many nuclei) formation. Cells grown in 96-well plates were treated with C34 (1,2 μM) in (A) or with P45 peptide: (C) 500 μM, (D) 250 μM, (E) 125 μM, and (F) 62.5 μM. (B) corresponds to untreated control.

that the sets P19−P21, P45−P47, P109 were more efficient in inhibiting the HXB2 virus than P11 and P34 and that P124 is more efficient in regard to BAL (Table 5).

Discussion

The understanding of how a nonpathogenic human virus, GBV-C, interferes with HIV related disease progression has been studied in the past years by means of epidemiological studies of HIV-infected cohorts and by in vitro approaches related to GBV-C/HIV co-infection. It has been proposed that the GBV-C E2 protein may modify HIV disease progression. In addition the GBV-C E2 protein, when added to $CD4^+$ T cells, inhibits HIV entry in a HIV-1 pseudotyped retrovirus single infection system. Moreover, polyclonal anti-E2 antibodies and murine monoclonal anti-E2 antibodies neutralized a broad panel of HIV-1 isolates in vitro.

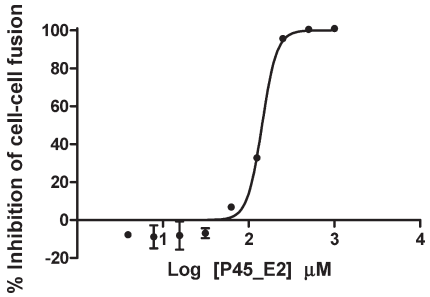

Figure 8. Inhibitory activity of P45 peptide of gp41-induced cell−cell fusion. Each data point represents the mean percent inhibition ± standard error (bars).

We here present data that peptides derived from the GBV-C E2 protein are able to reduce HIV-1 in vitro. We show that several regions of the GBV-C E2 represented by the following peptides (GBV-C $E2_{31-48}$, P11; GBV-C $E2_{55-78}$, P19−P21; GBV-C $E2_{100-118}$, P34; GBV-C $E2_{133-156}$, P45−P47; GBV-C $E2_{289-306}$, P97; GBV-C $E2_{325-342}$, P109; GBV-C $E2_{370-387}$, P124) can be implicated in the inhibition of the HIV-1 at the entry level.

The observed inhibition events were probably mediated by blocking virus entry, as observed by the biophysical assays performed in the presence of the gp41 HIV-1 fusion peptide like the inhibition of vesicular contents induced by the HIV-1 FP or the binding to POPG vesicles. As described, we could determine by calorimetric and surface plasmon resonance techniques the interaction of several domains of GBV-C E2 protein and the HIV-1 FP. According to the ITC results, the binding of both peptides is characterized by negative enthalpies, suggesting that there are a large number of favorable hydrogen bond contacts or van der Waals interactions between the E2 peptides and HIV-1 FP. On the other hand, the unfavorable entropic change could indicate that the binding

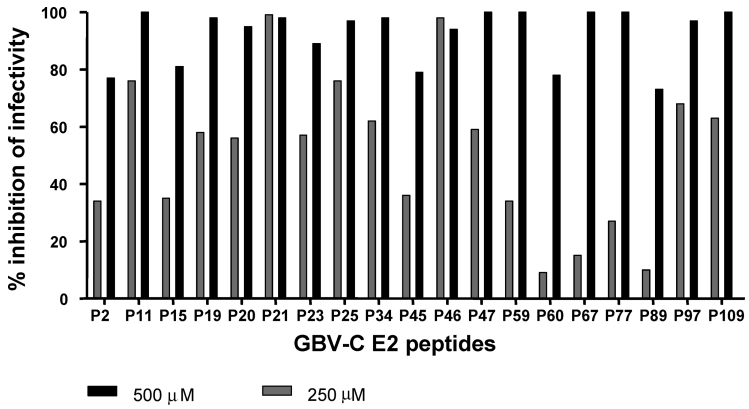

Figure 9. Inhibition of the HIV-1 infection of CEM174 by GBV-C E2 peptides.

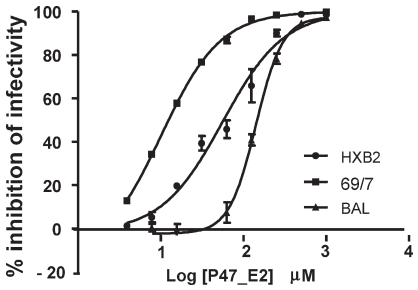

Figure 10. Susceptibilities of three different HIV-1 strains to P47 peptide in TZM-bl cells.

of E2 peptides to HIV-1 FP can be associated with structuring processes.[26]

The individual analysis of 124 overlapped GBV-C E2 peptides demonstrated that P11, P19−P21, P34, P45−P47, P109, and P124 inhibit the HIV-1 infection of X4, X4R5 DM, and/or R5 strains in a dose-dependent manner in TZM-bl cell cultures. Of note are that the potencies of E2 peptides to inhi bit the HIV-1 viral infection are modest (IC_{50} values in the micromolar range), the concentration needed to inhibit the viral infection being higher compared to another entry inhibitor,[27] and that the sensitivity of HIV-1 to these peptides was apparently modulated by the viral tropism.

In relation to the concentration of peptides required, it was highly reduced when the susceptibility assays were performed by using PBMCs. The activity enhancement observed in PBMCs vs TZM-bl cell line could be explained by the influence of the density of receptors and co-receptors and viral replication capacity in each cell type, as well as the target cell environment in which the induction of soluble factor release could hinder HIV-1 entry, as has been described elsewhere.[28−30] In any case, new studies are being conducted to analyze the effects of these particular peptides on uninfected PBMCs, and the chemical modification of peptides will be carried out to reduce the IC_{50s} observed.

In a comparison of the inhibitory activity of GBV-C E2 peptides on gp41-mediated cell−cell fusion and the susceptibility of HIV-1 to them, we consider the relevance mainly of domains GBV-C $E2_{55-78}$ and $E2_{133-156}$ in terms of future drug design. These domains might comprise useful leads for optimization because of the many advantages that peptides bring to the clinic, like potency, specificity, and lower rates of toxicity.

On the basis of the peptide sequences selected, the design and synthesis of new forms of peptide presentation are considered in order to enhance the antiviral activity of these synthetic molecules. The literature has described different strategies to increase the antiviral activity of synthetic peptides that prevent the limitations presented by this type of molecule in its clinical application, such as reduced stability and limited selectivity of action. Hence, the introduction of non-natural residues, such as D-amino acids, has recently been described to avoid peptide degradation by proteases or the introduction of intramolecular cyclical motives to encourage a more rigid structure with less flexibility in them.[19] Another recent approach consists of a modification of peptides by combining them with fatty acids, which favors enzymatic stability, improves pharmacokinetic properties, and encourages secondary structure in the synthetic peptide sequence. The modification of peptides that inhibit HIV fusion through the combination of fatty acids to increase their inhibiting activity has recently been described.[31] This inhibiting activity is correlated to the length of the fatty acid, the direction of the fatty acid attachment (N- or C-terminal) to the peptide sequence, and the peptide concentration in cells. It seems that the fatty acid allows the combined peptide to become attached to the cell membrane surface, increasing the concentration of the combined peptide at points of fusion.

In relation to the viral tropism, in general, the IC_{50} values observed for the HIV-1_{HXB2} (X4) were lower than those for HIV-$1_{69/7}$ (R5X4 DM) and lower than those for HIV-1_{BaL} (R5), reaching 1 $\log_{10}$ difference between the X4 strain and the R5 strain. This sensitivity profile was also observed in the PBMC susceptibility assays performed. The incubation of peptides and TZM-bl before the HIV-1 adsorption did not prevent the viral infection of either HIV-1_{HXB2} or HIV-1_{BaL} laboratory adapted strains. Thus, we discard that peptide−co-receptor binding as the cause of the differential susceptibility between both viral strains.

A similar phenomenon was observed in the T-20-gp41 interaction by Derdeyn et al.[32,33] in which the IC_{50} obtained for R5 isolates was 0.8 $\log_{10}$ higher than the mean IC_{50} for X4 isolates. This feature was interpreted as a consequence of the differential affinities of proteins during the cooperative process of CD4-gp120-CCR5 binding and the CD4-gp120-CXCR4 binding, leading to conformational changes that

Table 4. Phenotypic Susceptibilities of HIV-1 to E2 GBV-C Peptides in TZM-bl Cells

	HXB2		BAL		69-7[a]	
peptide	IC_{50}[b]	95% CI[c]	IC_{50}[b]	95% CI[c]	IC_{50}[b]	95% CI[c]
P11	162.1[d]	125.3−209.7	484.5	441.6−531.5	208.8	178.8−243.9
P19	46.0	34.5−61.2	194.3	171.2−220.5	71.4	64.7 − 78.7
P20	70.1	60.5−81.2	125.5	124.4−126.7	111.1[d]	104.8−117.7
P21	44.9	36.8−54.7	529.1	427.3−655.2	371.1[d]	326.4−421.9
P34	237.4	191.3−294.6	411.2	373.5−452.7	118.6	111.6 − 126.0
P45	48.8[d]	42.3−56.2	505.5	501.3−509.8	43.7	38.4−49.7
P46	39.9[d]	34.7−45.8	462.8	438.7−488.2	24.1	22.0−26.5
P47	58.6[d]	50.6−67.8	140.3	125.9−156.4	20.1	18.1−22.2
P109	37.5	31.8−44.3	294.8[d]	259.2−335.3	60.8	55.1−67.1
P124			94.7	79.9 − 112.3		
C34	nd[e]	nd[e]	0.012	0.010 − 0.013	nd[e]	nd[e]
T20	nd[e]	nd[e]	0.021	0.019 − 0.022	nd[e]	nd[e]
amphotericin B	0.175	0.167−0.185	0.136	0.129 − 0.145	nd[e]	nd[e]

[a] One replicate for each peptide in this assay. [b] IC_{50}: concentration (μM) of a peptide causing 50% inhibition of the infection, obtained from two independent experiments. [c] 95% CI: 95% confidence interval of IC_{50}. [d] Linear mathematical model, not sigmoidal. [e] nd: not determined.

Table 5. Concentrations of E2 Peptides (μM) up to Which the HIV-1 Infection of PBMCs Was Not Detected at Day 7 of Cell Culture by Qualitative Analysis of p24 Antigen

	HXB2	BAL
P11	31.2	62.5
P19	15.6	15.6
P20	7.8	15.6
P21	3.9	62.5
P34	31.2	62.5
P45	7.8	31.2
P46	7.8	7.8
P47	7.8	15.6
P109	7.8	15.6
P124	62.5	7.8

promote T-20 interaction with HR1 binding when the virus uses the CXCR4 co-receptor during virus-cell fusion. In our study, we do not discard the notion that the gp120-CXCR4 binding could also promote the display of g41-FP binding sites for the active GBV-C E2 peptides. On the other hand, despite the FP having a highly preserved 23 amino acid sequence among the HIV-1 strains, the polymorfism L/V was observed in the seventh position of the N-terminal FP of gp41 of the HIV-1_{BaL} laboratory adapted strain. This polymorphism located in the α-helix conformation of FP[34] did not appear as a consequence of an adaptive viral escape in the presence of peptides; however, its presence could be the cause of the differential affinity to the peptides observed between both laboratory adapted viral strains, independent of viral tropism. Future studies with the improved peptides will be carried out to assess this hypothesis.

To sum up, in the present article we describe certain E2 GBV-C domains that interfere with the HIV-1 fusion peptide−vesicle interaction, produce a notable decrease the cellular membrane fusion, and interfere with the HIV-1 infectivity in a dose-dependent manner. We provide insights into GBV-C E2 driven inhibition of HIV-1 replication that may lead to the identification of novel therapeutics, drug targets, and putative candidate vaccine antigens.

Experimental Section

Peptide Synthesis. The 124 peptides of the E2 GBV-C envelope protein were synthesized by semiautomated multiple solid-phase peptide synthesis on a peptide synthesizer (SAM, Multisyntech, Germany) as C-terminal carboxamides on a Tentagel RAM resin (Rapp Polymere GmbH, Germany) (100 mg, 0.2 meq/g) and following a 9-fluorenylmethoxycarbonyl (Fmoc) strategy. Amino acid side chain protection was effected by the following: triphenylmethyl (Trt) for glutamine, asparagine, histidine, and cysteine; *tert*-butyl (^{t}Bu) for aspartic acid, glutamic acid, serine, threonine, and tyrosine; 2,2,5,7,8-pentamethylchroman-6-sulfonyl (Pmc) for arginine, and *tert*-butoxycarbonyl (Boc) for lysine and tryptophan.

The coupling reaction was performed using 4-fold molar excesses of activated Fmoc-amino acids throughout the synthesis. The amino acids were activated essentially by means of treatment with 2-(1*H*-7-azabenzotriazole-1-yl)-1,1,3,3-tetramethyluranium hexafluorophosphate methanaminium (HATU) and a base such as diisopropylethylamine (DIPEA). The Fmoc-deprotection step was accomplished twice with 20% piperidine in dimethylformamide (DMF) for 10 min. The efficiency of these reactions was evaluated by the ninhydrin colorimetric reaction.

Once the synthesis was complete, the cleavage and deprotection processes of the peptidyl resins were carried out in a semiautomatic synthesizer using the Multisyntech accessories available for this purpose. These reactions took place by means of treatment with 94% trifluoroacetic acid (TFA) in the presence of scavengers, basically 2.5% H_2O, 2.5% 1,2-ethanedithiol (EDT), and 1% triisopropylsilane (TIS) for 4 h.

Peptides were isolated by precipitation with cold diethyl ether, centrifuged, and lyophilized in 10% acetic acid. The peptides were characterized by analytical HPLC on a Kromasil C-18 column (Teknokroma, 5 μm, 25 cm × 0.46 cm) with a linear gradient of 95−5% A in B over 20 min at a flow rate of 1 mL/min using 0.05% TFA in water (A) and 0.05% TFA in acetonitrile (B) as the eluting system. The peptides were up to 90% pure by analytical HPLC at 215 nm. Their identity was confirmed by electrospray mass spectrometry (ES-MS) (Table 1 in Supporting Information). Crude peptides were desalted using Oasis HLB Plus cartridge 225 mg/60 μg from Waters. These cartridges contain a polymeric water-wettable reversed phase sorbent.

The highly preserved gp41 FP, AVGIGALFLGFLGAAGSTMGAAS, was successfully synthesized in a 100% polyethylene glycol based resin, the ChemMatrix, that has proved to be a superior support for the solid-phase synthesis of hydrophobic and highly structured peptides.[35,36] Peptides synthesized manually (P2, P11, P19−21, P23, P25, P34, P45−47, P59, P97, P105, P109, P124, and FP gp41) were purified by preparative HPLC in a Kromasil-C8 column (Tecknochroma, 5 μm, 25 cm × 2.2 cm) and characterized by ES-MS. The purity by HPLC of all peptides was ≥95%.

Inhibition of the Release of Vesicular Contents Induced by the HIV-1 FP. In order to select the E2 GBV-C peptide sequences that have the capacity to inhibit the interaction and destabilization process of membranes induced by the HIV-1 fusion peptide,

the biophysical assay on the vesicle contents release described by Ellens[37] was performed in a PTI QM4CW spectrofluorimeter (Photon Technology Internacional). Unilamellar lipid vesicles (LUVs) containing fluorescent probes ANTS and DPX were prepared according to the protocol described by our work group.[38]

In order to carry out screening of the synthesized peptides, the concentration of the gp41(1−23) fusion peptide (HIV-1 FP) providing approximately half the total vesicle contents release was selected. Each GBV-C peptide sequence corresponding to the E2 protein was premixed with the HIV-1 FP in DMSO prior to its addition to a suspension of LUV liposomes. Dequenching of coencapsulated ANTS and DPX fluorescence resulting from dilution was measured to assess the leakage of aqueous contents from vesicles.

ANTS/DPX leakage out of the LUVs (100 μM lipids) was measured after 30 min of incubation at room temperature. Leakage was monitored by measuring the increase in ANTS/DPX fluorescence intensity at 520 nm, with an excitation of 355 nm. HIV-1 FP/E2 peptide ratios ranged from $^1/_1$ to $^1/_{10}$. The percentage of leakage was calculated as

$$\% \text{ leakage} = [(F - F_0)/(F_{100} - F_0)] \times 100$$

where F_0 is the initial fluorescence of LUVs, F is the fluorescence intensity after incubation with the peptide, and F_{100} is the fluorescence intensity after addition of 10 μL of a 10% (v/v) Triton-100 solution (complete lysis of the LUV).

Effect of E2 Peptides on the HIV-1 FP Binding to Model Membranes. POPG LUVs were prepared according the protocol described by Rojo et al.[39] Emission fluorescence spectra were recorded for peptides in tris(hydroxymethyl)aminomethane (Tris), 10 mM, pH 7.4, at 20 °C. Peptide−phospholipid interactions were assessed by monitoring the changes in the fluorescence spectra when LUV-POPG liposomes were incubated with 2 μM HIV-1 FP. Moreover, each E2 peptide (P59, P97, and P105) was premixed (1:1 ratio) with the HIV-1 FP in dimethyl sulfoxide (DMSO) prior to its titration with POPG liposomes. Regarding the presence of a Trp residue in both P11 and P45 sequences, these E2 peptides were not evaluated in this assay.

The fluorescence intensity was measured as a function of the lipid/peptide ratio. Suspensions were continuously stirred and were left to equilibrate for 1 min before recording the spectrum. Fluorescence intensities were corrected for contribution of light scattering by subtraction of the appropriate vesicle blank. The last correction was obtained from a parallel lipid tritation of *N*-acetyltryptophanamide (NATA), which is known to not interact with lipids.

According to Wimley and White[40] and assuming a two-state equilibrium between water-soluble aggregates and membrane-bound peptides, the apparent mole fraction partition coefficients were determined by fitting the binding curves to the equation $I = f_{\text{bound}} I_{\max} + (1 - f_{\text{bound}}) I_0$, for which I is the relative fluorescence intensity, I_0 is the intensity in the absence of lipid, and $f_{\text{bound}} = K_x L/(W + K_x L)$, where K_x is the mole fraction partition coefficient, L is the lipid concentration, and W is the molar concentration of water (55.3 M at 25 °C).

Surface Plasmon Resonance Studies. Surface plasmon resonance (SPR) studies were performed on a Biacore T100 instrument (GE, Healthcare). The surface of a CM5 chip with a dextrane matrix was activated by injecting a mixture of *N*-hydroxysuccinimide (NHS) and *N*-ethyl-*N*′-(dimethylaminopropyl)carbodiimide (EDC) for 7 min at a low rate of 10 mL/min. The HIV-1 FP was dissolved in sodium acetate buffer, pH 4.5, and the dissolution was filtered and injected onto the activated surface of the sensor chip until the immobilization level of 100−500 RU was reached. The surface was capped with a 1 M solution of ethanolamine at pH 8.0 to remove residual activated carboxylic acid functional groups. Control experiments were performed using sensor chips activated according to the protocol described but without any peptide coupled. The analytes (E2 peptides) were dissolved in HBS buffer (10 mM HEPES, pH 7.4, 150 mM NaCl, 3.4 mM EDTA, 0.05% surfactant P20) and injected onto the surface of the sensor chip diluted in a range of concentrations between 1.5 and 100 μM at a flow rate of 15 mL/min. The association and dissociation times were 180 s each. Regeneration was performed using a 50 mM NaOH and 1 M NaCl solution. The interaction parameters were analyzed and evaluated using the Biacore T100 GxP Evaluation software.

Isothermal Titration Calorimetry Studies. Isothermal titration calorimetric (ITC) experiments were recorded on VP-ITC microcalorimeter (MicroCal, LLC, Northampton, MA). Purified peptides were dissolved in DMSO and then degassed for 5 min prior to sample loading. Briefly, a solution of 0.5 mM peptides in DMSO was injected into a chamber containing 25 μM HIV-1 FP. The calorimeter was first equilibrated at 20 °C, and the baseline was monitored during equilibration. The time between injections was 5 min, and the stirring speed was 300 rpm. The heats of dilution were determined in control experiments by injecting E2 peptides into DMSO and subtracting from the heats produced in the corresponding peptide−peptide binding experiments. Control experiments were also performed by titrating DMSO into HIV-1 FP. The total observed heat effects were corrected for these small contributions. All titration data were subsequently analyzed using the Origin 7 software (MicroCal, LLC).

Inhibition of Cell Binding. Two cell lines were used: HeLa-env (donated by Dr. Blanco from Fundació IRSI Caixa) expressing the protein from the HIV-1 envelope and including the HIV-1 long terminal repeat (LTR) promoter in its genome, and TZM-bl (AIDS reagents catalogue no. 8129), which expresses the membrane receptor from CD4 lymphocytes and co-receptors CCR5 and CXCR4 and includes the luciferase and β-galactosidase genes in its genome.[41−43]

Cell lines were cultured in Dulbecco's modified Eagle medium (DMEM, PAA) containing L-glutamine and sodium pyruvate supplemented with 10% heat-inactivated fetal bovine serum (FBS), 100 μg/mL penicillin, and 100 μg/mL streptomycin. The cell cultures were maintained in a tissue culture incubator at 37 °C in a 5% of CO_2 atmosphere.

When both types of cells are cocultured, cell membrane fusion occurs and the luciferase is activated and produced the oxidation of luciferine. The level of oxiluciferine was quantified by using the Britelite kit (Perkin-Elmer) and SpectraMax M5 microplate reader.

In this study, the trial on the inhibition of cell binding induced by E2 GBV-C peptides consisted of the incubation of 2500 HeLa-env cells/well (Nunc plates, catalogue no. 136101) for 1 h at serial dilutions (5−1000 μM) of the peptides to be tested, followed by the addition of around 10 times (25 000 cells) TZM-bl/well and incubation for 24 h.

To control cell binding, wells without peptides were reserved and a known cell binding inhibitor, C-34 (AIDS Reagents, catalogue no. 9824), was used as a positive control.

The level of inhibition of cell binding was also qualitatively assessed by observing the formation of syncytia under the microscope.

Inhibition of HIV-1 Infection. Preliminary Screening of Peptides Inhibitory Effect on HIV-1. A preliminary susceptibility assay of HIV-1 against the 124 E2 GBV-C peptides was performed by infecting CEM-174 cell line (AIDS Reagents, catalogue no. 272) with 0.008 multiplicity of infection (moi) of HIV-$1_{92UG024}$ (R4 tropism, subtype D, AIDS Reagents no. 1649) and two different concentrations of each peptide (500 and 250 μM). Briefly, the 600 $TCID_{50}$ (50% tissue culture infective dose) of virus was first incubated, in triplicate with each concentration of each peptide prepared on RPMI-1640 cell medium supplemented with 10% of fetal bovine serum (FBS), for 2 h at 37 °C and 5% of CO_2. The peptide C34 (AIDS Reagents, no. 9824) at 1 μM was used as inhibition control. Later, 75 000 cells were added

and incubated for an additional 2 h at 37 °C and 5% of CO_2. After viral adsorption, the infected cells were washed three times with phosphate buffered saline (PBS) and incubated for 7 days in the presence of each concentration of each peptide in a final volume of 200 μL/well in 96-well tissue culture plates. Triplicates of infected cells without peptide and noninfected cells were included as positive and negative controls of infection, respectively. Viral infection was analyzed by cytopathic effect and by ELISA HIV-1 p24 ELISA p24 antigen-HIV-1 (Ag HIV, Innogenetics no. K1048).

Susceptibility Assay on TZM-bl. A set of peptides with potential capability for HIV-1 inhibition demonstrated by biophysical assays, cell−cell fusion assays, and preliminary assays on HIV-1 susceptibility in CEM 174 assay were investigated more deeply in a susceptibility assay on TZM-bl cells to assess if the inhibition of HIV-1 infection was in a dose-dependent manner.

Briefly, triplicates of 2-fold serial concentration of each peptide (0−500 μM) were preincubated along with a predetermined volume of either HIV-1_{BaL} strain (R5 tropism, AIDS Reagent) or HIV-1_{HXB2} strain (R4 tropism, obtained from pHXB2, kindly provided by Prof. C Boucher, University of Utrecht (AZU), The Netherlands) or a HIV-1 primary isolate named 69/7 (R5X4 dual or mixed tropism DM, isolated from an infected patient), in a final volume of 100 μL/well of DMEM with 10% FBS in 96-cell culture plates, for 2 h at 37 °C and 5% of CO_2. In addition, 2-fold serial concentration of either T-20 (AIDS Reagents, no. 9409) or C34 or amphotericin B (Bristol-Myers Squibb, SL) was used as a dose-dependent inhibition control of the assay. Later, an amount of 100 μL of cell media containing 15 000 TZM-bl cells was added to each well. In these conditions the final moi of each viral strain was 0.02 HIV-1_{BaL} and 0.01 for HIV-1_{HXB2} and HIV-$1_{69/7}$, respectively. A triplicate of each HIV-1 infected TZM-bl without peptides and a triplicate of noninfected cells were used as positive and negative controls, respectively, and they were included in each assay. After 72 h postinfection, the supernatant of each well was removed and to it was added 50 μL of lysis buffer (0.1% TritonX-100, 10 mM $MgCl_2$, 0.5 mM dithiotreitol (DTT) in PBS) along with 50 μL of 1.5 mM of chlorophenolred-β-D-galactopyranoside (CPRG). The β-galactosidase activity was analyzed by spectrophotometry (570 nm, SpectraMax M5 microplate reader). The optical densities obtained were transformed in percentage of inhibition, and the sigmoid curves were analyzed by nonlinear regression (GraphPad Prism software, version 5). In parallel, the toxicity effect on TZM-bl cells at each concentration of peptide assayed was analyzed by using the 3-(4,5-dimethylthiazol-2-yl)-2,5-diphenyltetrazolium bromide (MTT) assay as it is described below.

A modification of this procedure was also tested to determine if the inhibitory effect of the peptides was due to a direct interaction with the receptor or co-receptor of viral entry. In this case, the TZM-bl cells were incubated with the 2-fold serial concentrations of peptides for 2 h at 37 °C and 5% of CO_2 and washed three times with PBS prior to the viral adsorption period of 2 h. Later the cells were washed three times with PBS, incubated for 72 h in the absence of peptides, and analyzed as described above.

Susceptibility Assay on PBMCs. A qualitative assay of HIV-1 susceptibility based on the p24 HIV-1 antigen was performed by infecting PBMCs with HIV-1_{HXB2} and HIV-1_{BaL} to corroborate the peptide's inhibitory effect of HIV-1 infection of this type of cell. The PBMCs were obtained from healthy donor buffy coats by density gradient centrifugation (ACCUSPIN System-Histopaque-1077, Sigma Diagnostics) and activated with 5 μg/mL of phytohemaglutinine (PHA, Sigma-Aldhrich) in RPMI-1640 media (Lonza-BioWithaker) and 10% of FBS for 24−72 h prior the viral infection. The 2-fold serial concentrations of peptides (0−125 μM) were prepared in RPMI-1640 supplemented with 10% of FBS and 10 U/mL recombinant interleukine-2 (rIL-2, Roche Diagnostic Systems) and preincubated along with a predetermined volume of either HIV-1_{HXB2} or HIV-1_{BaL} for 2 h at 37 °C and 5% of CO_2. Later, 8×10^5 activated PBMCs were added and incubated for an additional 2 h to allow viral adsorption. Finally the infected cells were washed three times with PBS and incubated for 7 days, along with their corresponding concentrations of peptide, in 96-well cell culture plates containing 200×10^3 PBMC in 200 μL of RPMI-1640, 20% of FBS, and 10 U/mL of rIL-2 in the absence of peptides. Thus, the final moi for each viral strain was 0.001. Viral release was analyzed by qualitative ELISA p24 antigen-HIV-1 (Ag HIV, Innogenetics, no. K1048).

Cell Viability with MTT Assay. Cell toxicity of E2 peptides was analyzed in HeLa, TZM-bl, and PBMCs using the MTT assay. Cells were cultured with DMEM (15 000 cells/well) in a 96-well plate and incubated with the serial dilutions of each peptide at 37 °C for 72 h. Afterward, MTT was added to a final concentration of 7.5 mg/mL and incubated for 2 h at 37 °C. Later the medium was removed and 100 μL of DMSO was added to dissolve the formazan precipitate. Absorbance was measured at 570 nm after 45 min. Cell viability was determined by the quotient between the absorbance value of cells treated with peptide and untreated cells. The cytotoxic concentration (CC_{50}) was analyzed by nonlinear regression.

Statistical Analysis. To estimate the inhibitory concentration (IC_{50}) of E2 peptides and its 95% confidence intervals, nonlinear regression models were used assuming a symmetrical sigmoidal four-parameters curve[44] for the relationship (GraphPad Prism 5.0 software). This parametrization of the sigmoidal curve has good statistical properties.

The response was used in the log form ($\log_{10}$(dose)) rather than the dose itself. After convergence of the models, goodness-of-fit was checked by looking to the replicates test, the residuals, the covariance matrix of the estimated parameters, the dependence of each estimated parameter, and the determination coefficient (R^2). Constraints were used when necessary to improve the fit of the model.

Acknowledgment. This work was funded by Grants CTQ2006-15396-CO2-01/BQU and CTQ2009-13969-CO2-01/BQU from the Ministerio de Ciencia e Innovación, Spain. E.H. is the recipient of predoctoral grant (JAE program, CSIC, Spain). We also acknowledge Dr. Rafel Prohens (Scientific Parc of Barcelona), Dr. Ricardo Gutierrez (Pompeu Fabra University), and Dr. Julià Blanco (Fundació IRSI Caixa) for the discussion of ITC, SPR, and inhibition of cell−cell binding studies, respectively.The following reagent was obtained through the NIH AIDS Research and Reference Reagent Program, Division of AIDS, NIAID, NIH: HIV-1 IIIB C34 peptide from DAIDS, NIAID.

Supporting Information Available: Characterization of E2 GBV-C peptides; partitioning curves of FP and equimolecular mixtures of FP/E2 peptides (P59, P97, P105) in POPG LUVs; dose-response curves of inhibition of E2 GBV-C peptides for gp41-induced cell−cell fusion; dose-response curves of inhibition of E2 GBV-C peptides for HIV-1_{HXB2}, HIV-1_{BAL}, and primary isolate HIV-$1_{69/7}$ infection of TZM-bl cells; computerized prediction analysis of hydrophilicity, accessibility, and presence of β-turns in E2 protein. This material is available free of charge via the Internet at http://pubs.acs.org.

References

(1) Simons, J. N.; Leary, T. P.; Dawson, G. J.; Pilotmatias, T. J.; Muerhoff, A. S.; Schlauder, G. G.; Desai, S. M.; Mushahwar, I. K. Isolation of novel virus-like sequences associated with human hepatitis. *Nat. Med.* **1995**, *1*, 564–569.

(2) Linnen, J.; Wages, J., Jr.; Zhang-Keck, Z. Y.; Fry, K. E.; Krawczynski, K. Z.; Alter, H.; Koonin, E.; Gallagher, M.; Alter, M.; Hadziyannis, S.; Karayiannis, P.; Fung, K.; Nakatsuji, Y.; Shih, J. W.; Young, L.;

Piatak, M., Jr.; Hoover, C.; Fernandez, J.; Chen, S.; Zou, J. C.; Morris, T.; Hyams, K. C.; Ismay, S.; Lifson, J. D.; Hess, G.; Foung, S. K.; Thomas, H.; Bradley, D.; Margolis, H.; Kim, J. P. Molecular cloning and disease association of hepatitis G virus: a transfusion−transmissible agent. *Science* **1996**, *271*, 505–508.
(3) Mphahlele, M. J.; Lau, G. K.; Carman, W. F. HGV: the identification, biology and prevalence of an orphan virus. *Liver* **1998**, *18*, 143–55.
(4) Theodore, D.; Lemon, S. M. GB virus C, hepatitis G virus, or human orphan flavivirus? *Hepatology* **1997**, *25*, 1285–1286.
(5) Heringlake, S.; Ockenga, J.; Tillmann, H. L.; Trautwein, C.; Meissner, D.; Stoll, M.; Hunt, J.; Jou, C.; Solomon, N.; Schmidt, R. E.; Manns, M. P. GB virus C/hepatitis G virus infection: a favorable prognostic factor in human immunodeficiency virus-infected patients? *J. Infect. Dis.* **1998**, *177*, 1723–1726.
(6) Tillmann, H. L.; Heiken, H.; Knapik-Botor, A.; Heringlake, S.; Ockenga, J.; Wilber, J. C.; Goergen, B.; Detmer, J.; McMorrow, M.; Stoll, M.; Schmidt, R. E.; Manns, M. P. Infection with GB virus C and reduced mortality among HIV-infected patients. *N. Engl. J. Med.* **2001**, *345*, 715–724.
(7) Xiang, J.; Wunschmann, S.; Diekema, D. J.; Klinzman, D.; Patrick, K. D.; George, S. L.; Stapleton, J. T. Effect of coinfection with GB virus C on survival among patients with HIV infection. *N. Engl. J. Med.* **2001**, *345*, 707–714.
(8) Zhang, W.; Chaloner, K.; Tillmann, H. L.; Williams, C. F.; Stapleton, J. T. Effect of early and late GB virus C viraemia on survival of HIV-infected individuals: a meta-analysis. *HIV Med.* **2006**, *7*, 173–180.
(9) Van der Bij, A. K.; Kloosterboer, N.; Prins, M.; Boeser-Nunnink, B.; Geskus, R. B.; Lange, J. M.; Coutinho, R. A.; Schuitemaker, H. GB virus C coinfection and HIV-1 disease progression: The Amsterdam Cohort Study. *J. Infect. Dis.* **2005**, *191*, 678–685.
(10) Williams, C. F.; Klinzman, D.; Yamashita, T. E.; Xiang, J.; Polgreen, P. M.; Rinaldo, C.; Liu, C.; Phair, J.; Margolick, J. B.; Zdunek, D.; Hess, G.; Stapleton, J. T. Persistent GB virus C infection and survival in HIV-infected men. *N. Engl. J. Med.* **2004**, *350*, 981–990.
(11) Xiang, J.; George, S. L.; Wunschmann, S.; Chang, Q.; Klinzman, D.; Stapleton, J. T. Inhibition of HIV-1 replication by GB virus C infection through increases in RANTES, MIP-1alpha, MIP-1beta, and SDF-1. *Lancet* **2004**, *363*, 2040–2046.
(12) Jung, S.; Knauer, O.; Donhauser, N.; Eichenmuller, M.; Helm, M.; Fleckenstein, B.; Reil, H. Inhibition of HIV strains by GB virus C in cell culture can be mediated by CD4 and CD8 T-lymphocyte derived soluble factors. *AIDS* **2005**, *19*, 1267–1272.
(13) Moenkemeyer, M.; Schmidt, R. E.; Wedemeyer, H.; Tillmann, H. L.; Heiken, H. GBV-C coinfection is negatively correlated to Fas expression and Fas-mediated apoptosis in HIV-1 infected patients. *J. Med. Virol.* **2008**, *80*, 1933–1940.
(14) Jung, S.; Eichenmuller, M.; Donhauser, N.; Neipel, F.; Engel, A. M.; Hess, G.; Fleckenstein, B.; Reil, H. HIV entry inhibition by the envelope 2 glycoprotein of GB virus C. *AIDS* **2007**, *21*, 645–647.
(15) Xiang, J.; McLinden, J. H.; Chang, Q.; Kaufman, T. M.; Stapleton, J. T. An 85-aa segment of the GB virus type C NS5A phosphoprotein inhibits HIV-1 replication in CD4+ Jurkat T cells. *Proc. Natl. Acad. Sci. U.S.A.* **2006**, *103*, 15570–15575.
(16) Chang, Q.; McLinden, J. H.; Stapleton, J. T.; Sathar, M. A.; Xiang, J. Expression of GB virus C NS5A protein from genotypes 1, 2, 3 and 5 and a 30 aa NS5A fragment inhibit human immunodeficiency virus type 1 replication in a CD4+ T-lymphocyte cell line. *J. Gen. Virol.* **2007**, *88*, 3341–3346.
(17) Xiang, J.; McLinden, J. H.; Chang, Q.; Jordan, E. L.; Stapleton, J. T. Characterization of a peptide domain within the GB virus C NS5A phosphoprotein that inhibits HIV replication. *PLoS One* **2008**, *3*, No. e2580.
(18) Burton, A. Enfuvirtide approved for defusing HIV. *Lancet Infect. Dis.* **2003**, *3*, 260.
(19) Munch, J.; Standker, L.; Adermann, K.; Schulz, A.; Schindler, M.; Chinnadurai, R.; Pohlmann, S.; Chaipan, C.; Biet, T.; Peters, T.; Meyer, B.; Wilhelm, D.; Lu, H.; Jing, W.; Jiang, S.; Forssmann, W. G.; Kirchhoff, F. Discovery and optimization of a natural HIV-1 entry inhibitor targeting the gp41 fusion peptide. *Cell* **2007**, *129*, 263–275.
(20) Boggiano, C.; Jiang, S.; Lu, H.; Zhao, Q.; Liu, S.; Binley, J.; Blondelle, S. E. Identification of a D-amino acid decapeptide HIV-1 entry inhibitor. *Biochem. Biophys. Res. Commun.* **2006**, *347*, 909–915.
(21) Smith, J. M.; Ellenberger, D.; Butera, S. Protein Engineering for HIV Therapeutics. In *Medicinal Protein Engineering*; Khudyakov, Y. E., Ed.; CRC Press: Boca Raton, FL, 2009; pp 385−406.
(22) Herrera, E.; Gómara, M. J.; Mazzini, S.; Ragg, E.; Haro, I. Synthetic peptides of hepatitis G virus (GBV-C/HGV) in the selection of putative peptide inhibitors of the HIV-1 fusion peptide. *J. Phys. Chem. B* **2009**, *113*, 7383–7391.
(23) Hopp, T. P.; Woods, K. R. Prediction of protein antigenic determinants from amino acid sequences. *Proc. Natl. Acad. Sci. U.S.A.* **1981**, *78*, 3824–3828.
(24) Janin, J. Surface and inside volumes in globular proteins [20]. *Nature* **1979**, *277*, 491–492.
(25) Chou, P. Y.; Fasman, G. D. Prediction of the secondary structure of proteins from their amino acid sequence. *Adv. Enzymol. Relat. Areas Mol. Biol.* **1978**, *47*, 45–148.
(26) Schön, A.; Madani, N.; Klein, J. C.; Hubicki, A.; Ng, D.; Yang, X.; Smith, A. B.; Sodroski, J.; Freire, E. Thermodynamics of binding of a low-molecular-weight CD4 mimetic to HIV-1 gp120. *Biochemistry* **2006**, *45*, 10973–10980.
(27) Naider, F.; Anglister, J. Peptides in the treatment of AIDS. *Curr. Opin. Struct. Biol.* **2009**, *19*, 473–482.
(28) Doms, R. Beyond receptor expression: the influence of receptor conformation, density and affinity in HIV-1 infection. *Virology* **2000**, *276*, 229–237.
(29) Rusert, P.; Mann, A.; Huber, M.; von Wyl, V.; Gunthard, H. F.; Trkola, A. Divergent effects of cell environment on HIV entry inhibitory activity. *AIDS* **2009**, *23*, 1319–1327.
(30) Nattermann, J.; Nischalke, H. D.; Kupfer, B.; Rockstroh, J.; Hess, L.; Sauerbruch, T.; Spengler, U. Regulation of CC chemokine receptor 5 in hepatitis G virus infection. *AIDS* **2003**, *17*, 1457–1462.
(31) Wexler-Cohen, Y.; Shai, Y. Demonstrating the C-terminal boundary of the HIV 1 fusion conformation in a dynamic ongoing fusion process and implication for fusion inhibition. *FASEB J.* **2007**, *21*, 3677–3684.
(32) Derdeyn, C. A.; Decker, J. M.; Sfakianos, J. N.; Wu, X.; O'Brien, W. A.; Ratner, L.; Kappes, J. C.; Shaw, G. M.; Hunter, E. Sensitivity of human immunodeficiency virus type 1 to the fusion inhibitor T-20 is modulated bu coreceptor specificity defined by the V3 loop of gp120. *J. Virol.* **2000**, *74*, 8358–8367.
(33) Derdeyn, C. A.; Decker, J. M.; Sfakianos, J. N.; Zhang, Z.; O'Brien, W. A.; Ratner, L.; Shaw, G. M.; Hunter, E. Sensitivity of human immunodeficiency virus type 1 to fusion inhibitors targeted to the gp41 first heptad repeat involves distinct regions of gp41 and is consistently modulated by gp120 interaction with the coreceptor. *J. Virol.* **2001**, *75*, 8605–8614.
(34) Gordon, L. M.; Mobley, P. W.; Pilpa, R.; Sherman, M. A.; Waring, A. J. Conformational mapping of the N-terminal peptide of HIV-1 gp41 in membrane environments using ^{13}C-enhanced Fourier transform infrared spectroscopy. *Biochim. Biophys. Acta* **2002**, *1559*, 96–120.
(35) Garcia-Martin, F.; Quintanar-Audelo, M.; Garcia-Ramos, Y.; Cruz, L. J.; Gravel, C.; Furic, R.; Cote, S.; Tulla-Puche, J.; Albericio, F. ChemMatrix, a poly(ethylene glycol)-based support for the solid-phase synthesis of complex peptides. *J. Comb. Chem.* **2006**, *8*, 213–220.
(36) Garcia-Martin, F.; White, P.; Steinauer, R.; Cote, S.; Tulla-Puche, J.; Albericio, F. The synergy of ChemMatrix resin and pseudoproline building blocks renders RANTES, a complex aggregated chemokine. *Biopolymers* **2006**, *84*, 566–575.
(37) Ellens, H.; Bentz, J.; Szoka, F. C. pH-induced destabilization of phosphatidylethanolamine-containing liposomes: role of bilayer contact. *Biochemistry* **1984**, *23*, 1532–1538.
(38) Larios, C.; Casas, J.; Alsina, M. A.; Mestres, C.; Gomara, M. J.; Haro, I. Characterization of a putative fusogenic sequence in the E2 hepatitis G virus protein. *Arch. Biochem. Biophys.* **2005**, *442*, 149–159.
(39) Rojo, N.; Gomara, M. J.; Alsina, M. A.; Haro, I. Lipophilic derivatization of synthetic peptides belonging to NS3 and E-2 proteins of GB virus-C (hepatitis G virus) and its effect on the interaction with model lipid membranes. *J. Pept. Res.* **2003**, *61*, 318–330.
(40) Wimley, W. C.; White, S. H. Designing transmembrane alpha-helices that insert spontaneously. *Biochemistry* **2000**, *39*, 4432–4442.
(41) Sackett, K.; Wexler-Cohen, Y.; Shai, Y. Characterization of the HIVN-terminal fusion peptide-containing region in context of key gp41 fusion conformations. *J. Biol. Chem.* **2006**, *281*, 21755–21762.
(42) Wei, X. P.; Decker, J. M.; Liu, H. M.; Zhang, Z.; Arani, R. B.; Kilby, J. M.; Saag, M. S.; Wu, X. Y.; Shaw, G. M.; Kappes, J. C. Emergence of resistant human immunodeficiency virus type 1 in patients receiving fusion inhibitor (T-20) monotherapy. *Antimicrob. Agents Chemother.* **2002**, *46*, 1896–1905.
(43) Nussbaum, O.; Broder, C. C.; Berger, E. A. Fusogenic mechanisms of enveloped-virus glycoproteins analyzed by a novel recombinant vaccinia virus-based assay quantitating cell fusion-dependent reporter gene activation. *J. Virol.* **1994**, *68*, 5411–5422.
(44) Ratkowsky, D. A. *Handbook of Nonlinear Regression Models*; Dekker: New York, 1990; Vol. 107, p 241.

Biochimica et Biophysica Acta 1808 (2011) 1567–1573

Contents lists available at ScienceDirect

Biochimica et Biophysica Acta

journal homepage: www.elsevier.com/locate/bbamem

Study of the inhibition capacity of an 18-mer peptide domain of GBV-C virus on gp41-FP HIV-1 activity

I. Haro [c], M.J. Gómara [c], R. Galatola [c], O. Domènech [a], J. Prat [a,b], V. Girona [a,b], M.A. Busquets [a,b,*]

[a] Physical Chemistry Department, IN2UB, University of Barcelona, Avda, Joan XXIII, s/n. 08028 Barcelona, Spain
[b] Associated Unit to the CSIC: Peptides and Proteins: Physicochemical studies, Faculty of Pharmacy, University of Barcelona, Avda. Joan XXIII, s/n. 08028 Barcelona, Spain
[c] Unit of Synthesis and Biomedical Application of Peptides, Department of Biomedical Chemistry, IQAC-CSIC, Jordi Girona 18, 08034, Barcelona, Spain

ARTICLE INFO

Article history:
Received 24 August 2010
Received in revised form 23 February 2011
Accepted 25 February 2011
Available online 4 March 2011

Key words:
HIV-1
GBV-C
AFM
Lipid monolayer
Peptide–peptide binding

ABSTRACT

The peptide sequence (175–192) RFPFHRCGAGPKLTKDLE (P59) of the E2 envelope protein of GB virus C (GBV-C) has been proved to decrease cellular membrane fusion and interfere with the HIV-1 infectivity in a dose-dependent manner. Based on these previous results, the main objective of this study was to deepen in the physicochemical aspects involved in this interaction. First, we analyzed the surface activity of P59 at the air–water interface as well as its interaction with zwitterionic or negatively charged lipid monolayers. Then we performed the same experiments with mixtures of P59/gp41-FP. Studies on lipid monolayers helped us to understand the lipid–peptide interaction and the influence of phospholipids on peptide penetration into lipid media. On another hand, studies with lipid bilayers showed that P59 decreased gp41-FP binding to anionic Large Unilamellar Vesicles. Results can be attributed to the differences in morphology of the peptides, as observed by Atomic Force Microscopy. When P59 and gp41-FP were incubated together, annular structures of about 200 nm in diameter appeared on the mica surface, thus indicating a peptide–peptide interaction. All these results confirm the gp41-FP–P59 interaction and thus support the hypothesis that gp41-FP is inhibited by P59.

1. Introduction

A large number of studies have arisen from the need to overcome AIDS infection and transmission, and to improve therapy. Several authors [1–5] have provided evidence of a significant reduction in HCV-related liver morbidity associated with GB virus C (GBV-C) (formerly known as hepatitis G virus) viremia in HCV/HIV-coinfected patients. GBV-C infection contributes to unpredictable clinical outcomes in these patients. It has also been proposed that GBV-C is a good indicator for demonstrating nosocomial parenteral transmission of viral agents [6]. Thus, GBV-C could be used to predict hospital-acquired infection, as this virus is common in North America and Western Europe [7,8].

Most reported studies cover clinical or genotypic aspects of the potential interaction between HIV and GBV-C virus [1,9–11]. However, little attention has been given to the interactions between the viral fusion peptides of these two viral families and the cell membrane. These interactions are crucial to our understanding of the mechanisms by which viruses enter cells and why GBV-C coinfection with HIV decreases AIDS virulence. A full account of these mechanisms should consider the concomitance between E2 protein of GBV-C and gp41 protein of HIV-1. In particular, we need to establish whether E2 affects protein folding and whether it forms a non-active complex with gp41-FP.

We previously described the interaction of peptide sequences of E1 and E2 envelope proteins of GBV-C with liposomes or lipid monolayers [12–14]. All these initial studies agree on the occurrence of electrostatic interactions between the peptides and the polar heads of the lipids [15]. However, to our knowledge, there is no published description of the structural and morphological changes induced as a result of the concomitance of gp41-FP with any GBV-C peptide sequence.

Here we performed a series of studies to determine peptide–membrane or peptide–peptide interactions in an attempt to elucidate the mechanism by which GBV-C prevents HIV entry into cells. For this purpose, we chose a linear peptide that belongs to the region (175–192) of the E2 GBV-C envelope protein (P59) because it has shown a high capacity to inhibit cell-cell fusion. P59 inhibits syncitium formation in a dose-dependent manner (IC_{50}: 530 μM) with a lack of toxicity at the peptide concentrations studied [16].

In the first set of experiments, liposomes or lipid monolayers were used as model membranes to explore the mode of action of the following: i) P59; ii) gp41-FP fusion peptide (gp41-FP) and; iii) a mixture of the two peptides after their incubation at a P59/gp41-FP molar ratio of 5:1.

Abbreviations: LUVs, Large Unilamellar Vesicles; P59, Peptide sequence (175–192): RFPFHRCGAGPKLTKDLE, of the E2 envelope protein of GBV; gp41 FP, HIV-1 FP; PC, L-α-phosphatidylcholine (egg); PS, L-α-phosphatidylserine (bovine); π_{sat}, saturation pressure; π_{max}, maximum insertion pressure; π_o, initial surface pressure; $\Delta\pi$, pressure increase; TRIS, Tris hydroxymethylaminomethane; GBV-C, GB virus C

* Corresponding author at: Physical Chemistry Department, Faculty of Pharmacy, Avda Joan XXIII, s/n. 08028 Barcelona, Spain. Tel.: +34934024556; fax: +34934035987.
E-mail address: mabusquetsvinas@ub.edu (M.A. Busquets).

0005-2736/$ – see front matter © 2011 Elsevier B.V. All rights reserved.
doi:10.1016/j.bbamem.2011.02.019

In addition, membrane fluidity, determined by the nature of the lipids chosen, also affected the balance between the electrostatic forces at the interface and the hydrophobic forces that drive the interaction inside the membrane. The Langmuir film studies reported here showed that these peptides bind strongly to membranes, their intercalation into lipid monolayers being enhanced by the presence of negatively charged phospholipids.

The second set of experiments was designed to analyze the morphological changes associated with the P59–gp41-FP interaction. For this purpose, we used Atomic Force Microscope (AFM) [17–19] to view the peptides alone and also mixed. AFM images of gp41-FP and P59 showed spherical structures on a mica surface, indicating aggregation of the peptides when deposited on a flat surface. In contrast, when incubated together at a ratio of 5:1 (P59–gp41-FP, mol/mol) annular structures of 200 nm in diameter appeared on the mica surface. These structures were aligned in chains in which each link could be the association of one gp41-FP peptide surrounded by five P59 peptides. These annular structures suggest changes in the organization of the peptides as a result of the exposure of regions to the medium. The new organization may be due to the protection of these regions, which provides a more stable structure in the media.

All these results confirm the gp41-FP–P59 interaction and, consequently, the hypothesis that P59 inhibits gp41-FP.

2. Materials and methods

2.1. Surface activity

The experiments were carried out on a NIMA Langmuir Balance (Coventry, UK). Several volumes of a concentrated solution of P59, gp41-FP or P59/gp41-FP (5:1) were injected into a cylindrical Teflon trough with a capacity of 35 mL filled with 10 mM Tris buffer, pH: 7.4. The subphase was stirred continuously with a miniature Teflon-coated rod spinning at 150 rpm. Surface pressure, π, was monitored continuously by an electronic microbalance with an accuracy of ± 0.05 mN m^{-1} using a platinum plate as the pressure sensor. Changes in surface pressure over time were recorded for a minimum of 60 min. All the experiments were carried out in triplicate at room temperature (20 ± 1 °C). Each experiment was preceded by a thorough rinse and wipe of the troughs with 70% ethanol, several times with hot deionized water and finally with double distilled water.

2.2. Kinetics of penetration and maximum insertion pressure

To determine the capacity of lipid monolayers to host the selected peptide sequence, we studied the penetration kinetics of P59, gp41-FP and mixtures of P59/gp41-FP (5:1 molar ratio). Lipids from a concentrated solution (1 mg mL^{-1} in chloroform/methanol 2:1, v/v) were spread at the air/water interface in the same Teflon trough as in the above experiment, to reach the desired initial surface pressure (π_o). The spreading solvent was left to evaporate for 10 min. A peptide concentration, slightly lower than the equilibrium spreading pressure found in the surface activity measurements, [20] was then injected into the subphase through a lateral hole to prevent monolayer perturbation. Depending on both the peptide surface activity and affinity for the lipid monolayer, surface pressure increases to a steady-state upon peptide/monolayer binding, which is called the equilibrium adsorption pressure (π_e). The difference between π_e and π_o at different π_o, named surface pressure increase, $\Delta\pi$, allows the determination of the maximum insertion pressure (π_{max}) of a molecule by extrapolating the regression of the plot $\Delta\pi$ versus π_o.

P59 was injected under PC, PS or PC/PS (3:2) monolayers at several π_o, while gp41-FP, mixtures of P59/gp41-FP (5:1) and P59/gp41-FP (1:1) were studied only on the latter (3:2).

All the experiments were performed at 20° ± C.

2.3. Liposomes

PC/PS (3:2) large unilamellar vesicles (LUVs) were prepared following the protocol described by Rojo et al. [21]. Briefly, LUVs were prepared by hydration of the lipid film with tris(hydroxymethyl)aminomethane (TRIS) 10 mM, pH 7.4 buffer followed by 10 freeze–thaw cycles. This preparation was extruded 10 times through two 100-nm pore-size polycarbonate filters (Nucleopore, Pleasanton, CA, USA) in a high-pressure extruder (Lipex, Biomembranes, Vancouver, Canada).

2.4. Binding assay

The effect of E2(175–192) on the HIV-1 fusion protein (FP) binding to model membranes was studied by the protocol described below.

Emission fluorescence spectra were recorded for peptides in TRIS buffer 10 mM, pH 7.4, at 20 °C. Peptide–phospholipid interactions were assessed by monitoring the changes in the fluorescence spectra when LUV-PC/PS liposomes were incubated with 2 μM peptide concentration of [^{8}W] gp41-FP. Moreover, the E2 peptide was premixed with the [^{8}W] gp41-FP in dimethylsulphoxide (DMSO) in a 5:1 ratio prior to titration with PC/PS liposomes.

The fluorescence intensity was measured as a function of the lipid: peptide ratio. Suspensions were stirred continuously and left to equilibrate for 1 min before recording the spectrum. Fluorescence intensities were corrected for contribution of light scattering, by subtraction of the appropriate vesicle blank. The last correction was obtained from a parallel lipid titration of N-acetyl-tryptophanamide (NATA), which does not interact with lipids.

Assuming a two-state equilibrium between water-soluble aggregates and membrane-bound peptides, the apparent mole fraction partition coefficients were determined by fitting the binding curves to the equations: $I = f_{bound}\, I_{max} + (1 - f_{bound})\, I_0$, in which I is the relative fluorescence intensity, I_0 is the intensity in the absence of lipid; and $f_{bound} = K_x\, L/(W + K_x\, L)$, where K_x is the mole-fraction partition coefficient, L the lipid concentration and W the molar concentration of water (55.3 M at 25 °C). This procedure follows Wimley & White [22].

2.5. Atomic force microscopy

Mica squares (0.25 cm^2) were glued onto a steel disc, cleaned carefully with water before use and cleaved to obtain a flat and uniform surface. Immediately, an aliquot of 10 μL of peptides (P59 at 25 μM, gp41-FP 5 μM in milliQ water) was deposited on the mica surface and incubated for 60 min at room temperature.

Sample was thereafter washed with milliQ water to eliminate non-adsorbed peptides and dried to dryness. AFM contact mode images in water were obtained using a Nanoscope IV Multimode AFM (Veeco Metrology Group, Santa Barbara, CA) with V-shaped Si_3N_4 cantilevers (MSNL, Veeco, CA) with a nominal spring constant of 0.10 N × m^{-1}. Instrument was equipped with an "E" scanner (15 μm). To minimize the applied force on the sample, set point was continuously adjusted during imaging. Images were acquired at 0º scan angle with a scan rate of 1.5 Hz. All images were processed using the Veeco software.

3. Results

3.1. Peptide synthesis

E2(175–192) was chosen because it strongly inhibits the interaction and destabilization of membranes induced by the HIV FP, as shown by several biophysical techniques as isothermal titration calorimetry, surface plasmon resonance or vesicle content release assays [16,23]. It bears a net positive charge and contains 4 positively charged amino acids, which could be important for the interaction with negatively charged phospholipid membranes.

3.2. Surface activity measurements

Surface activity experiments give information about the capacity of a peptide to adsorb or incorporate into the air-buffered interface through the recording of the temporal change in surface pressure, π, at constant area, after peptide injection into the subphase. The adsorption kinetics of P59 or gp41-FP into the air-buffered interface was measured in the subphase at a range of peptide concentrations. A slight gradual adsorption of the peptide was observed at low concentration. The higher the peptide concentration in the subphase, the faster the incorporation and the higher the surface pressure achieved. Fig. 1A illustrates the adsorption isotherm profile. The shape of the surface activity curve approached a rectangular hyperbola, and it was fitted to Eq. (1) via nonlinear least-squares regression analysis:

$$\pi = \frac{c\pi_{sat}}{K + c}, \quad (1)$$

where c is the concentration, π^1_{sat} the saturation pressure or maximum pressure that can be achieved, and K is a characteristic constant equal to the peptide concentration that reaches half π_{sat}.

Fitting the data of P59, the values obtained were $\pi_{sat} = 13.80 \pm 1.8$ mN m^{-1}; $K = 167.0 \pm 62.6$ nM (R^2: 0.9576). A slightly lower value of K, 138 nM, was chosen for further penetration studies as it corresponds to the optimum peptide concentration that should be used in the bulk subphase for experiments of penetration kinetics, lower than the equilibrium spreading pressure of the peptide [20]. For gp41-FP results were $\pi_{sat} = 79.50 \pm 4.1$ mN m^{-1}; $K = 521.0 \pm 35.5$ nM (R^2: 0.9720).

On the basis of these results, it is possible to calculate the peptide surface excess concentration by applying the Gibbs adsorption equation in its simplest form (Eq. (2)).

$$\Gamma = \frac{1}{RT}\frac{\Delta\pi}{\Delta\, lnc}, \quad (2)$$

where R is the gas constant (8.314 J K^{-1} mol^{-1}), T is the temperature (293 K), $\Delta\pi$ is the pressure increase achieved 30 min after injection, and c is the peptide concentration.

The surface excess concentration was 1.28×10^{-6} and 4.75×10^{-6} mol m^{-2}, for P59 and gp41-FP, respectively which correspond to a molecular surface area of 1.29 nm^2 for P59 and 0.35 nm^2 for gp41-FP as calculated with Eq. (3):

$$A = \frac{1}{\Gamma N} \quad (3)$$

where N is Avogadro's constant.

The values are of the same order as those found for other peptide sequences of the same family [14,15,24].

In order to find out the effect of P59 on gp41-FP surface activity, the same set of experiments was done with the P59/gp41-FP (5:1 mixture). Results are reported as surface pressure versus P59 concentration (Fig. 1B). When the equivalent concentration of gp41-FP in the mixture was injected alone, the surface pressure was higher. Therefore, when P59 was incubated with gp41-FP and then injected, the rectangular hyperbola approached the values registered for P59 alone, suggesting that gp41-FP activity was neutralized ($\pi_{sat} = 19.1 \pm 2.1$ mN m^{-1}; $K = 250.0 \pm 9.5$ nM; R^2: 0.9836). These results indicate an inhibitory effect of P59 on gp41-FP surface activity.

[1] Many authors express this concept as π_{max} but in the present paper we name it π_{sat} to avoid misunderstanding with the maximum insertion pressure, expressed as π_{max} that will appear in the next section.

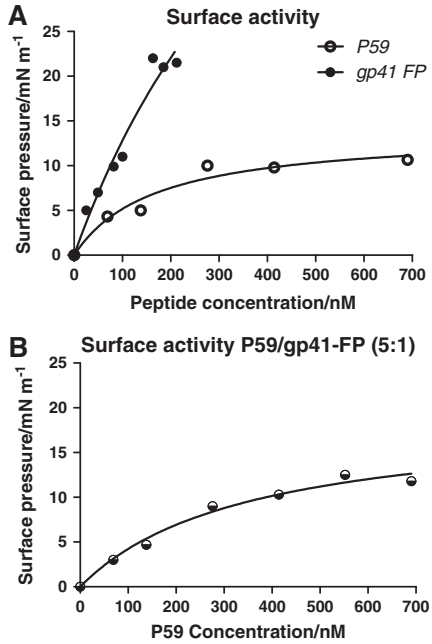

Fig. 1. Surface activity of A) P59 and gp41-FP and, B) P59/gp41-FP mixture (5:1) against free air-Tris buffered interface versus concentration. The subphase was continuously stirred.

3.3. Kinetics of penetration and maximum insertion pressure

The Langmuir film studies revealed that P59 and gp41-FP bind strongly to membranes, their intercalation into lipid monolayers being enhanced by the zwitterionic/negatively PC/PS (3:2) mixture. PC is the major component of the outer leaflet of uninfected cells, whereas PS, a hallmark of programmed cell death, is expressed at elevated levels in HIV-1-infected T cells and macrophages because of the association of apoptosis with the progression of AIDS [25–28].

The maximum insertion pressure (π_{max}) corresponds to the maximum surface pressure (minimum surface area) of the monolayer at which the interaction of a peptide with the lipids is energetically favorable. It is a useful parameter to determine the capacity of molecules of interest, in the present case peptides, to penetrate cell membranes. In lipid monolayers, π_{max} values of proteins are useful to characterize protein adsorption and lipid specificity without the need to use radiolabels or other tags [29]. Large π_{max} values (34–36 mN m^{-1}) have been reported for apolipoproteins and their C-terminal amphipathic α-helix. In contrast, low values of π_{max} (17–29 mN m^{-1}) correlate well with the lower capacity of N-terminal α-helices of apoproteins for the same function. Therefore, given that the membrane lateral pressure has been estimated to be between 30 and 35 mN m^{-1}, values found below this range indicate a lack of penetration while those above are characteristic of membrane-active compounds [30].

We performed various P59 penetration experiments using two phospholipids that differed in the nature of the head group: PC, zwitterionic, and PS, negatively charged, and a mixture of PC/PS (3:2). All the monolayers are in the liquid expanded state at the temperature used (ca 20 °C).

When the monolayer was of pure PC, a linear plot of $\Delta\pi$ versus π_o was obtained. The higher the π_o, the lower the $\Delta\pi$ regardless of peptide concentration in the subphase. In contrast, for PS monolayers, $\Delta\pi$ was highly dependent on P59 concentration. The initial experiments with P59 were done by injecting this peptide into the Teflon trough at a final concentration of 276 nM. In these experiments, $\Delta\pi$ was very similar to each initial surface pressure assayed, π_o, except for

π_o higher than 30 mN m^{-1} as an indication of monolayer saturation. When the concentration of P59 in the subphase was lower than 138 nM, a linear relationship was observed. Consequently, we chose this concentration for further experiments. These results show not only the high electrostatic component of the P59/membrane interaction, but also the utility of surface activity measurements to calculate the appropriate amount of sample to be injected into the subphase.

π_{max} values found for P59 were slightly higher for PS and for PC/PS (3:2) (around 41 mN m^{-1}) than for PC (36 mN m^{-1}), thereby indicating a better uptake by negatively charged phospholipids. Therefore, the PC/PS mixture (3:2) was chosen for the following experiments.

The next step was to analyze the interaction of gp41-FP and a P59/gp41-FP (5:1) mixture with PC/PS (3:2) monolayers. The various plots of pressure variation versus the initial surface pressure are shown in Fig. 2.

The maximum insertion pressures on PC/PS (3:2) monolayers obtained from extrapolation of the $\Delta\pi$ plot versus π_o to $\Delta\pi = 0$ were as follows: 41 mN m^{-1} for P59; 32 mN m^{-1} for gp41-FP and 46 mN m^{-1} for P59/gp41-FP (5:1). The π_{max} values of P59 alone or after incubation with gp41-FP were similar, what makes difficult the elucidation of the mechanism of the interaction. However, these values were consistent with surface activity measurements.

Given that the P59/gp41-FP molar ratio seems to be crucial for the inhibition, the kinetics of peptide insertion into PC/PS (3:2) monolayers was also studied at a P59/gp41-FP molar ratio of 1:1. Leakage experiments showed that when P59 was present at this molar ratio, it did not inhibit gp41-FP activity. In contrast, synergism between the two peptides was observed. Results gave a π_{max} of 38 mN m^{-1}, lower than the 46 mN m^{-1} found for the P59/gp41-FP (5:1) molar ratio. In both experiments, the concentration of gp41-FP injected into the subphase was the same (28 nM) but the concentration of P59 was lowered to 28 nM. At this concentration, P59 did not show a significant pressure increase even at low π_o but there was an increase in the π_{max} of gp41-FP when incubated with P59. If the behavior observed in penetration kinetics were a consequence of the activity of gp41-FP and P59 in an independent way, one would have expected a lower π_{max}, equal to π_{max} of gp41-FP when injected alone. Therefore, the increase in pressure appears to be a consequence of a P59–gp41-FP complex.

Although the data obtained with the Langmuir method are not enough to draw a clear conclusion, the results support the hypothesis of the formation and interaction of a P59–gp41-FP complex.

However, taking into consideration the charge of the peptides and the AFM observations (see below), we can relate electrostatic interactions of the peptides with the results on the kinetics of penetration. On the basis of the peptide sequences, P59 has 6 positive and 2 negative charges while gp41-FP has a single positive charge at the N-terminus (Table 1). Taking into account the charge distribution in the molecules, there may be an electrostatic attraction between the positive charge of gp41-FP and one of the negative charges of P59. Such an attractive force would lead to the formation of a peptide complex P59/gp41-FP and would be responsible for the increases in surface pressures observed. This longer structure would have two regions, one composed of neutral amino acids acting as hydrophobic tail, and another with positively charged amino acids, behaving as a polar head. Therefore, the activity of the P59/gp41-FP complex in PC/PS (3:2) monolayers would be the consequence of both electrostatic and hydrophobic interactions, as observed for P59 alone.

It is also relevant to point out that these results were observed only when peptides were incubated before their injection into the subphase; however, this effect was not detected when peptides were injected in a sequential way, first P59 and then gp41-FP or vice versa.

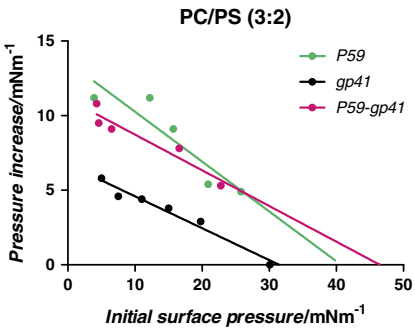

Fig. 2. Variation of the surface pressure as a function of the initial surface pressure of the PC/PS (3:2) phospholipid monolayer: black: gp41-FP; green: P59; red: P59–gp41-FP (5:1). P59 and gp41-FP concentration into the subphase (Tris pH:7.4) was 138 nM and 28 nM. This same concentration was injected when studying the mixture P59/gp41-FP (5:1).

3.4. Binding results

The interaction of P59 E2 peptide with HIV-1 FP or gp41-FP was examined by measuring its partitioning into PC/PS liposomes. The maximum wavelength of Trp emission (λ_{max}) of HIV-1 FP or gp41-FP shifted toward the blue in the presence of PC/PS LUVs (Fig. 3A). Specifically, λ_{max} decreased by more than 10 nm, which is consistent with the movement of HIV-1 FP or gp41-FP FP into a non polar environment of vesicle bilayers. The incubation of P59 with HIV-1 FP or gp41-FP prior to PC/PS titration prevented the shift of the Trp emission fluorescence (Fig. 3B). This observation thus indicates an interaction of E2 P59 with HIV-1 FP or gp41-FP that prevents the movement of the Trp residue to an environment of lower polarity provided by the vesicles.

Fluorescence titration was used to measure HIV-1 FP or gp41-FP partitioning quantitatively by measuring fluorescence intensity at the λ_{max} (346 nm). The partitioning isotherms (Fig. 3C) show that HIV-1 FP or gp41-FP partitioned strongly into PC/PS vesicles ($K_x = 1.9 \times 10^6$). The mole-fraction partition coefficient for HIV-1 FP or gp41-FP/P59 was 2.7×10^5, indicating that P59 impeded HIV-1 FP or gp41-FP binding to the PC/PS, the partition coefficient resulting one order of magnitude lower.

The interaction of synthetic peptides derived from HIV-gp41-FP and model membranes has been reported in several studies. Some agree in the efficiency of these peptides in inducing lipid mixing of negatively charged membranes whereas their activity toward zwitterionic membranes is very low [31,32]. However, a study of Kliger et al. [33] of a synthetic peptide (DP178) corresponding to a segment of gp41 of HIV-1 with either negatively charged or zwitterionic vesicles yielded similar results in binding experiments. In our study, as far as the physicochemical aspect of the interaction is concerned, results evidence the important role of both electrostatics and hydrophobic contribution in the fusion mechanism.

3.5. AFM observations

Up to know there are few references reporting the interaction of gp41-FP with lipid membranes by AFM [28]. Recently, Bitler et al. [34]

Table 1
Peptides characterization.

Peptide	Amino acid sequence[a]	Net charge	HPLC (k')[b]	ES-MS[c]
E2(175–192)	***R***FPF***HR***CGAGP***K***LT***K***DLE	+4	3.8	2072,42
gp41 FP	AVGIGALFLGFLGAAGSTMGAAS	+1	4.7	2036,80
[^{8}W] gp41 FP	AVGIGALWLGFLGAAGSTMGAAS	+1	3.4	2076,40

High performance liquid chromatography (HPLC) conditions: A: H_2O 0,05% trifluoroacetic acid (TFA)]; B: acetonitrile (0,05% TFA). Gradient 95% A to 5% A in 30 min, 1 mL min^{-1}. Kromasil C-18 column. Detection 215 and 280 nm.

[a] In italics and bold the cationic amino acid, underlined the anionic amino acid.
[b] Capacity factor.
[c] Electrospray mass spectrometry.

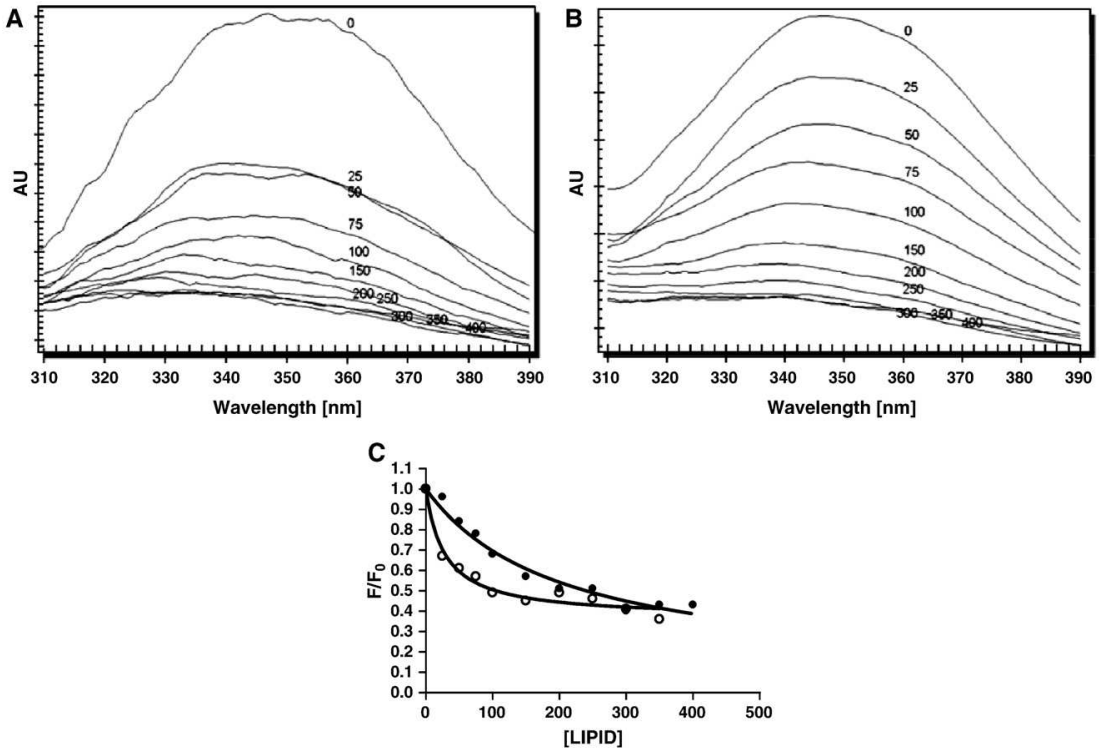

Fig. 3. Fluorescence emission spectra of: A) HIV-1 FP or gp41-FP and B) HIV-1 FP or gp41-FP/ P59 (1/5) mixture upon titration with PC/PS LUVs. C) Partitioning curves as estimated from the fractional change in Trp fluorescence in the presence of increasing amounts of PC/PS LUVs. The solid lines correspond to the best fits of the experimental values to a hyperbolic function. ○ HIV-1 FP or gp41-FP ; ● HIV-1 FP or gp41-FP / P59 (1/5).

have published a real-time kinetic study of the activity of gp41-FP and two mutants in the post-fusion state with nanometer resolution by AFM. AFM images revealed differences in the interaction of the three types of protein with zwitterionic and negatively charged membranes.

In the present work, AFM was used to study the structure and self-assembly of the two peptides and their mixture on the mica surface. Large round aggregates of peptide gp41-FP formed all over the surface (Fig. 4A). These aggregates showed a step height of 82 ± 10 nm with a mean diameter of 330 ± 30 nm. Aggregates were randomly distributed over the mica surface and no individual peptides were observed. In contrast round P59 peptide aggregates were smaller than gp41-FP aggregates with a height of 9.1 ± 1.6 nm with a mean diameter of 150 ± 30 nm (Fig. 4B). In this case, the mica surface was fully covered with a thin film. Although peptide aggregates were stable against contact mode scanning, the thin film was not. This effect can be observed from the enlargement of some soft features in the direction of the scan (horizontal).

Fig. 5 shows the adsorption of a mixture of P59 and gp41-FP (5:1, mol/mol) on the mica surface. The mixed peptides adsorbed aligned in preferential directions to form lines (Fig. 5A). Fig. 5B is a zoom image of these lines with an angle of $130 \pm 5°$ from the scan direction (horizontal). These lines can be identified as chains where each link is the pattern that repeats. Links (Fig. 5C) are rings with elliptical shape with a height of 1.3 ± 0.4 nm, first diameter of 130 ± 30 nm nm, second diameter of 98 ± 15 nm and with a ring thickness of 26 ± 6 nm.

The capacity of gp41-FP to form larger aggregates on mica (polar surface) than P59 suggests that peptides differ in their behavior when they interact with mica. The image of gp41-FP indicates more hydrophobic interactions than P59 (strongly charged), which can form a thin film on the mica surface.

Annular structures suggest morphological changes in the organization of peptides when gp41-FP and P59 were mixed in solution before deposition on the mica surface. P59 might stabilize gp41-FP molecules in solution, thereby protecting hydrophobic regions from the media. One possible scenario for the links could be the formation of mixed micelles: gp41-FP hydrophobic regions could arrange to form concentric and elongated structures. Positively charged amino acid on gp41-FP may be on the surface of the tube where P59 could be adsorbed (electrostatic interaction), thus stabilizing the structure against the media (Fig. 6).

When the same experiments were done with a mixture of P59/gp41-FP (1:1, mol/mol), these structures were not observed. These results do not match with the obtained with Langmuir studies in which no differences in interaction where observed at different P59/gp41-FP molar ratios. However, the AFM studies were performed under different experimental conditions to the monolayer experiments. While monolayers were done with samples in solution, in AFM, peptides were fixed to a negatively charged mica surface.

4. Conclusions

Using various techniques, here we have shown the capacity of P59, a sequence of the E2 protein of GBV-C virus, to inhibit gp41-FP.

Monolayer experiments showed a high surface activity of gp41-FP and to a lesser extent of P59. However, when peptides were mixed, surface activity was of the same order as that of P59, much lower than that observed for gp41-FP alone. Furthermore, P59, gp41-FP and their mixtures interacted with negatively charged lipid monolayers and to a lesser extent with zwitterionic monolayers. The values of π_{max} obtained

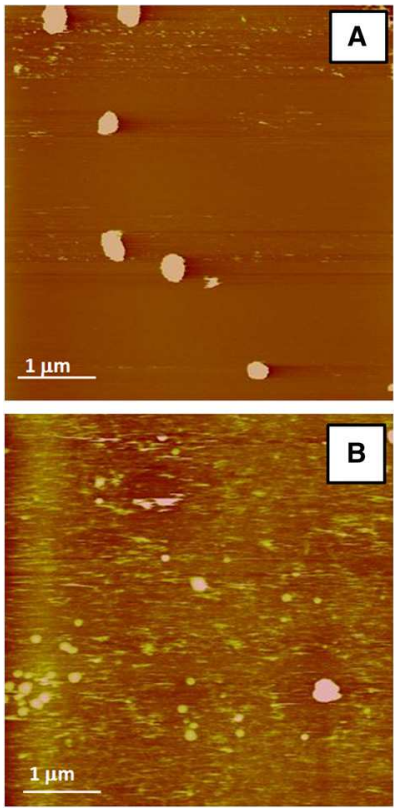

Fig. 4. AFM images of adsorbed peptide on mica surface, A) gp41-FP at a concentration of 5 μM and B) P59 at a concentration of 25 μM. Contact mode in liquid. Height scale bar is 20 nm.

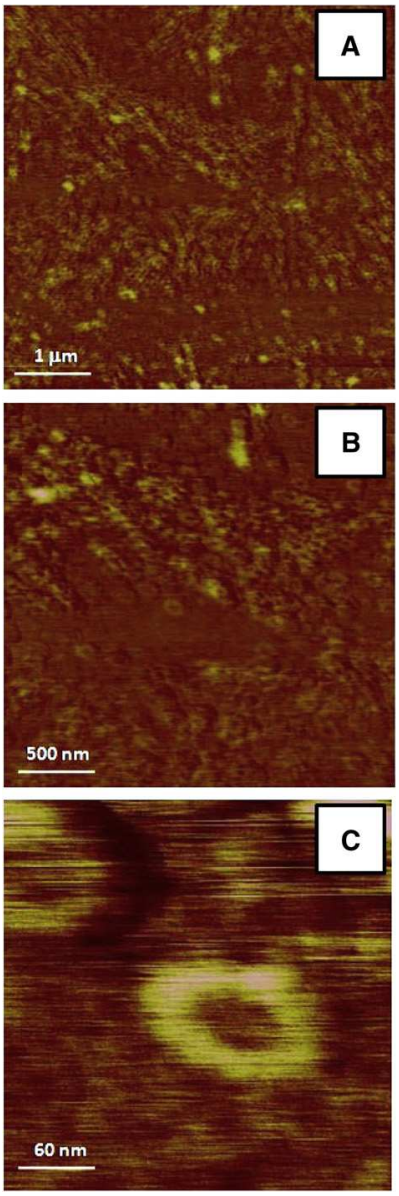

Fig. 5. A) AFM image of absorbed peptide mixture of gp41-FP and P59 (5:1, weight/weight) on mica surface. B) Zoom image from a) where chains are formed by links, and C) High magnification of one of these links. Contact mode in liquid. Height scale bar is 20 nm.

for P59, gp41-FP and the mixture P59/gp41-FP (5:1) indicate their strong affinity for phospholipid monolayers. Indeed, most of the π_{max} were over 30 mN m^{-1}, i.e., above the estimated lateral pressure of membranes. This observation suggests that the interactions of the peptides with biological membranes are thermodynamically favorable. Despite the high values of π_{max} for all the samples, the mixture P59/gp41-FP showed a lower value than the one observed for gp41-FP alone indicating a change in activity of gp41-FP in the vicinity of the monolayer. In addition, we propose that peptide/s–lipid monolayer interactions (at P59/gp41-FP molar ratios of 5:1 and 1:1) are governed mainly by electrostatic interactions but a hydrophobic contribution is also present.

Studies performed with lipid vesicles also indicated the capacity of P59 to decrease gp41-FP contact with the lipid membrane. This interaction was confirmed by AFM images showing different interaction of peptides with the polar surface of mica. While individual peptides aggregated in a different manner on the mica surface, the mixture formed a particular structure at a molar ratio of P59:gp41-FP (5:1) but not at a molar ratio of P59:gp41-FP (1:1). It is necessary here to clarify that peptide interactions with mica surface are not the same as those found with lipid membranes. In addition, the interaction of peptides with mica provides information on the interactions of peptides alone, and especially on the capacity of the mixture at a molar ratio of P59:gp41-FP (5:1) to modify their structure to form more stable aggregates in solution. One working hypothesis is that, at the nanoscale, gp41-FP molecules are surrounded by P59 molecules, which thus prevent the fusion of gp41-FP molecules with membranes.

Furthermore, many events at the membrane level are caused by conformational changes of peptide sequences when they are in the vicinity of the host cell. P59 has a short chain of 18 amino acids and it adopts an amphipathic random coil structure in aqueous solution, like other peptides of the same family [23]. In contrast, gp41-FP adopts a β−turn structure under the same conditions [35]. Herrera et al. [13] have shown that E2(259–287) interacts with HIV-1 FP and modifies its conformation. Therefore further studies should be developed to clarify the role of P59 in gp41-FP inhibition. This line of research should cover not only the conformational aspects of the interaction but also the stoichiometry of binding or the depth in which the sequences interact with the host membrane.

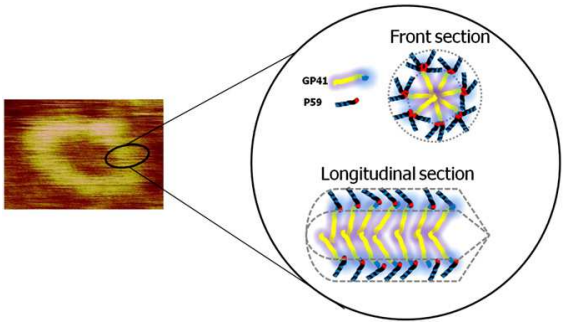

Fig. 6. Cartoon showing the possible organization of P59 and gp41-FP mixtures (P59/gp41-FP: 5:1, mol/mol) deduced from AFM results. Left) AFM image; Top Right) Cut of the wire showing the proposed mixed micellar structure formed by electrostatic attraction between the positive terminal charge of gp41-FP and one of the negative terminal charges of P59. Bottom Right) longitudinal view of the wire organized as an annular structure formed by P59/gp41-FP mixtures.

Acknowledgements

This work was supported by Grants CTQ2009-13969-C02-01/02 from the Ministerio de Ciencia e Innovación and by 2009SGR560 from the Generalitat de Catalunya, Spain. We thank Mrs. Tania Ballesteros for her technical assistance in the monolayer section. We are grateful to Robin Rycroft and Tanya Yates of the *Serveis Lingüístics* (UB) for their careful correction of grammar and stile. Finally, we would like to thank the referees for their suggestions to improve the manuscript.

References

[1] H.M.H. Mostafa, P. Ali-Akbar, M. Minoo, S. Zahra, A. Sedigheh, A. Mahnaz, S. Shahram, N. Mahin, M. Reza, Evaluation of circulating natural type 1 interferon-producing cells in HIV/GBV-C and HIV/HCV coinfected patients: a preliminary study, Arch. Med. Res. 38 (2007) 868–875.
[2] H.L. Tillmann, T. Kaiser, Z. Fox, S. Staszewski, F. Antunes, A. Monforte, P. Vernazza, A. Hill, U.B. Dragsted, J.D. Lundgren, Impact of coinfection with HIV-1 and GB virus C in patients receiving a ritonavir-boosted HAART regimen: a substudy to the MaxCmin1 trial, J. Acquir. Immune Defic. Syndr. 40 (2005) 378–380.
[3] C.F. Williams, D. Klinzman, T.E. Yamashita, J. Xiang, P.M. Polgreen, C. Rinaldo, C. Liu, J. Phair, J.B. Margolick, D. Zdunek, et al., Persistent GB-virus C infection and survival in HIV-infected men, N. Engl. J. Med. 350 (2004) 981–990.
[4] M.D. Berzsenyi, D.S. Bowden, S.K. Roberts, P.A. Revill, GB virus C genotype 2 predominance in a hepatitis C virus/HIV infected population associated with reduced liver disease, J. Gastroenterol. Hepatol. 24 (2009) 1407–1410.
[5] M.D. Berzsenyi, D.S. Bowden, S.K. Roberts, GB virus C: insights into co-infection, J. Clin. Virol. 33 (2005) 257–266.
[6] P. Björkman, L. Flamholc, V. Molnegren, A. Marshall, N. Güner, A. Widell, Enhanced and resumed GB virus C replication in HIV-1-infected individuals receiving HAART, AIDS 21 (2007) 1641–1643.
[7] M. Fernández-Vidal, M.D. Cubero, G. Ercilla, M.J. Gomara, I. Haro, I. Application of a chimeric synthetic peptide in the development of a serologic method for the diagnosis of hepatitis G virus infection, Protein Pept. Lett. 14 (2007) 865–870.
[8] M.J. Gomara, I. Haro, Synthetic peptides for the immunodiagnosis of human diseases Cur, Med. Chem. 14 (2007) 531–546.
[9] W.B. Supapol, R.S. Remis, J. Raboud, M. Millson, J. Tappero, R. Kaul, P. Kulkarni, M.S. McConnell, P.A. Mock, M. Culnane, et al., Reduced mother-to-child transmission of HIV associated with infant but not maternal GB virus C infection, J. Infect. Dis. 197 (2008) 1369–1377.
[10] J.T. Stapleton, K. Chaloner, J. Zhang, D. Klinzman, I.E. Souza, J. Xiang, A. Landay, J. Fahey, R. Pollard, R. Mitsuyasu, GBV-C viremia is associated with reduced CD4 expansion in HIV-infected people receiving HAART and interleukin-2 therapy, AIDS 23 (2009) 605–610.
[11] E.L. Mohr, J.T. Stapleton, GB virus type C interactions with HIV: the role of envelope glycoproteins, J. Viral. Hepat. 16 (2009) 757–768.
[12] S. Mazzini, M. Fernandez-Vidal, V. Galbusera, F. Castro-Roman, M.C. Bellucci, E. Ragg, I. Haro, 3D-Structure of the interior fusion peptide of HGV/GBV-C by 1H NMR, CD and molecular dynamics studies, Arch. Biochem. Biophys. 465 (2007) 187–196.
[13] E. Herrera, M.J. Gomara, S. Mazzini, E. Ragg, I. Haro, Synthetic peptides of hepatitis G virus (GBV-C/HGV) in the selection of putative peptide inhibitors of the HIV-1 fusion peptide, J. Phys. Chem. B 113 (2009) 7383–7391.
[14] O. Fontvila, C. Mestres, M. Munoz, I. Haro, M.A. Alsina, M. Pujol, Surface behavior and peptide–lipid interactions of the E1(3–17)R and E1(3–17)G peptides from E1 capsid protein of GBV-C/HGV virus, Coll. Surf. A Physicochemical Eng. Aspects 321 (2008) 175–180.
[15] S. Pérez-Lopez, M. Nieto-Suarez, C. Mestres, M.A. Alsina, I. Haro, N. Vila-Romeu, Behaviour of a peptide sequence from the GB virus C/hepatitis G virus E2 protein in Langmuir monolayers: its interaction with phospholipid membrane models, Biophys. Chem. 141 (2009) 153–161.
[16] E. Herrera, S. Tenckhoff, M.J. Gomara, R. Galatola, M.J. Bleda, C. Gil, G. Ercilla, J.M. Gatell, H.L. Tillmann, I. Haro, Effect of synthetic peptides belonging to E2 envelope protein of GB virus C on human immunodeficiency virus Type 1 infection, J. Med. Chem. 53 (2010) 6054–606316.
[17] K. El Kirat, S. Morandat, Y.F. Dufrene, Nanoscale analysis of supported lipid bilayers using atomic force microscopy, Biochim. Biophys. Acta 1798 (2010) 750–765.
[18] O. Domenech, G. Francius, P.M. Tulkens, F. Van Bambeke, Y. Dufrêne, M.P. Mingeot-Leclercq, Interactions of oritavancin, a new lipoglycopeptide derived from vancomycin, with phospholipid bilayers: Effect on membrane permeability and nanoscale lipid membrane organization, Biochim. Biophys. Acta 1788 (2009) 1832–1840.
[19] K.J. Weronski, P. Cea, I. Diez-Pérez, M.A. Busquets, J. Prat, V. Girona, Time-lapse atomic force microscopy observations of the morphology, growth rate, and spontaneous alignment of nanofibers containing a peptide–amphiphile from the hepatitis G virus (NS3 Protein), J. Phys. Chem. B 114 (2010) 620–625.
[20] M. Rafalski, J.D. Lear, W.F. DeGrado, Phospholipid interactions of synthetic peptides representing the N-terminus of HIV gp41, Biochemistry 29 (1990) 7917–7922.
[21] N. Rojo, M.J. Gómara, M.A. Busquets, M.A. Alsina, I. Haro, Interaction of E2 and NS3 synthetic peptides of GB virus C with model lipid membranes, Talanta 60 (2003) 395–404.
[22] W.C. Wimley, S.H. White, Designing transmembrane alpha-helices that insert spontaneously, Biochemistry 39 (2000) 4432–4442.
[23] M.J. Gomara, M. Lorizate, N. Huarte, I. Mingarro, E. Perez-Paya, J.L. Nieva, Hexapeptides that interfere with HIV-1 fusion peptide activity in liposomes block GP41-mediated membrane fusion, FEBS Lett. 580 (2006) 2561–2566.
[24] M.J. Sanchez-Martin, I. Haro, M.A. Alsina, M.A. Busquets, M. Pujol, A Langmuir monolayer study of the interaction of E1(145–162) Hepatitis G virus peptide with phospholipid membranes, J. Phys. Chem. B 114 (2010) 448–456.
[25] M.K. Callahan, P.M. Popernack, S. Tsutsui, L. Truong, R.A. Schlegel, A.J. Henderson, Phosphatidylserine on HIV envelope is a cofactor for infection of monocytic cell, J. Immunol. 170 (2003) 4840–4845.
[26] G. Ma, T. Greenwell-Wild, K. Lei, W. Jin, J. Swisher, N. Hardegen, C.T. Wild, S.M. Wahl, Secretory leukocyte protease inhibitor binds to annexin II a cofactor for macrophage HIV-1 infection, J. Exp. Med. 200 (2004) 1337–1346.
[27] H. Garg, R. Blumenthal, Role of HIV gp41 mediated fusion/hemifusion in bystander apoptosi, Cell. Mol. Life Sci. 65 (2008) 3134–3144.
[28] N. Lev, Y. Fridmann-Sirkis, L. Blank, A. Bitler, R.F. Epand, R.M. Epand, Y. Shai, Conformational stability and membrane interaction of the full-length ectodomain of HIV-1 gp41: implication for mode of action, Biochemistry 48 (2009) 3166–3175.
[29] P. Calvez, S. Bussières, E. Demers, C. Salesse, Parameters modulating the maximum insertion pressure of proteins and peptides in lipid monolayers, Biochimie 91 (2009) 718–733.
[30] D. Marsh, Lateral pressure in membranes, Biochim Biophys. Acta 1286 (1996) 183–193.
[31] R. Pascual, M. Contreras, A. Fedorov, M. Prieto, J. Villalain, Interaction of a peptide derived from the N-heptated repeat region of gp41 Env ectodomain with model membranes. Modulation phospholipid phase behavior, Biochemistry 44 (2005) 14275–14288.
[32] M.R. Moreno, M. Giudici, J. Villalain, The mebranotropic regions of the endo and ecto domains of HIV gp41 envelope glycoprotein, Biochim. Biophys. Acta 1758 (2006) 111–123.
[33] Y. Kliger, S.A. Gallo, S.J. Peisajovich, I. Muñoz-Barroso, S. Avkin, R. Blumenthal, Y. Shai, Mode of action of an antiviral peptide from HIV-1, J. Biol. Chem. 12 (2001) 1391–1397.
[34] A. Bitler, N. Lev, Y. Fridmann-Sirkis, L. Blank, S.R. Cohen, Y. Shai, S. Yechiel, Kinetics of interaction of HIV fusion protein (gp41) with lipid membranes studied by real-time AFM imaging, Ultramicroscopy 110 (2010) 694–700.
[35] K. Sackett, M.J. Nethercott, R.F. Epand, R.M. Epand, D.R. Kindra, Y. Shai, D.P. Keliky, Comparative analysis of membrane-associated fusion peptide secondary structure of HIV gp41 constructs that model the early pre-hairpin intermediate and final hairpin conformations, J. Mol. Biol. 397 (2010) 301–315.

Introduction

Theranostic approaches are in the borderline among several scientific disciplines, including chemistry, biology, medicine, pharmacy, nanotechnology and imaging (1) and aim at the simultaneous diagnostic and therapy of diseases (2). These methods constitute a very useful tool to visualize solid tumors, abnormal proteins and perturbating events in living cells, and are normally based on the use of radioisotopic or fluorimetric techniques. Radionuclide-based agents have the advantage of allowing the exploration of inner target tissues, which is not possible with the currently available fluorescence-based imaging systems. This limitation notwithstanding, fluorimetric agents are being increasingly adopted for *in vitro* studies in cell and tissue cultures. Furthermore, fluorescent probes present the outstanding advantage of avoiding the hazards inherent to the handling of radioactive substances. In this context, we report here preliminary studies of the use of styrylquinolines as theranostic agents for Alzheimer's disease on the basis of their potential pharmacological activity and their suitable fluorescence solvatochromic effect.

Results and discussion

Styrylbenzoxazoles have been recently employed to detect β-amyloid plaques (3). A library of styrylquinoline derivatives was synthesized (4) to test their activity against protein misfolding diseases. Three compounds belonging to this library were selected to study their binding ability towards amyloid fibrils. The flexible ethylene chain makes the probes sensitive to different conformational states of the biomolecules and the presence of aromatic moieties conjugated to ethylene chain makes them good candidates to discriminate between the amyloid fibrils and the aggregates of the amyloid plaques on the basis of changes in their fluorescence properties (5). Figure 1 shows the chemical structures and the fluorescence emission maxima of the compounds under study in aqueous solution. These compounds have shown to be very sensitive to changes in the environment (solvent and pH). Thus, the protonation of the quinoline nitrogen under acidic conditions (pH < 2.0) causes a red shift in the fluorescence emission maxima of compounds **1** and **2**, but a blue shift in the fluorescence emission wavelength of the amino derivative **3**. The spectral shape as well as the position and intensity of the maxima of styrylquinoline sensors are dependent also on the solvent polarity. As can be appreciated in Figure 2, in the case of compound **1**, the fluorescence emission maximum is shifted from 311 nm in cyclohexane to 405 in water. A good correlation between solvent polarity (evaluated as dielectric constant or E_T (30) values) and the position of the emission maxima was observed. In all compounds the fluorescence maxima were red-shifted in aqueous solution with regard to the emission observed in polar or apolar organic solvents. Consequently, these compounds are good candidates to recognize the characteristic fibrilar aggregates appearing in Alzheimer's disease, as the sensors in aqueous solution showed a red-shifted emission band and the fluorescence emission is expected to be blue-shifted in the presence of β-amyloid fibril aggregate, as corresponds to a lower-polarity and more rigid environment. In conclusion, the simplicity and sensitivity of fluorescence techniques in the studies of the interactions between probes and proteins make fluorimetry (6) a valuable screening method for developing β-amyloid image sensors.

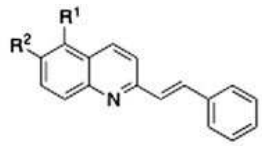

COMPOUND	R^1	R^2	λ_{em} (nm) (water)	λ_{em} (nm) (acidic water)
1	-H	$-CH_3$	405	447
2	-H	-OCH3	412	457
3	$-NH_2$	$-CH_3$	560	430

Figure 1. Chemical structures and fluorescence emission wavelengths of the styrylquinolines studied in aqueous solution.

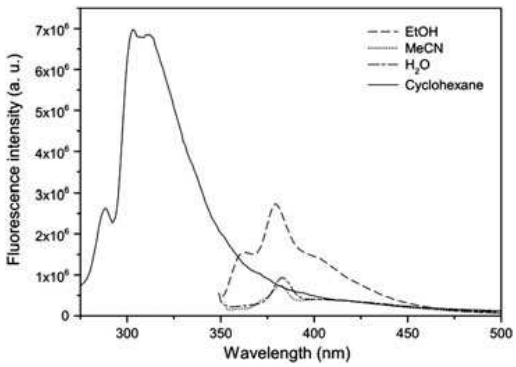

Figure 2. Solvent polarity effect on the fluorescence spectra of compound **1** in different solvents.

Acknowledgements

Financial support from MICINN, Spain (grants CTQ 2009-11312-BQU and CTQ2009-12320-BQU) and Grupos de Investigación UCM (GR35/10-A-920234) are gratefully acknowledged. V. González-Ruiz is grateful to MEC, Spain, for a FPU Research Fellowship.

References

1. Nystrom AM, Wooley KL. The Importance of chemistry in creating well-defined nanoscopic embedded therapeutics: devices capable of the dual functions of imaging and therapy. Acc Chem Res 2011;44:969–78.
2. Lammers T, Aime S, Hennink WE, Storm G, Kiessling F. Theranostic nanomedicine. Acc Chem Res 2011;44:1029–38.
3. Morais GR, Miranda HV, Santos IC, Santos I, Outeiro TF, Paulo A. Synthesis and in vitro evaluation of fluorinated styryl benzazoles as amyloid-probes. Bioorg Med Chem. 2011;19:7698–710.
4. Sridharan V, Avendaño C, Menéndez, JC. Convenient, two-step synthesis of 2-styrylquinolines: an application of the CAN-catalyzed vinylogous type-II Povarov reaction. Tetrahedron 2009;65: 2087–96.
5. Peter K, Nilsson R. Small organic probes as amyloid specific ligands-Past and recent molecular scaffolds. FEBS Lett 2009;583:2593–9.
6. Beckford G, Owens E, Henary M, Patonay G. The solvatochromic effects of side chain substitution on the binding interaction of novel tricarbocyanine dyes with human serum albumin. Talanta 2012;92: 45–52.

Study of the interaction between the HIV-1 fusion peptide and E1/E2 GB virus c derived peptides

R. Galatola[1], M. J. Gómara[1,3], M. Escarrà[1], M. J. Bleda[1], M. Pujol[2,3], M. A. Alsina[2,3], I. Haro[1,3]
[1]Unit of Synthesis and Biomedical Applications of Peptides. IQAC-CSIC. Jordi Girona, 18-26 08034 Barcelona, Spain
[2]Physical Chemistry Department, Faculty of Pharmacy. University of Barcelona. Av. Joan XXIII s/n, 08028 Barcelona, Spain
[3]Grupo de Péptidos y Proteínas: Estudios Fisicoquímicos. Unidad Asociada UB-CSIC

LUMINESCENCE
The Journal of Biological and Chemical Luminescence

Keywords: GB virus C; HIV-1 Fusion peptide; E1/E2 peptides; Solid-Phase Peptide Synthesis; Leakage assay

Recent studies of GBV-C and its interaction with host cells provide new insights into the observed associations between GBV-C infection and improved survival in HIV-positive individuals (reviewed in ref.1). One of the proposed mechanisms by which GBV-C modulates HIV infection and AIDS progression involves inhibiting HIV replication by GBV-C proteins. In our hands, certain 18-mer peptide sequences of the E2 envelope protein of the GB virus C

Peptide	Primary Sequence	Peptide	Primary Sequence
E1P8 (parent)	APEDIGFCLEGGCLVALG	**E2P45 (parent)**	SDRDTVVELSEWGVPCAT
P8-1	AAEDIGFCLEGGCLVALG	**P45-1**	ADRDTVVELSEWGVPCAT
P8-2	APADIGFCLEGGCLVALG	**P45-2**	SARDTVVELSEWGVPCAT
P8-3	APEAIGFCLEGGCLVALG	**P45-3**	SDADTVVELSEWGVPCAT
P8-4	APEDAGFCLEGGCLVALG	**P45-4**	SDRATVVELSEWGVPCAT
P8-5	APEDIAFCLEGGCLVALG	**P45-5**	SDRDAVVELSEWGVPCAT
P8-6	APEDIGACLEGGCLVALG	**P45-6**	SDRDTAVELSEWGVPCAT
P8-7	APEDIGFALEGGCLVALG	**P45-7**	SDRDTVAELSEWGVPCAT
P8-8	APEDIGFCAEGGCLVALG	**P45-8**	SDRDTVVALSEWGVPCAT
P8-9	APEDIGFCLAGGCLVALG	**P45-9**	SDRDTVVEASEWGVPCAT
P8-10	APEDIGFCLEAGCLVALG	**P45-10**	SDRDTVVELAEWGVPCAT
P8-11	APEDIGFCLEGACLVALG	**P45-11**	SDRDTVVELSAWGVPCAT
P8-12	APEDIGFCLEGGALVALG	**P45-12**	SDRDTVVELSEAGVPCAT
P8-13	APEDIGFCLEGGCAVALG	**P45-13**	SDRDTVVELSEWAVPCAT
P8-14	APEDIGFCLEGGCLAALG	**P45-14**	SDRDTVVELSEWGAPCAT
P8-15	APEDIGFCLEGGCLVAAG	**P45-15**	SDRDTVVELSEWGVACAT
P8-16	APEDIGFCLEGGCLVALA	**P45-16**	SDRDTVVELSEWGVPAAT
P8-17	APQDIGFCLEGGCLVALG	**P45-17**	SDRDTVVELSEWGVPCAA
P8-18	APENIGFCLEGGCLVALG	**P45-18**	SDRDTVVQLSQWGVPCAT
P8-19	APEDIGFCLQGGCLVALG	**P45-19**	SNRNTVVELSEWGVPCAT
P8-20	APQNIGFCLQGGCLVALG	**P45-20**	SNRNTVVQLSQWGVPCAT
P8-21	APRDIGFCLEGGCLVALG	**P45-21**	SNXNTVVQLSQWGVPCAT
P8-22	APRRIGFCLEGGCLVALG	**P45-22**	SDXDTVVELSEWGVPCAT
P8-23	APRRIGFCLRGGCLVALG	**P45-23**	SDRDTVVELSEFGVPCAT

Table 1. Primary sequence of E1P8 and E2P45 peptide analogues

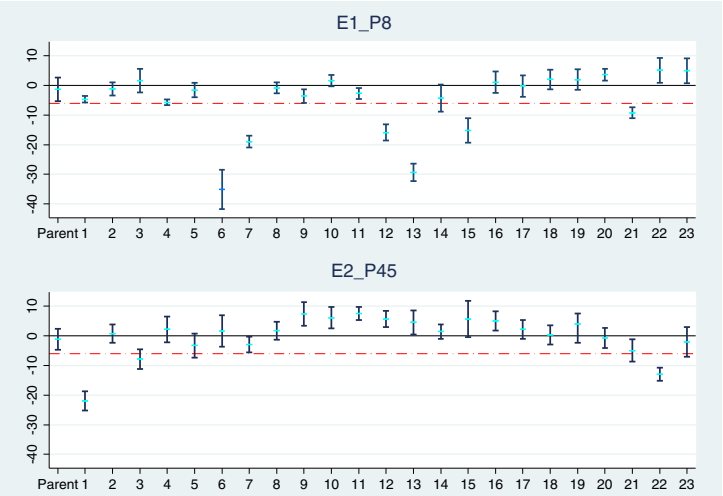

Figure 1. Inhibitory effect of E1P8 and E2P45 peptide analogues on HIV-1 FP induced leakage. The molar ratio of the HIV-1 FP : GBV-C peptides is 1:10.

(GBV-C) notably decrease cellular membrane fusion and interferes with the HIV-1 infectivity highlighting their potential utility in future anti-HIV-1 therapies[2]. Besides, the interaction of other GBV-C peptide sequences of the E1 envelope protein with the HIV-1 fusion peptide as well as the inhibition of the membrane fusion process has been determined through the use of several biophysical techniques[3]. Based on these findings, two peptide sequences from E2 and E1 GBV-C proteins, E2(133-150) (namely E2P45) and E1(22-39) (namely E1P8), have been selected. In order to perform a systematic trial on the structure-activity relationship of these sequences, forty six peptide analogues were analysed in which each of the amino acid residues was replaced by L-Ala (Table 1). The influence of the total net load of the peptides on the activity through the replacement of residues loaded with neutral amino acids was also studied. Thus, the critical residues for the interaction of the parent peptides with HIV-1 Fusion Peptide (FP) were determined.

The E1 and E2 peptide analogues were evaluated in regard to their capacity to inhibit the destabilisation process of lipid vesicles induced by the HIV-1 FP. Thus, the biophysical assay on vesicular content leakage was performed. Unilamellar lipid vesicles containing fluorescent probes 8-aminonaphtalene-1,3,6-trisulfonic acid disodium salt (ANTS) and p-xylenebispiridinium bromide (DPX) were prepared according to the protocol previously described (2,3). Peptides were mixed with the HIV-1 FP in DMSO prior to their addition to the liposome suspension, recording the emission of the ANTS probe at 520 nm. The trials were performed in a PTI QM4CW spectrofluorimeter. The screening of the peptide was carried out in 96 well plates. Intra- and inter-assay fluorescence variations were analysed by performing each plate by triplicate and repeated five times in different days using Quantile Regression Models (Median Regression) (4). Five E1 (P8-6, P8-7, P8-12, P8-13 and P8-15) and three E2 (P45-1, P45-3 and P45-22) peptide analogues were selected on the basis of a higher estimated median difference effect comparing to parent peptides (Figure 1). Both sets of most active analogues deserve more attention and will be evaluated in further biological studies such as cell-cell fusion or viral inhibition assays to analyse their potential as anti-HIV-1 agents.

Acknowledgements
This work was funded by grants CTQ2009-13969-CO2-01/02 from the Ministerio de Ciencia e Innovación, Spain and FIPSE 36-0735-09

References

1. Bhattarai N, Stapleton JT. GB virus C: the good boy virus? Trends in Microbiology 2012;20:124–30.
2. Herrera E, Tenckhoff S, Gómara MJ, Galatola R, Bleda MJ, Gil, C, Ercilla G, Gatell JM, Tillmann H, Haro I. Effect of synthetic peptides belonging to E2 envelope protein of GB virus C on human immunodeficiency virus type 1 infection. J Med Chem 2010;53:6054–63.
3. Sánchez-Martín MJ, Hristova K, Pujol M, Gómara MJ, Haro I, Alsina MA, Busquets MA. Analysis of HIV-1 fusion peptide inhibition by synthetic peptides from E1 protein of GB virus C. J. Colloid Interface Sci. 2011;360:124–31.
4. Koenker R. In: *Quantile Regression*. New York: Cambridge University Press, 2005.

Autofluorescence characterization of the pattern formation of gurken distribution in drosophila oogenesis by lie group analysis

J.C. Wang[1]; K.L. Wu[1]; W.C. Lin[1]; L.M. Pai[2]; P.Y. Wang[2]; R.R. Huang[1]; H.I. Chen[1]; C.H. Fan[1]; and T.E. Nee[1,*]
[1]Graduate Institute of Electro-Optical Engineering and Department of Electronic Engineering, Chang Gung University, Kwei-Shan, Tao-Yuan 333, Taiwan, Republic of China.
[2] Department of Biochemistry, Chang Gung University, Kwei-Shan, Tao-Yuan 333, Taiwan, Republic of China, E-mail: neete@mail.cgu.edu.tw

Keywords: Autofluorescence; Drosophila oogenesis; Gurken; Lie group

Introduction

The morphogen distributions are crucial for understanding their effects on cell-fate determination, yet it is difficult to quantitate and obtain such information through direct measurements. The developments of higher organisms are derived from

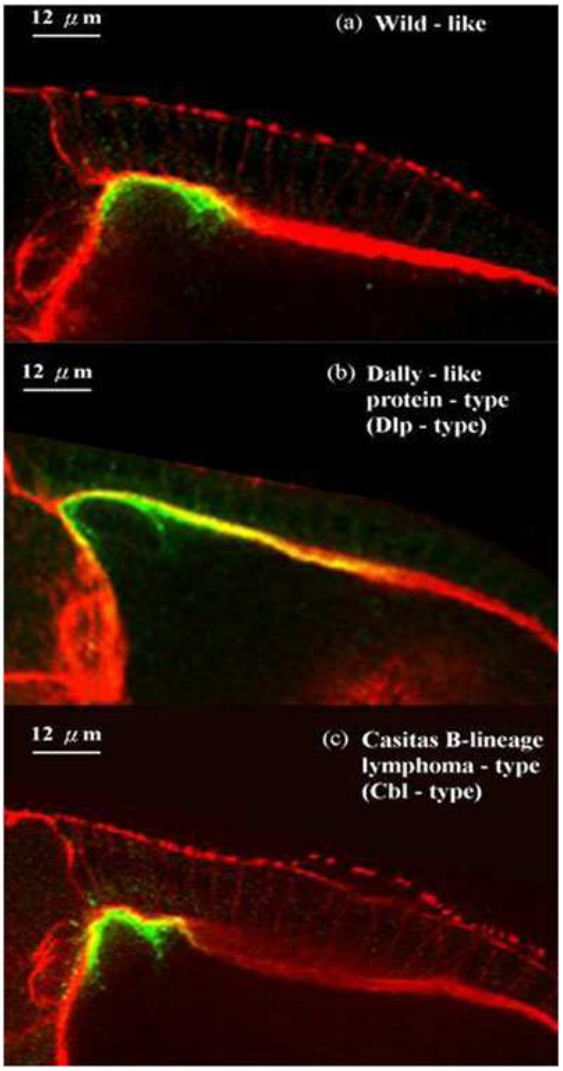

Figure 1. The partial distribution of the Gurken gradient in the stage 10A egg chambers for (a) wild-type, (b) overexpressing Dlp, and (c) overexpressing Cbl. The scale bars both are 12 μm in Figures. 1 (a), (b) and (c), respectively.

FINAL

Send Orders for Reprints to reprints@benthamscience.net

Current Medicinal Chemistry, 2013, *20*, ????-????

HIV-1 Inhibiting Capacity of Novel Forms of Presentation of GB Virus C Peptide Domains is Enhanced by Coordination to Gold Compounds

María J. Gómara[1], Ramona Galatola[1], Alejandro Gutiérrez[2], María C. Gimeno[2], José M. Gatell[4], Víctor Sánchez-Merino[3], Eloísa Yuste[3] and Isabel Haro[1]

[1]*Unit of Synthesis and Biomedical Applications of Peptides, IQAC-CSIC, Spain;* [2]*Departamento de Química Inorgánica, Instituto de Síntesis Química y Catálisis Homogénea ISQCH-CSIC, Spain;* [3]*AIDS Research Unit-HIVACAT, Institut d'Investigacions Biomediques August Pi i Sunyer Barcelona, Spain;* [4]*Infectious Diseases Unit- HIVACAT, Hospital Clinic, Barcelona, Spain.*

Abstract: Following the report of beneficial effects of co-infection by GB virus C (GBV-C) for HIV-infected patients, we have studied synthetic GBV-C peptides and their relationship with HIV type-1. This paper reports the design and synthesis of new forms of presentation of two peptide inhibitors corresponding to the envelope proteins E1 and E2 of GBV-C, together with a study of their anti-HIV-1 activity. Homogeneous and heterogeneous multiple antigenic peptides (MAPs), lipophilic derivatizations, cyclization and peptide–gold conjugations are the chemical design strategies adopted. Our aim is to enhance the anti-viral potency of the GBV-C peptide domains. Of all the GBV-C peptide derivatives studied, peptide–gold complexes derived from the (22-39) sequence of the GBV-C E1 protein were the most active entry inhibitors. These results support the putative modulation of HIV-1 infection by the GBV-C E1 protein and open new perspectives for the development of novel peptide-derived HIV-1 entry inhibitors.

Keywords: Anti-HIV assays, cell–cell fusion assays, cyclic peptides, GBV-C, HIV-1, lipopeptides, multiple antigenic peptides, peptide–gold complexes.

INTRODUCTION

The use of synthetic peptides as human immunodeficiency virus type-1 (HIV-1) inhibitors has been the subject of research over recent years. A large number of peptides that could be used to target different stages of the HIV-1 life cycle continue to be studied for their clinical application in the fight against HIV-1 infection. The main advantages of synthetic peptides as therapeutic agents are their low systemic toxicity and the possibility of structurally modifying them so they mimic certain substrates or epitopes.

HIV-1-inhibiting peptides have been identified and/or developed using different methods. Some therapeutic peptides such as Enfuvirtide, already approved for clinical use [1], are derived from HIV-1. Others are natural peptides such as chemokines, defensins or the "virus inhibitory peptide" (VIRIP) [2]; while still others have been designed and synthesized from crystallographic data on HIV-1 proteins or from peptide libraries [3].

Initial attempts to derive therapeutic applications focused on HIV-coded enzymes (reverse transcriptase, protease and, more recently, integrase). Currently, however, structural HIV proteins and, more specifically, the mechanisms by which the virus infects the cell and replicates are also considered therapeutic targets.

*Address correspondence to this author at the Unit of Synthesis and Biomedical Applications of Peptides, IQAC-CSIC, Spain;
Tel: 34934006109; E-mail: isabel.haro@iqac.csic.es

At present, interest in viral fusion and entry inhibitors is growing significantly [4], since they can be applied in combined therapies or when resistance to other antiretroviral drugs is encountered. Furthermore, these inhibitors act before the virus enters the cell, which could have the same potential as the inducing of immunity by a vaccine.

Following the report of beneficial effects for HIV-infected patients of co-infection by GB virus C (GBV-C) [5], our research group decided to study synthetic GBV-C peptides and their relationship with HIV-1. Recent studies of GBV-C and its interaction with host cells provide new insights into the associations observed between GBV-C infection and improved survival in HIV-positive individuals. Although the mechanism by which GBV-C modulates HIV infection and the progression of AIDS is not fully understood, the existing data on potential mechanisms by which GBV-C interferes with HIV has recently been reviewed [6]. One of the proposed mechanisms involves the inhibition of HIV replication by GBV-C proteins (E2 glycoprotein and NS5A phosphoprotein) [7-9]. It has been reported that the GBV-C E2 protein directly inhibits HIV pseudovirus entry, and that peptides derived from this E2 protein interfere with HIV cellular binding and fusion, independently of the viral effect on CD4 cell homeostasis [8, 10]. The same group has now identified the region of the GBV-C E2 protein involved in HIV inhibition [11] and proposed that this region, the E2(276-292) peptide, does not inhibit HIV replication unless it is fused to a TAT protein transduction domain for cellular uptake. Presumably, it does not present the structural motif

0929-8673/13 $58.00+.00

required to inhibit HIV on its own, but needs to be combined with an element capable of penetrating the cell membrane. The peptide has to be taken up by or expressed within cells to effectively inhibit HIV entry and replication. The inhibition seems to be specific to HIV, as the entry of neither the yellow fever virus (YFV) nor the mumps virus was inhibited in cells expressing GBV-C E2. Addition of the GBV-C E2 peptide motif to the HIV TAT protein inhibited different HIV isolates including T-20-resistant strains; which suggests that the mechanism of entry inhibition is different from that of T-20 and other HIV gp41 peptides.

In different research, gold-based drugs have been effectively used in the treatment of many diseases [12] and recently their anti-HIV activity has been reported. Okada *el al.* demonstrated that some commercial drugs, such as *Aurothioglucose* and *Aurothiomalate*, are inhibitors of HIV. The inhibition takes place through coordination of the gold(I) fragment to the exposed acidic thiol groups of the viral surface proteins as well as by inhibition of the reverse transcriptase [13]. Administration of gold–phosphine complexes, such as the antiarthritic agent *Auranofin*, led to an increase in the CD4+ count of an HIV patient being treated for psoriatic arthritis [14], and other gold(I)–phosphine complexes have been shown to inhibit reverse transcriptase or protease [15]. Furthermore, several compounds of gold(III) with porphyrins or Schiff bases have been patented due to their considerable anti-HIV activity [16]. Recently, Bowman *et al.* demonstrated that multivalent gold nanoparticles can inhibit HIV fusion [17].

We have previously shown that certain 18-mer peptide sequences of the GBV-C E2 envelope protein decrease cellular membrane fusion and interfere with HIV-1 infectivity; which indicates their potential utility in future anti-HIV-1 therapies [18]. The interaction of other GBV-C peptide sequences from the E1 envelope protein with the HIV-1 fusion peptide has also been established through the use of several biophysical techniques [19]. Furthermore, the same research has shown that some of those peptide sequences inhibit the HIV-1 membrane fusion process.

Based on these findings, two peptide sequences from the GBV-C E1 and E2 proteins—E1(22-39) and E2(133-150)—were selected for study. In this work, we report the design and synthesis of new forms of presentation of the selected GBV-C envelope peptide sequences, together with an evaluation of their anti-HIV-1 activity. Our aim is to discover novel presentations of the parent peptides with enhanced antiviral activity.

MATERIALS AND METHODS

1. Synthesis of Peptides

1.1. Multiple Synthesis of Peptide Analogues

Twenty-three peptide analogues from the (22-39) sequence of the GBV-C E1 protein (E1P8: APEDIGFCLEGGCLVALG) and 23 analogues from the (133-150) sequence of the GBV-C E2 protein (E2P45: SDRDTVVELSEWGVPCAT) were synthesized by semi-automated multiple solid-phase peptide synthesis on a peptide synthesizer (SAM, Multisyntech, Germany) as C-terminal carboxamides on a Tentagel RAM resin (Rapp Polymere GmbH, Germany) (100 mg, 0.28 meq/g) and following a 9-fluorenylmethoxycarbonyl (Fmoc) strategy. Couplings were performed by 2-(1H-7-azabenzotriazole-1-yl)-1,1,3,3-tetramethyluronium hexafluorophosphate (HATU) and diisopropylethylamine (DIEA) activation, with three-fold molar excesses of amino acids. The Fmoc deprotection step was performed twice with 20% piperidine in dimethylformamide (DMF) for 10 min. Peptide isolation from the peptidyl resins was carried out as described elsewhere [20]. The crude peptides were desalted using Oasis HLB Plus cartridges (225 mg/60 μg) from Waters.

The peptides were characterized by analytical HPLC on a 1260 Infinity chromatograph (Agilent Technologies) with an Eclipse Plus C18 column (Agilent, 3.5 μm, 4.6 × 100 mm). The E2P45 analogues were analysed with a linear gradient of 80%-30% A in B over 20 min at a flow rate of 1 mL/min using 0.05% trifluoroacetic acid (TFA) in water (A) and 0.05% TFA in acetonitrile (B) as the eluting system. A linear gradient (5%-95%) of 0.05% ammonium acetate in acetonitrile (solvent B) into 0.05% ammonium acetate in water (solvent A) over 20 min at a 1 mL/min flow rate was used for separation of the E1P8 analogues. The peptides were 95% pure by analytical HPLC at 220 nm. Their identity was confirmed by electrospray ionization mass spectrometry (ESI-MS) (Tables **1** and **2**). ESI-MS was performed with a liquid chromatograph–time of flight (LC-TOF) detector, LCT Premier XE (Micromass Waters) coupled to Analytical Ultra Performance Liquid Chromatography apparatus (UPLC, Waters). Samples were dissolved in a mixture of acetonitrile/water (1:1, v/v) and analysed previously in the UPLC at a flow rate of 0.3 mL/min. Mass spectra were recorded in positive ion mode for E2P45 analogues and in negative ion mode for E1P8 peptides (in the m/z 500-2500 range). UPLC was performed in an Acquity UPLC BEH C_{18} reverse-phase column (2.1×100 mm, 1.7 μm particle size) and with an Acquity UPLC (Waters) chromatograph. Solvent A was 20 mM formic acid in water and solvent B was 20 mM formic acid in acetonitrile for E2P45 analogues; and 10 mM ammonium acetate in water (solvent A) and 10 mM ammonium acetate in methanol (solvent B) for E1P8 peptides. Elution was performed with linear gradients of solvent B into A over 10 min at 0.3 mL/min.

1.2. Multiple Antigenic Peptides (MAPs)

Homogeneous MAP_4E1P8 and MAP_4E2P45 were synthesized manually as C-terminal carboxamides on H-PAL ChemMatrix® resin (Aldrich) (Fig. **2**). The Cys residues were replaced by Ser or 2-aminobutyric acid (Abu) residues. The first amino acid coupled was β-Ala. The tetravalent lysine core was obtained by sequential coupling of 0.4 and 0.8 mmol of Fmoc-Lys(Fmoc)-OH which was essentially incorporated by means of treatment with HATU and DIEA. The E1P8 and E2P45 peptide sequences were then assembled at both Nα- and Nε-lysine positions. Twelve-fold molar excesses of Fmoc-amino acids, diisopropylcarbodiimide (DIP-CDI) and hydroxybenzotriazole (HOBt) were used throughout the synthesis. The efficiency of these reactions was evaluated by Kaiser's (ninhydrin) test and repeated couplings were carried out when a positive ninhydrin test was observed. The tetrameric MAPs were concomitantly side chain-deprotected and cleaved from the resin by treatment with a

Table 1. Alanine Scanning of E1P8 Sequence and Inhibition of gp41-Mediated Cell–Cell Fusion

Peptide	Primary Sequence	HPLC (k')[a]	$[M+H^+]_{exp}$ [b]	% Inhib. Fusion Assay[c]
E1P8	APEDIGFCLEGGCLVALG	5.3	1762.9 (1763.0)	80 (128.1±8.7)
E1P8-1	A**A**EDIGFCLEGGCLVALG	5.4	1736.8 (1737.0)	15
E1P8-2	AP**A**DIGFCLEGGCLVALG	6.7	1704.8 (1705.0)	16
E1P8-3	APE**A**IGFCLEGGCLVALG	6.6	1718.8 (1719.0)	92 (85.4±5.2)
E1P8-4	APED**A**GFCLEGGCLVALG	5.7	1720.7 (1720.9)	32
E1P8-5	APEDI**A**FCLEGGCLVALG	6.6	1776.9 (1777.1)	91 (94.8±4.3)
E1P8-6	APEDIG**A**CLEGGCLVALG	5.7	1685.7 (1686.9)	84 (140.7±6.7)
E1P8-7	APEDIGF**A**LEGGCLVALG	5.4	1730.9 (1731.0)	34
E1P8-8	APEDIGFC**A**EGGCLVALG	5.2	1720.8 (1720.9)	75 (160.1±9.3)
E1P8-9	APEDIGFCL**A**GGCLVALG	6.3	1704.8 (1705.0)	32
E1P8-10	APEDIGFCLE**A**GCLVALG	6.9	1776.9 (1777.1)	48
E1P8-11	APEDIGFCLEG**A**CLVALG	7.0	1776.9 (1777.1)	61 (97.2±2.2)
E1P8-12	APEDIGFCLEGG**A**LVALG	6.1	1730.9 (1731.0)	34
E1P8-13	APEDIGFCLEGGC**A**VALG	5.7	1720.8 (1720.9)	38
E1P8-14	APEDIGFCLEGGCL**A**ALG	6.2	1734.8 (1735.0)	29
E1P8-15	APEDIGFCLEGGCLVA**A**G	5.4	1720.8 (1720.9)	44
E1P8-16	APEDIGFCLEGGCLVAL**A**	6.1	1776.9 (1777.1)	38

[a]*HPLC conditions. Eluents:(A) 0.05% (v/v) ammonium acetate in water, (B) 0.05% ammonium acetate in acetonitrile. Linear gradient 5%-95% of B into A over 20 min at a flow rate of 1 mL/min.*

[b]*Experimental mass obtained by Electrospray (ESI-MS) in negative ion mode. Theoretical mass in parenthesis*

[c] *% inhibition tested at a peptide concentration of 200 μM. Maximum non-toxic concentration >200 μM Calculated IC_{50} (μM) values in parenthesis.*

mixture of TFA in the presence of triisopropylsilane (TIS) and water as scavengers (TFA:TIS:H_2O, 9.5:2.5:2.5) for 3 h with occasional agitation at room temperature. The solvent was removed in vacuum and the crude peptides were precipitated with diethyl ether. The solids were dissolved in 30% acetic acid in water and lyophilized.

Heterogeneous MAP_4(E1P8-E2P45) was synthesized following essentially the same protocol as that used for the homogeneous tetrameric MAPs (Fig. **2**). However, for this synthesis the orthogonal N-protecting group, 1-(4,4-dimethyl-2,6-dioxocyclohexylidene)-3-methylbutyl (ivDde) was used to synthesized the core oligolysine-based dendrimer [21].

Table 2. Alanine Scanning of E2P45 Sequence and Inhibition of gp41-Mediated Cell–Cell Fusion

Peptide	Primary Sequence	HPLC (k')[a]	$[M+H^+]_{exp}$ [b]	% Inhib. Fusion Assay[c]
E2P45	SDRDTVVELSEWGVPCAT	3.5	1964.2 (1964.1)	54 (198.3±3.4)
E2P45-1	**A**DRDTVVELSEWGVPCAT	3.4	1948.0 (1948.1)	0
E2P45-2	S**A**RDTVVELSEWGVPCAT	3.4	1920.0 (1920.1)	14
E2P45-3	SD**A**DTVVELSEWGVPCAT	3.6	1877.9 (1879.0)	9
E2P45-4	SDR**A**TVVELSEWGVPCAT	3.5	1921.0 (1920.1)	23
E2P45-5	SDRD**A**VVELSEWGVPCAT	3.5	1934.1 (1934.1)	0
E2P45-6	SDRDT**A**VELSEWGVPCAT	3.4	1937.0 (1936.1)	1
E2P45-7	SDRDTV**A**ELSEWGVPCAT	3.4	1937.0 (1936.1)	0
E2P45-8	SDRDTVV**A**LSEWGVPCAT	3.5	1907.0 (1906.1)	62 (154.4±12.3)
E2P45-9	SDRDTVVE**A**SEWGVPCAT	3.2	1921.9 (1922.0)	28
E2P45-10	SDRDTVVEL**A**EWGVPCAT	3.5	1949.0 (1948.1)	25
E2P45-11	SDRDTVVELS**A**WGVPCAT	3.5	1907.0 (1906.1)	0
E2P45-12	SDRDTVVELSE**A**GVPCAT	3.2	1848.9 (1849.1)	15
E2P45-13	SDRDTVVELSEW**A**VPCAT	3.5	1979.0 (1978.2)	47
E2P45-14	SDRDTVVELSEWG**A**PCAT	3.4	1935.9 (1936.1)	22
E2P45-15	SDRDTVVELSEWGV**A**CAT	3.5	1937.9 (1938.1)	45
E2P45-16	SDRDTVVELSEWGVPA**A**T	3.4	1931.9 (1932.1)	48
E2P45-17	SDRDTVVELSEWGVPCA**A**	3.6	1934.4 (1934.1)	49

[a]*HPLC conditions. Eluents:(A) 0.05% (v/v) TFA in water, (B) 0.05% TFA in acetonitrile. Linear gradient 30%-80% of B into A over 20 min at a flow rate of 1 mL/min.*
[b]*Experimental mass obtained by Electrospray (ESI-MS) in positive ion mode. Theoretical mass in parenthesis*
[c] *% inhibition tested at a peptide concentration of 200 μM. Maximum non-toxic concentration >200 μM Calculated IC_{50} (μM) values in parenthesis.*

Thus, the tetravalent lysine core was obtained by sequential coupling of 0.4 mmol of Fmoc-Lys(Fmoc)-OH and 0.8 mmol of Fmoc-Lys(ivDde)-OH, which were incorporated through HATU:DIEA (1:2)-mediated carboxyl activation. The peptide sequence E1P8 was then assembled at both Nα-lysine positions. Eight-fold molar excesses of Fmoc-amino acids and DIPCDI/HOBt were used throughout the synthesis. The N-terminal amino acid was introduced as a tert-butoxycarbonyl (Boc) Nα-protected residue. The *Nε*-Dde-protecting group was removed by treatment with 2% hydrazine in DMF [22]. The E2P45 sequence was then assembled at both exposed lysine Nε- amino groups of the monoepi-

topic MAP resin intermediate. Cleavage and final deprotection of the crude peptide was performed as described above for the homogeneous MAPs. The crude peptides were desalted using Oasis HLB Plus cartridges (225 mg/60 μg) from Waters.

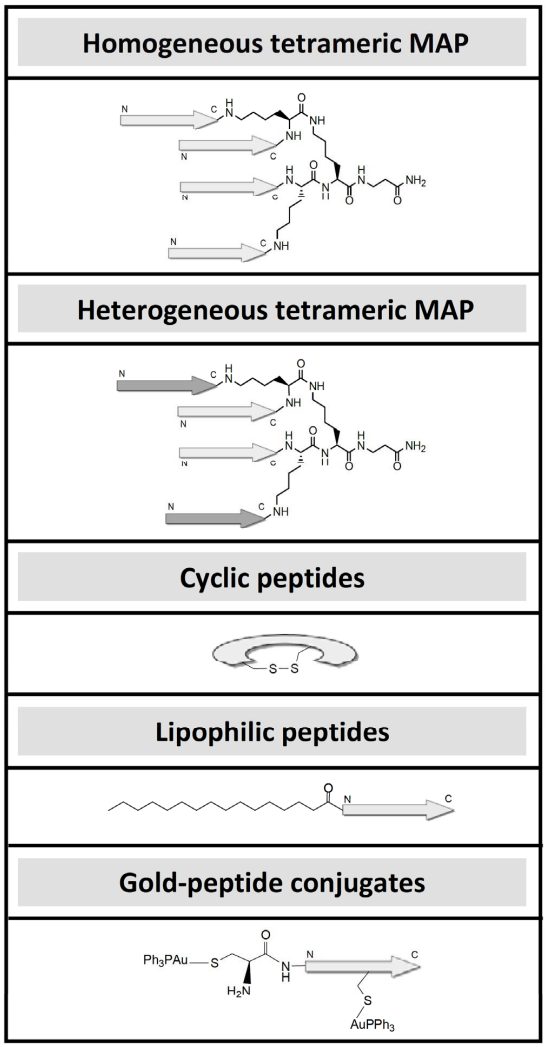

Fig. (1). Chemical modifications to design new forms of presentations of GBV-C peptide domains.

The desalted molecules were purified by semipreparative HPLC (1260 Infinity, Agilent Technologies) in an XBridge™ BEH300 Prep C18 column (Waters, 5 μm, 10×250 mm) at a flow rate of 3.5 mL/min. The MAP_4E2P45 was purified using a linear gradient of 50%-100% B (0.05% (v/v) TFA in acetonitrile) into A (0.05% (v/v) TFA in water) for 25 min at a flow rate of 1 mL/min. The purification yield was 7%. For the purification of MAP_4E1P8, a linear gradient of 50%-100% B into A (A:10 mM ammonium acetate in water; and B: 10 mM ammonium acetate in methanol) for 25 min at a flow rate of 1 mL/min was used. A yield of 9% was obtained upon purification.

Purification of MAP_4E2P45-E1P8 was carried out using the same eluents as those used for homogeneous tetrameric MAP_4E1P8. A linear gradient of 65%-90% B into A for 25 min at a flow rate of 1 mL/min was used to obtain a purification yield of 14%.

Analytical HPLC, MALDI-TOF and ESI-MS characterization of pure MAPs (min. 95% purity) are shown in (Figs. **1A-C**) of the Supportive/Supplementary Material. MALDI-TOF mass spectra were recorded on an Autoflex III Smartbeam (Bruker Daltonics), using 2,5-dihydroxybenzoic acid matrix (DHB) on an MTP 384 target plate (Bruker).

1.3. Cyclic Peptides

To obtain the disulphide cyclic peptides, (S^{29},S^{34}cyclo [$Cys^{29,34}$])E1(22-39) (cycE1P8) and (S^{132},S^{148}cyclo [$Cys^{132,148}$])E2(132-150) (cycE2P45), cysteine residues protected with trityl groups were introduced at the specified positions. The corresponding linear peptides were synthesized manually as C-terminal carboxamides on a NovaSyn TGR resin NovaSyn® (Novabiochem, Merck Millipore, Merck KGaA, Darmstad, Germany) and finally cleaved from the resin with TFA/ethanedithiol (EDT)/triisopropylsilane (TIS)/H2O (95/2/1/2) and precipitated from ice-cold diethyl ether. Finally, they were dissolved in 10% aqueous acetic acid and lyophilized. Characterization of the resulting peptides was carried out by analytical HPLC and UPLC-ESI/MS as described above. The linear crude peptides were purified by semipreparative HPLC (1260 Infinity, Agilent Technologies) in an XBridge™ PrepBEH130 C18 column (Waters, 5 μm, 10×250 mm). The purification yield was about 25%. For cyclization, the peptides were dissolved in 0.1 M ammonium bicarbonate (0.3 mg/mL). The solution was left to stand open to the atmosphere and stirred for 24 h. The formation of cyclic disulphides was checked by the Ellman test. Cyclic peptides were desalted using Oasis HLB Plus cartridges, 225 mg/60 μg, from Waters and were characterized by analytical UPLC and ESI-MS mass spectrometry (Supportive/Supplementary Material Figs. **2A-B**). Cyclic peptides were obtained with 95% purity.

1.4. Lipophilic Peptides

E1P8 and E2P45 were synthesized manually as C-terminal carboxamides on a NovaSyn TGR resin NovaSyn® (Novabiochem, Merck Millipore, Merck KGaA, Darmstad, Germany). Once the peptide sequences were completed and prior to the cleavage and deprotection processes of peptidyl resins, palmitic and myristic acids were introduced at the N-terminus of different fractions of each peptidyl resin. The coupling reaction was performed using three-fold molar excesses of activated fatty acids with *N*',*N'* diisopropylcarbodiimide (DIPCDI) and 1-hydroxybenzotriazole (HOBt). The mixtures were set aside at room temperature overnight. The efficiency of these reactions was evaluated by the ninhydrin colorimetric reaction. Crude peptides were obtained after cleavage with TFA/EDT/TIS/H_2O (95/2/1/2) and were desalted using Oasis HLB Plus cartridges (225 mg/60 μg) from Waters. Purification yields by solid phase extraction cartridges were in the range of 15%-20%. Lipophylic peptides

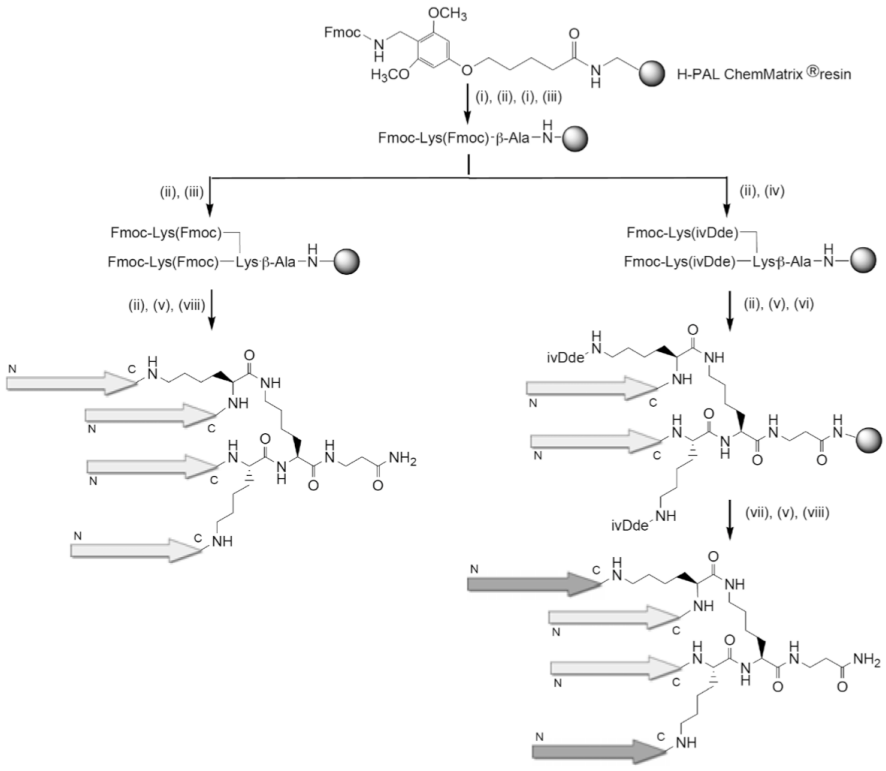

Fig. (2). Synthesis of homogeneous and heterogeneous MAPs: (**i**) 20% piperidine/DMF; (**ii**) Fmoc-βAla-OH/HATU/DIEA, DMF; (**iii**) Fmoc-Lys(Fmoc)-OH/HATU/DIEA, DMF; (**iv**) Fmoc-Lys(ivDde)-OH/HATU/DIEA, DMF; (**v**) Fmoc SPPS; (**vi**) Boc-Ala-OH/DIPCDI/HOBt, DMF; (**vii**) 2% hydrazine, DMF; (**viii**) TFA/TIS/H_2O (95/2.5/2.5).

were characterized by analytical UPLC and ESI-MS mass spectrometry as described for the E1P8 and E2P45 analogues (Supportive/Supplementary Material Figs. **3A-B**). The peptides were 95% pure by analytical HPLC at 220 nm.

1.5. Au–peptide Conjugates

The reaction of the peptides E1P8 and E2P45 with two equivalents of [Au(acac)(PPh_3)] (acac = acetylacetonate) was carried out in acetonitrile under an argon atmosphere. The mixture was stirred for 2 h and then evaporation of the solvent to dryness gave the Au–peptide conjugates E1P8-(2H)-$(AuPPh_3)_2$ (MW = 2680; yield: 91%) and P45-E2-(-2H)-$(AuPPh_3)_2$ (MW = 2983; yield: 86%), respectively. In the reaction, the acetylacetone cleanly deprotonates the cysteine residues, forming acetylacetone, and the $AuPPh_3^+$ fragment coordinates to the thiolate peptide ligand. $^{31}P\{^1H\}$ NMR spectra were acquired on a Bruker Avance 400 spectrometer in dmso-d6 (referenced to external 85% H_3PO_4): E1P8-(2H)-$(AuPPh_3)_2$, δ: 35.8; P45-E2-(2-H)-$(AuPPh_3)_2$, δ: 34.6.

2. INHIBITION OF CELL–CELL FUSION ASSAYS

Cell–cell fusion assays were performed in triplicate as described elsewhere [18], but the quantification of syncytia formation was determined by fluorescence instead of luminescence.

Two cell lines were used: HeLa-env (donated by Dr. Blanco of the Fundació IRSI-Caixa) expressing the protein from the HIV-1 envelope and including the HIV-1 long terminal repeat (LTR) promoter in its genome; and TZMbl (AIDS reagents catalogue no. 8129), which expresses the membrane receptor from CD4 lymphocytes and co-receptors CCR5 and CXCR4, and includes the luciferase and β-galactosidase genes in its genome. The cell lines were cultured in Dulbecco's modified Eagle medium (DMEM, PAA) containing L-glutamine and sodium pyruvate supplemented with 10% heat-inactivated foetal bovine serum (FBS), 100 UI/mL penicillin, and 100 μg/mL streptomycin. The cell cultures were maintained in a tissue culture incubator at 37ºC in a 5% CO_2 atmosphere.

When both types of cells are cocultured, cell membrane fusion occurs and the β-galactosidase gene is activated. In this study, the trial for the inhibition of cell binding induced by the E2P45 and E1P8 peptide derivatives consisted of incubation of 2500 HeLa-env cells/well (Nunc plates, catalogue no. 136101) for 1 h at serial dilutions (5-200 μM) of the peptides to be tested, followed by the addition of around 10 times (25000 cells) TZMbl/well and incubation for 24 h.

Subsequently, 5 μL of a solution of 20% Igepal in phosphate buffer (100 mM, pH 7.2, 0.1 mM $MgCl_2$) was added to each well. After 1-2 min, 50 μL was taken from each well and added to a new plate. Then 50 μL of a 1 mM solution of 4-methylumbelipheryl-β-D-galactopiranoside in phosphate buffer (100 mM, pH 7.2, 0.1 mM $MgCl_2$) was added to each well and the plate was incubated for 30 min at 37ºC. Finally, upon the addition of 150 μL Glycine-NaOH buffer (100 mM, pH 10.6), fluorescence was quantified in a SpectraMax M5 (Molecular Devices) microplate reader using an excitation λ of 355 nm and emission λ of 460 nm. To control cell binding, wells without peptides were reserved and a known cell binding inhibitor, C-34 (AIDS Reagents, catalogue no. 9824), was used as a positive control. The level of inhibition of cell binding is shown as an average of three independent assays and was also qualitatively assessed by observing the formation of syncytia under the microscope.

3. INHIBITION OF HIV INFECTION

Virus stock was produced by transfection of 293T cells using the calcium phosphate method according to the manufacturer's instructions (ProFection mammalian transfection system; Promega, Madison, WI, USA). To perform infection inhibition assays, 96-well plates were set up as follows: to the first two columns, 25 μL of medium (DMEM, 10% FBS) was added; to each of the other columns (columns 3 through 12), 25-μL aliquots of serial 2-fold dilutions for each compound in DMEM–10% FBS were added. Virus in a total volume of 75 μL was then added to each well in columns 2 through 12. Virus-free medium was added to column 1 (mock infected). The amount of virus chosen was the lowest level of viral input sufficient to give a clear luciferase signal within the linear range. The plate was incubated for 2 h at 37°C. After incubation, 10^4 target cells (TZM-bl) in a volume of 100 μL were added to each well. The plate was then placed into a humidified chamber within a CO_2 incubator at 37°C. After 72 h of incubation at 37°C, supernatants were removed and the cell-associated luciferase activity for each well was determined on a microplate luminometer (Turner Biosystems, Sunnyvale, CA) using a luciferase assay kit (Biotherma, Sweden). The values are expressed as the concentration of compound that reduces infectivity by 50% (IC_{50}). IC_{50} values in (Table **4**) are the average of two or three independent inhibition assays.

4. CELL VIABILITY WITH MTT ASSAY

Cell toxicity of E2 peptides was analysed in HeLa-env and TZM-bl cells using the MTT assay. The cells were cultured with DMEM (15,000 cells/well) in a 96-well plate and incubated with the serial dilutions of each peptide at 37ºC for 72 h. Afterwards, MTT was added to a final concentration of 7.5 mg/mL and the plate was incubated again for 2 h at 37ºC. Subsequently, the medium was removed and 100 μL of DMSO was added to dissolve the formazan precipitate. After 45 min, absorbance was measured at 570 nm. Cell viability was established via the quotient between the absorbance value of cells treated with the peptide and untreated cells. The maximum non-toxic concentration of each peptide derivative was used in the cell–cell fusion and inhibition of HIV infection assays.

RESULTS AND DISCUSSION

This paper presents the design and synthesis of new forms of presentation of two peptide domains corresponding to the GBV-C E1 and E2 envelope proteins, together with a study of their anti-HIV-1 activity. Our aim is to enhance the anti-viral potency of the GBV-C peptide domains.

From the GBV-C E2 protein, the (133-150) peptide sequence (namely E2P45) was first selected [18]. Of the 124 overlapping peptides spanning the E2 protein, the 18-mer peptide sequence E2P45 was found to be one of those that are capable of interfering with the HIV-1 fusion peptide (FP)–vesicles interaction, and it produced a notable decrease in cellular membrane fusion and HIV-1 infectivity.

Our studies of the GBV-C E1 protein using several biophysical techniques, such as isothermal titration calorimetry, confocal microscopy, monolayers and fluorescence-based binding assays, allowed us to establish that certain peptide sequences from this protein interact with the HIV-1 FP [19]. Further analysis demonstrated that the (22-39) sequence of the E1 protein (namely E1P8) was capable of inhibiting membrane fusion as well as the interaction of HIV-1 FP with bilayers [23], and this peptide sequence was therefore proposed as a putative HIV-1 entry inhibitor.

Based on these results, the E1P8 and E2P45 peptides were selected as parent peptides to have their structures chemically modified and then be tested for activity against HIV-1 through cell–cell fusion and HIV-1 NL4-3 infectivity assays. HeLa-env cells express the HIV-1 envelope protein and TZM-bl cells express the membrane receptor of the host cell as well as the co-receptors CCR5 and CXCR4. Thus, by means of the inhibition of cell–cell fusion of these cells, we analysed the capacity of the newly designed E1 and E2 peptides to inhibit virus entry. Meanwhile, the HIV-1 NL4-3 infectivity assay was taken as a measure of the capacity of the selected peptides to inhibit HIV infection.

Firstly, Alanine scanning (reviewed in Ref [24]) was performed to identify specific amino acid residues responsible for the activity of E1P8 and E2P45. All the possible positions in the original peptides were replaced by Ala to determine which residues are critical for their activity. The characterization of the peptide analogues obtained by solid-phase multiple syntheses is shown in (Tables **1** and **2**). All the peptides were tested at a non-toxic concentration determined by MTT assays (200 μM) in cell–cell fusion assays and the degree of reduction in activity was taken as a relative measure of the importance of the substituted residue. Assuming that the substitution of an essential amino acid would result in a clear reduction in peptide activity, only those changes resulting in cell–cell fusion inhibition of at least 20% less than that of the corresponding parent peptides were taken into account. Thus, peptides with a degree of inhibition equal to or lower than 16% (E1P8 analogues) and 10% (E2P45 analogues) were considered to have been obtained after the modification of essential positions within the parent sequences. Our results highlighted the specific contribution to cell–cell fusion inhibition of the N-terminal residues Pro^{23} and Glu^{24} in E1P8, and Ser^{132}, Arg^{134}, Thr^{136}, Val^{137}, Val^{138} and Glu^{142} in E2P45.

Other E1P8 and E2P45 analogues produced results that were similar to or even better than those of the parent sequences after performing the inhibition assay at a concentration of 200 μM. The corresponding IC_{50} values were obtained and compared to those of the parent peptides (Tables **1** and **2**). However, no substantial improvement was observed since the IC_{50} values for the most active analogues were 82-97 μM and 147 μM for the analogues of E1P8 (IC_{50}=128.1±8.7 μM) and E2P45 (IC_{50}=198.3±3.4 μM), respectively.

The influence of the total net charge of the parent peptides on their activity was also studied through the replacement of non-essential residues. In this way, several new E1P8 and E2P45 analogues were obtained in the solid phase and the inhibition of both cell–cell fusion and HIV-1 NL4-3 replication in cell cultures was determined. Our results indicate that the net negative charge (2-) of both peptides seems to be important for their activity. As shown in (Table **3**), in general all the analogues tested showed lower activity in the cell–cell fusion assay. This finding was reinforced after performing the HIV-1 inhibition assay: in no case was inhibition of viral replication observed and some peptide analogues even led to the promotion of cellular growth (data not shown). For this reason, the parent sequences were structurally modified as described below.

Different strategies for increasing the antiviral activity of synthetic peptides that circumvent the limitations they present in clinical applications, such as low stability and limited selectivity of action, have been described in the literature. We performed different chemical modifications on E1P8 and E2P45, in order to enhance their antiviral activity. Homogeneous and heterogeneous MAPs, lipophilic derivatizations, cyclization and peptide–gold conjugations were the chemical strategies used to design new forms of presentation of the GBV-C peptide domains (Fig. **1**).

The relatively large and stereochemically complex protein–protein interfaces usually hamper the binding of short inhibiting peptides, which do not have enough affinity to and specificity for the protein target site to bind to it. An alternative antiviral strategy based on the multimerization of linear parent peptides has been devised and the design of new anti-HIV peptides through sequence multimerization has been reported [25-27]. In this work, we synthesized two homogeneous tetrameric molecules containing four copies of the E1P8 and E2P45 peptides (Fig. **2**) by solid-phase methods. This kind of multimeric peptide molecule was initially described by Tam [28-29] and is formed of a lysine core that provides a backbone for the peptide antigens, thereby allowing the stabilization of the secondary structure. Moreover, the use of orthogonally-protected lysine derivatives allows several copies of two different peptide sequences to be presented in the same molecule, which could lead to an increase in antiviral activity. We therefore also synthesized a heterogeneous tetrameric MAP containing both the E1P8 and E2P45 sequences in Nα and Nε positions, with respect to the tetralysine core (Fig. **2**). To avoid secondary reactions due to the presence of multiple Cys residues in the macromolecule, they were replaced by Ser or Abu. The toxicity of these compounds, as evaluated in the MTT assay, was higher than that of the corresponding linear peptides; the maximum non-toxic toxic concentration of the homogeneous MAP peptide was 25 μM. In spite of their higher toxicity, the multimeric peptides showed increased activity compared to their monomeric parents. Particularly, homogeneous MAP_4E1P8 inhibited HIV-1 infection at the low μM level (IC_{50} 8.7 μM) (Table **4**). Moreover, the activity of this MAP in the gp41 cell–cell fusion assay (IC_{50} 17.6±3.0 μM) demonstrated that this macromolecule may be used to target the HIV-1 fusion step. It is worthy of note that the tetra-lysine core did not show any activity at the highest concentration tested (100 μM).

Regarding the heterogeneous MAP_4E2P45-E1P8, the LC_{50} (lethal concentration 50%), was 14.4 μM. The maximum non-toxic concentration of this heterogeneous multimeric peptide evaluated in cell–cell fusion assays was 2.5 μM, with an inhibition of only 23%. Similar results were obtained for the inhibition of viral replication, since no significant inhibition was observed at the non-toxic concentrations evaluated for the heterogeneous MAP. The unexpected results obtained from the incorporation of the two different peptide sequences into one multimeric molecule demonstrate the difficulty in achieving a precise spatial arrangement of the sequences within each MAP for optimal binding to the target site. A degree of unpredictability concerning the optimal composition and configuration of heterogeneous MAPs is normally observed.

The introduction of intramolecular cyclical motifs to encourage a less flexible and more rigid structure has recently been reported to increase the anti-HIV activity of linear peptides [30, 31]. Here, the cyclic peptides cycE1P8: (S^{29},S^{34}cyclo[$Cys^{29,34}$])E1(22-39) and cycE2P45: (S^{132},S^{148} cyclo[$Cys^{132,148}$])E2(132-150) were obtained in solution via the formation of disulphide bridges. To this end, it was necessary to insert a Cys residue into the N-terminus of the E2P45 parent sequence (Fig. **3**). Table **4** shows the inhibitory activity of the cyclic analogues. Regarding the inhibition of replication of HIV-1 NL4-3 in cell cultures, cycE1P8 and cycE2P45 showed IC_{50} values of 7.8±3.2 and 32.5±17.7 μM, respectively; the first being almost 20-fold more potent than the corresponding linear peptide. These results support the idea that constrained peptides inhibit HIV-1 replication more effectively. It seems that the cyclic counterparts become more specific ligands than their parent peptides because of their increased rigidity. Such conformationally restricted molecules constitute a promising alternative for inhibiting the protein–protein interactions involved in the fusion process and subsequent HIV-1 entry into the cell.

The modification of peptides by combining them with fatty acids favours enzymatic stability, improves pharmacokinetic properties and promotes secondary structures in synthetic peptide sequences. In fact, the modification of peptides that inhibit HIV fusion via combination with fatty acids to increase their inhibiting activity was recently reported [32-34]. It has been suggested that the fatty acid allows the peptide to become attached to the cell membrane surface, thereby increasing peptide concentration at points of fusion. Although inhibiting activity has been correlated to the length of the fatty acid, we found no significant differences between myristic and palmitic acid-derived peptides. A correlation was found between the inhibitory activity of cell–cell fusion and HIV infectivity assays; in general, lower IC_{50} values

Table 3. Net Charge Contribution of E1P8 and E2P45 Peptides in the Inhibition of gp41-Mediated Cell–Cell Fusion

Peptide	Primary Sequence[a]	HPLC (k')[b]	$[M+H^+]_{exp}$[c]	Net charge	% Inhib. Fusion Assay[d]
Parent E1P8	A**PE**DIGFCLEGGCLVALG			2-	80
	A**PE***N*IGFCLEGGCLVALG	6.4	1761.8 (1762.1)	1-	37
	A**PE**DIGFCL***Q***GGCLVALG	6.3	1761.8 (1762.1)	1-	44
	A**PE**DIGFCL***R***GGCLVALG	6.4	1789.9 (1790.1)	0	65
	A**P*****Q***NIGFCL***Q***GGCLVALG	6.0	1857.9 (1760.1)	1+	0
	A**PE*****R***IGFCL***R***GGCLVALG	5.7	1829.9 (1831.2)	2+	27
Parent E2P45	**S**D**R**D**TVV**ELS**E**WGVPCAT			2-	54
	SD**R**D**TVV*****Q***LS**E**WGVPCAT	3.5	1964.1 (1963.2)	1-	52
	S***N*****R*****N*****TVV**ELS**E**WGVPCAT	3.3	1963.0 (1962.2)	0	7
	S***N*****R*****N*****TVV*****Q***LS***E***WGVPCAT	3.6	1962.0 (1961.2)	1+	0
	S**N****R****N****TVV*****Q***LS***Q***WGVPCAT	3.4	1961.1 (1960.2)	2+	69

[a] *Underlined are represented considered essential residues. In italics the introduced modifications in parent sequences*

[b] *HPLC conditions:*

E1P8 derived peptides: Eluents:(A) 0.05% (v/v) ammonium acetate in water, (B) 0.05% ammonium acetate in acetonitrile.

Linear gradient 5%-95% of B into A over 20 min at a flow rate of 1 mL/min.

E2P45 derived peptides: Eluents:(A) 0.05% (v/v) TFA in water, (B) 0.05% TFA in acetonitrile.

Linear gradient 30%-80% of B into A over 20 min at a flow rate of 1 mL/min.

[c] *Experimental mass obtained by Electrospray (ESI-MS) in negative(E1P8 derived peptides) and positive (E2P45 derived peptides) ion mode. Theoretical mass in parenthesis*

[d] *% inhibition tested at a peptide concentration of 200 μM. Maximum non-toxic concentration >200 μM.*

Table 4. Inhibitory Activity of E2P45 and E1P8 Derivatives in gp41-Mediated Cell–Cell Fusion and HIV-1 NL4-3 Infectivity Assays

Peptide	% Inhib. Fusion Assay[a]	Fusion Assay IC_{50}(μM)	HIV-1 Assay IC_{50}(μM)
E1P8 derivatives			
E1P8	80	128.1±8.7	150±50
MAP_4E1P8	60[b]	17.6±3.0	8.7±6.0
cycE1P8	68	164.2±19.3	7.8±3.2
Palm-E1P8	94	32.4±3.3	12.0±4.2
Mir-E1P8	96	32.0±2.2	13.5±9.2
E1P8-Au	96[c]	0.73±0.03	<0.5
E2P45 derivatives			
E2P45	54	198.3±3.4	>110
MAP_4E2P45	34[b]	ND	24.5±7.8
cycE2P45	40	ND	32.5±17.7

(Table 4) contd….

Peptide	% Inhib. Fusion Assay[a]	Fusion Assay IC_{50}(μM)	HIV-1 Assay IC_{50}(μM)
E2P45 derivatives			
Palm-E2P45	93	78.8±3.1	82.5±24.7
Mir-E2P45	98	41.7±2.1	30.0±7.1
E2P45-Au	72[c]	1.01±0.46	1.2±1.1
E2P45-E1P8 derivatives			
MAP_4E1P8-E2P45	23[d]	ND	ND

ND: not determined

C34 (240 nM) 90% inhibition IC_{50}=5 nM

[a] *% inhibition tested at a peptide concentration of 200 μM*

[b] *% inhibition tested at the MAP maximum non-toxic concentration (25 μM)*

[c] *% inhibition tested at the Au–peptide maximum non-toxic concentration (2 μM)*

[d] *% inhibition tested at the MAP_4E2P45-E1P8 non-toxic concentration (2.5 μM).*

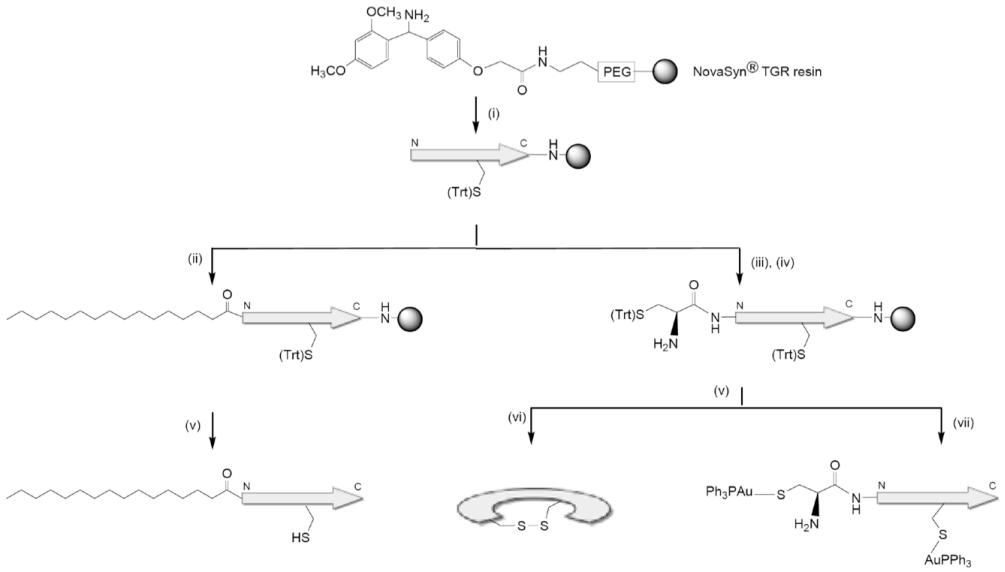

Fig. (3). Synthesis of modified E2P45 peptides: (**i**) Fmoc SPPS; (**ii**) Palmitic acid/DIPCDI/HOBt, DMF; (**iii**) Fmoc-Cys(Trt)-OH/HATU/DIEA, DMF; (**iv**) 20% piperidine/DMF (**v**) TFA/EDT/TIS/H_2O (95/2/1/2); (**vi**) 0.1M ammonium bicarbonate; (**vii**) [Au(acac)(PPh_3)], acetonitrile, argon atmosphere.

were found for E1P8 lipopeptides than for E2P45 lipophilic derivatives. In the HIV-1 NL4-3 infectivity assay, IC_{50} values of 12.0±4.2 μM and 13.5±9.2 μM were obtained for palmitoylated and myristoylated E1P8 peptides, respectively (Table **4**). No inhibition was found for the corresponding control compound (palmitic acid) at a concentration lower than 30 μM. Thus, the conjugation of the parent peptides with saturated fatty acids could increase the concentration of the inhibitor in the cell membrane and allow the lipopeptides to locate in lipid rafts. Enriching the peptide entry inhibitors with saturated fatty acids represents a useful strategy to enhance their efficacy when it comes to penetrating membrane domains.

Finally, the anti-HIV activity of a great variety of metallic compounds, and particularly of gold complexes, has recently been reported [12]. Gold compounds used as antiarthritic drugs have been proven to possess antiretroviral activity via their inhibition of reverse transcriptase [13, 14]. Furthermore, several gold(III) compounds with porphyrins or Schiff bases have been patented due to their considerable anti-HIV activity [16]. Here, we coordinated gold(I) to the E1P8 and E2P45 peptides. The amino acid sequence of the E2P45 peptide, which contains a cysteine at position 148, was modified by the insertion of a second cysteine residue into the N-terminus to allow for greater or more stable coordination of the gold atom, or more specifically of the

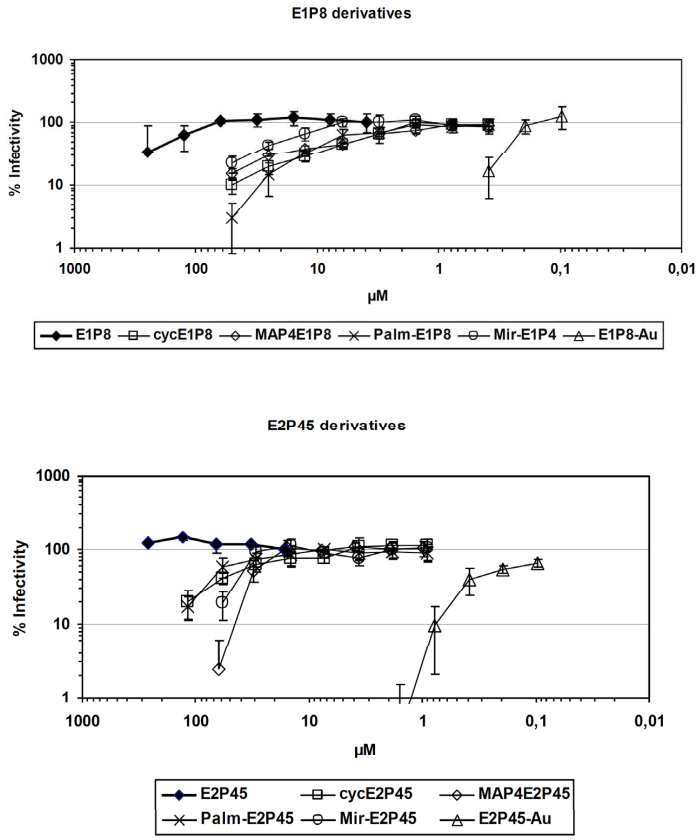

Fig. (4). Dose-response curves for E1P8 and E2P45 derivatives.

$AuPPh_3^+$ fragment, to the peptide (Fig. **3**). In this way, both the cysteine residues allow the gold(I) atom to bind with the sulphurs to form thiolate complexes. The E1P8 peptide sequence was not modified since it already contains 2 Cys residues. The coordination of the gold(I) centres was carried out through the reaction of the peptides with the basic complex $[Au(acac)(PPh_3)]$, which allows straightforward substitution of the cysteine acid protons by the $AuPPh_3^+$ fragment. $^{31}P\{^1H\}$ NMR spectra allowed us to characterize the final peptide–thiolate–gold complexes, as they were clean spectra with an upfield displacement compared to the initial gold precursor; this chemical shift is characteristic of gold–thiolate–phosphine complexes (not shown). The main advantages that the final gold–peptide conjugates may offer would be that the peptides already present antiviral activity on their own (they correctly locate the target) while the gold–phosphine fragments present good cellular uptake and possible inhibitory activity. The maximum non-toxic concentration of the peptide–gold complexes assayed was 2 μM. The gold complexes tested as controls (a chloro and an irrelevant peptide–gold(I)–phosphine complex) showed some cellular fusion inhibitory activity, but considering that the IC_{50} values of the gold–E1 and gold–E2 peptide conjugates described are 10 times lower (about 0.5 μM), they can be considered clearly specific. These results agree well with previous findings of significant antiproliferative effects of gold(I)–phosphine complexes in cultured human tumour cell lines [35]. The authors of those findings attributed the cytotoxic activity of $[AuCl(PPh_3)]$ to its uptake into the cells. Gold–phosphine complexes are more lipophilic than non-phosphine analogues, and this enhances transport of the gold compound through cellular membranes and facilitates the association of the gold complex with the active intracellular site. In general, it seems that for good cytotoxic activity of gold complexes, the ligands are important for the transport of the metal to the biological target; but it is the gold itself which possesses the cytotoxic activity. Remarkably, the inhibitory concentrations of the E1P8 and E2P45 gold(I) complexes obtained in both cell–cell fusion and HIV-1 NL4-3 antiretroviral assays, were 3 orders of magnitude lower than those corresponding to the parent peptides. In particular, the IC_{50} value of the E1P8 peptide gold complex was submicromolar (<0.5 μM) (Table **4**).

CONCLUSIONS

This work demonstrates that the modification of two GBV-C peptide domains, E1P8 and E2P45, by different chemical strategies improves the antiviral potencies of these short linear HIV-inhibiting peptides: the modified products

decrease the infectivity of HIV-1 NL4-3 in a dose-dependent manner (Fig. **4**). The increased activity of these new derivatives might be due to either suitable presentation of the required structural motif, or increased cellular uptake of the peptides. So, we propose the derivatization of synthetic GBV-C peptides with fatty acids as well as their multimerization as potential routes to therapeutic advances. Moreover, the coordination of the peptides to gold(I) phosphine could enhance their cellular uptake and could therefore be of considerable interest for the development of novel antiretroviral drugs. Of all the GBV-C peptide derivatives studied in this work, the peptide–gold complexes were the most active entry inhibitors. Specifically, peptide molecules derived from the (22-39) sequence of the GBV-C E1 protein were more potent as HIV-1 inhibitors than derivatized peptides from the (133-150) sequence of the GBV-C E2 protein. These results also support the putative modulation of HIV-1 infection by the GBV-C E1 protein and open new perspectives for the development of novel peptide-derived HIV-1 entry inhibitors.

CONFLICT OF INTEREST

The author(s) confirm that this article content has no conflicts of interest.

ACKNOWLEDGEMENTS

This work was funded by Grants CTQ2009-13969-C02-01/BQU and CTQ2012-37589-C02-01/BQU from the Ministerio de Economía y Competitividad, Spain and FIPSE 36-0735-09 from the Fundación para la Investigación y Prevención del SIDA en España.

R.G. is the recipient of predoctoral grant (JAE program, CSIC, Spain). We are grateful to Dr. Meritxell Egido for performing cell-cell fusion assays. We are also grateful to Anna Paús and Raymond Ulldemolins for the technical assistance in solid phase peptide synthesis and Alberto Merino-Mansilla for performing the HIV assays. The following reagent was obtained through the NIH AIDS Research and Reference Reagent Program, Division of AIDS, NIAID, NIH: HIV-1 IIIB C34 peptide from DAIDS, NIAID.

SUPPORTIVE/SUPPLEMENTARY MATERIAL

Characterization of homogeneous and heterogeneous tetrameric MAPs. Characterization of cyclic derivatives. Characterization of lipophilic derivatives.

ABBREVIATIONS

AIDS	=	Acquired immunodeficiency syndrome
DIPCDI	=	Disopropylcarbodiimide
DIPEA	=	Diisopropylethylamine
DMEM	=	Dulbecco's modified Eagle medium
EDT	=	Ethanedithiol
FBS	=	Foetal bovine serum
FP	=	Fusion peptide
GBV-C	=	GB virus C
HATU	=	2-(1H-7-azabenzotriazole-1-yl)-1,1,3,3-tetramethyluronium hexafluorophosphate
HIV	=	Human immunodeficiency virus
HOBt	=	Hydroxybenzotriazole
H-PAL	=	5-[3,5-Dimethoxy-4-(Fmoc-aminomethyl)phenoxy]pentanoic acid
ivDde	=	1-(4,4-dimethyl-2,6-dioxocyclo hexylidene)-3-methylbutyl
LTR	=	Long terminal repeat promoter
LC_{50}	=	Lethal concentration 50%
MAP	=	Multiple antigenic peptide
MTT	=	(3-(4,5-dimethylthiazol-2-yl)-2,5-diphenyltetrazolium bromide
TIS	=	Triisopropylsilane
YFV	=	Yellow fever virus
VIRIP	=	Virus inhibitory peptide

REFERENCES

[1] Burton, A. Enfuvirtide approved for defusing HIV. *Lancet Infect. Dis.*, **2003**, *3*, 260.

[2] Munch, J.; Standker, L.; Adermann, K.; Schulz, A.; Schindler, M.; Chinnadurai, R.; Pohlmann, S.; Chaipan, C.; Biet, T.; Peters, T.; Meyer, B.; Wilhelm, D.; Lu, H.; Jing, W.; Jiang, S.; Forssmann, W. G.; and Kirchhoff, F. Discovery and optimization of a natural HIV-1 entry inhibitor targeting the gp41 fusion peptide. *Cell,* **2007**, *129*, 263-275.

[3] Boggiano, C.; Jiang, S.; Lu, H.; Zhao, Q.; Liu, S.; Binley, J.; and Blondelle, S. E. Identification of a D-amino acid decapeptide HIV-1 entry inhibitor. *Biochem. Biophys. Res. Commun*., **2006**, *347*, 909-915.

[4] Smith,J.M.; Ellenberger,D.; and Butera,S. Protein Engineering for HIV Therapeutics. In *Medicinal Protein Engineering.* Khudyakov, Y. E. Ed.; CRC Press: Boca Raton, **2009**; pp 385-406.

[5] Heringlake, S.; Ockenga, J.; Tillmann, H. L.; Trautwein, C.; Meissner, D.; Stoll, M.; Hunt, J.; Jou, C.; Solomon, N.; Schmidt, R. E.; and Manns, M. P. GB virus C/hepatitis G virus infection: a favorable prognostic factor in human immunodeficiency virus-infected patients? *J. Infect. Dis.*, **1998**, *177*, 1723-1726.

[6] Bhattarai, N. and Stapleton, J. T. GB virus C: the good boy virus? *Trends Microbiol.*, **2012**, *20*, 124-130.

[7] Chang, Q.; McLinden, J. H.; Stapleton, J. T.; Sathar, M. A.; and Xiang, J. Expression of GB virus C NS5A protein from genotypes 1, 2, 3 and 5 and a 30 aa NS5A fragment inhibit human immunodeficiency virus type 1 replication in a CD4+ T-lymphocyte cell line. *J. Gen.Virol.*, **2007**, *88*, 3341-3346.

[8] Jung, S.; Eichenmuller, M.; Donhauser, N.; Neipel, F.; Engel, A. M.; Hess, G.; Fleckenstein, B.; and Reil, H. HIV entry inhibition by the envelope 2 glycoprotein of GB virus C. *AIDS*, **2007**, *21*, 645-647.

[9] Xiang, J.; McLinden, J. H.; Chang, Q.; Kaufman, T. M.; and Stapleton, J. T. An 85-aa segment of the GB virus type C NS5A phosphoprotein inhibits HIV-1 replication in CD4+ Jurkat T cells. *Proc. Natl. Acad. Sci. U. S A*, **2006**, *103*, 15570-15575.

[10] Koedel, Y.; Eissmann, K.; Wend, H.; Fleckenstein, B.; and Reil, H. Peptides Derived from a Distinct Region of GB Virus C Glycoprotein E2 Mediate Strain-Specific HIV-1 Entry Inhibition. *J. Virol.*, **2011**, *85*, 7037-7047.

[11] Xiang, J.; McLinden, J.H.; Kaufman, T.M.; Mohr, E.L.; Bhattarai, N.; Chang, Q.; Stapleton, J.T. Charcaterization of a peptide domain within the GB virus C envelope glycoprotein (E2) that inhibits HIV replication. Virology, **2012**, 430, 53-62.

[12] Gielen, M.; Tiekink, E.R.T. *Metallotherapeutic Drugs & Metal-based Diagnostic Agents: The Use of Metals in Medicine*; Wiley: Chichester, **2005**.

[13] Okada, T.; Patterson, B. K.; Ye, S. Q.; and Gurney, M. E. Aurothiolates Inhibit Hiv-1 Infectivity by Gold(I) Ligand-Exchange with A Component of the Virion Surface. *Virology*, **1993**, *192*, 631-642.

[14] Shapiro, D. L. and Masci, J. R. Treatment of HIV associated psoriatic arthritis with oral gold. *J. Rheumatol.*, **1996**, *23*, 1818-1820.

[15] Fonteh, P. and Meyer, D. Novel gold(I) phosphine compounds inhibit HIV-1 enzymes. *Metallomics*, **2009**, *1*, 427-433.

[16] Che, C. M. Methods for using gold(III)complexes as anti-tumor and anti-HIV agents. U.S. [WO/2004/024146]. **2004.**

[17] Bowman, M. C.; Ballard, T. E.; Ackerson, C. J.; Feldheim, D. L.; Margolis, D. M.; and Melander, C. Inhibition of HIV fusion with multivalent gold nanoparticles. *J. Am. Chem. Soc.*, **2008**, *130*, 6896-6897.

[18] Herrera, E.; Tenckhoff, S.; Gomara, M. J.; Galatola, R.; Bleda, M. J.; Gil, C.; Ercilla, G.; Gatell, J. M.; Tillmann, H. L.; and Haro, I. Effect of Synthetic Peptides Belonging to E2 Envelope Protein of GB Virus C on Human Immunodeficiency Virus Type 1 Infection. *J. Med. Chem.*, **2010**, *53*, 6054-6063.

[19] Sanchez-Martin, M. J.; Hristova, K.; Pujol, M.; Gomara, M. J.; Haro, I.; Alsina, M. A.; and Busquets, M. A. Analysis of HIV-1 fusion peptide inhibition by synthetic peptides from E1 protein of GB virus C. *J. Colloid Interf. Sci.*, **2011**, *360*, 124-131.

[20] Malakoutikhah, M; Gomara, M.J.; Gomez-Puerta, J.A.; Sanmarti, R.; Haro, I. The use of chimeric vimentin citrullinated peptides for the diagnosis of Rheumatoid Arthritis. *J. Med. Chem.*, **2011**, 54, 7486-7492.

[21] Chhabra, S. R.; Hothi, B.; Evans, D. J.; White, P. D.; Bycroft, B. W.; and Chan, W. C. An appraisal of new variants of Dde amine protecting group for solid phase peptide synthesis. *Tetrahedron Lett.*, **1998**, *39*, 1603-1606.

[22] Bycroft, B. W.; Chan, W. C.; Chhabra, S. R.; and Hone, N. D. A Novel Lysine-Protecting Procedure for Continuous-Flow Solid-Phase Synthesis of Branched Peptides. *J. Chem. Soc., Chem. Commun.*, **1993**, 778-779.

[23] Sanchez-Martin, M. J.; Urban, P.; Pujol, M.; Haro, I.; Alsina, M. A.; and Busquets, M. A. Biophysical Investigations of GBV-C E1 Peptides as Potential Inhibitors of HIV-1 Fusion Peptide. *Chemphyschem*, **2011**, *12*, 2816-2822.

[24] Morrison, K.L. and Weiss G.A. Combinatorial alanine-scanning. *Curr. Opin. Chem. Biol.*, **2001**, *5*(3), 302-307.

[25] Nomura, W.; Hashimoto, C.; Ohya, A.; Miyauchi, K.; Urano, E.; Tanaka, T.; Narumi, T.; Nakahara, T.; Komano, J. A.; Yamamoto, N.; and Tamamura, H. A Synthetic C34 Trimer of HIV-1 gp41 Shows Significant Increase in Inhibition Potency. *Chemmedchem*, **2012**, *7*, 205-208.

[26] Shi, W. G.; Qi, Z.; Pan, C. G.; Xue, N.; Debnath, A. K.; Qie, J. K.; Jiang, S. B.; and Liu, K. L. Novel anti-HIV peptides containing multiple copies of artificially designed heptad repeat motifs. *Biochem. Biophysl. Res. Comm.*, **2008**, *374*, 767-772.

[27] Welch, B. D.; VanDemark, A. P.; Heroux, A.; Hill, C. P.; and Kay, M. S. Potent D-peptide inhibitors of HIV-1 entry. *Proc. Natl. Acad. Sci. U. S A,* **2007**, *104*, 16828-16833.

[28] Tam, J. P. Synthetic Peptide Vaccine Design - Synthesis and Properties of A High-Density Multiple Antigenic Peptide System. *Proc. Natl. Acad. Sci. U. S A*, **1988**, *85*, 5409-5413.

[29] Tam, J. P. and Spetzler, J. C. Synthesis and application of peptide dendrimers as protein mimetics. *Curr. Protoc. Immunol.*, **2001**, *Chapter 9*, Unit 9.6.

[30] Hayouka, Z.; Hurevich, M.; Levin, A.; Benyamini, H.; Iosub, A.; Maes, M.; Shalev, D. E.; Loyter, A.; Gilon, C.; and Friedler, A. Cyclic peptide inhibitors of HIV-1 integrase derived from the LEDGF/p75 protein. *Bioorgan. Med. Chem.*, **2010**, *18*, 8388-8395.

[31] Jia, Q. Y.; Jiang, X. F.; Yu, F.; Qiu, J. Y.; Kang, X. Y.; Cai, L. F.; Li, L.; Shi, W. G.; Liu, S. W.; Jiang, S. B.; and Liu, K. L. Short cyclic peptides derived from the C-terminal sequence of alpha 1-antitrypsin exhibit significant anti-HIV-1 activity. *Bioorgan. Med. Chem. Lett*., **2012**, *22*, 2393-2395.

[32] Wexler-Cohen, Y. and Shai, Y. Demonstrating the C-terminal boundary of the HIV 1 fusion conformation in a dynamic ongoing fusion process and implication for fusion inhibition. *FASEB J.*, **2007**, *21*, 3677-3684.

[33] Wexler-Cohen, Y. and Shai, Y. Membrane-Anchored HIV-1 N-Heptad Repeat Peptides Are Highly Potent Cell Fusion Inhibitors via an Altered Mode of Action. *Plos Path.*, **2009**, *5,* e1000509.

[34] Zhang, H. Y.; Schneider, S. E.; Bray, B. L.; Friedrich, P. E.; Tvermoes, N. A.; Mader, C. J.; Whight, S. R.; Niemi, T. E.; Silinski, P.; Picking, T.; Warren, M.; and Wrings, S. A. Process development of TRI-999, a fatty-acid-modified HIV fusion inhibitory peptide. *Org. Process Res. Dev.*, **2008**, *12*, 101-110.

[35] Scheffler, H.; You, Y.; and Ott, I. Comparative studies on the cytotoxicity, cellular and nuclear uptake of a series of chloro gold(I) phosphine complexes. *Polyhedron*, **2010**, *29*, 66-69.

Received: ????? **Revised: ?????** **Accepted: ?????**